MONITORING OF SOIL MOISTURE AND HUMAN BREATH USING COLORIMETRIC HUMIDITY SENSORS

by

Emily Bialka

A Thesis Submitted in

Partial Fulfillment of the

Requirements for the Degree of

Master of Science

in Chemistry

at

The University of Wisconsin-Milwaukee

August 2021

ABSTRACT

MONITORING OF SOIL MOISTURE AND HUMAN BREATH USING COLORIMETRIC HUMIDITY SENSORS

by

Emily Bialka

The University of Wisconsin-Milwaukee, 2021
Under the Supervision of Professor Jian Chen

The monitoring of soil moisture is essential to optimize plant growth, harvest, and water use, and respiration monitoring is one of the major vital signs of human health. Current soil moisture sensors are either costly or ineffective, and current breath sensors which also detect humidity levels are electronic-based with narrow humidity ranges. The following study targets these two needs by developing a cost-effective, high-sensitivity soil moisture sensor and breath monitor. Responsive interference coloration humidity sensors which utilize thin-film interference are applied to track soil moisture content over time, and to monitor breath humidity levels and respiratory rate in various scenarios. The ease of use and cost-effectiveness associated with the sensor and its analysis makes it suitable even for at-home use.

TABLE OF CONTENTS

LIST OF FIGURES

LIST OF TABLES

LIST OF ABBREVIATIONS

KGM Konjac Glucomannan

RH Relative Humidity

RIC Responsive Interference Coloration

VWC Volumetric Water Content

ACKNOWLEDGEMENTS

This work would not be possible without the support from my family and friends, and guidance from my advisor, Dr. Jian Chen. His outstanding ideas and support throughout my studies is what created great developments during this endeavor. I am forever appreciative of his leadership as it has shaped me to be a better chemist. I would also like to sincerely thank members of my committee: Dr. Mark Dietz and Dr. Alan Schwabacher for their time, support, and contributions.

I would like to acknowledge Dr. Heather Owen, for her assistance with the sputter coater. To Elise Nicks, Wendy Grober, Kevin Blackburn, and Shelly Hagen, thank you so much for the continual support throughout my years at UW-Milwaukee. I would also like to thank my group member Milad Momtaz for his instruction, advice, encouragement, and support.

I am so grateful now and forever for the support everyone has offered me during my time completing my masters.

Introduction

The following study employs the principal of thin-film interference coloration with a responsive interference coloration (RIC) humidity sensor developed by Momtaz and Chen[1] to applications of soil moisture sensing and breath monitoring. The water vapor on a soil's surface and the high humidity of a human's exhale breath can be monitored with this colorimetric humidity sensor. The reflected color observed on said sensor is dependent on the film's thickness, refractive index, and the angle of incidence, as seen in Equation 1.

$$m\lambda = 2n_2 d_2 \cos\theta \quad (1)$$

Where m is a positive integer of the order of interference, λ is the wavelength of light reflected, n_2 and d_2 are the refractive index and thickness of the film, respectively, and θ is the angle of incidence.

Konjac glucomannan (KGM) polymer is used as the thin film in the present study. When presented with water vapor, the hydrogel swells, increasing the thickness of the polymer and changing the reflected wavelength. The trilayer RIC sensor for thin-film interference was used in the following studies as it has been shown to exhibit sensitivity to relative humidity (RH) from 0-100%.[1] The layers consist of a KGM film, an ultrathin layer of iridium, and a glass substrate (Figure 1). The layer of iridium acts as an optical filter, enhancing the color of the polymer, otherwise colorless on glass.[2]

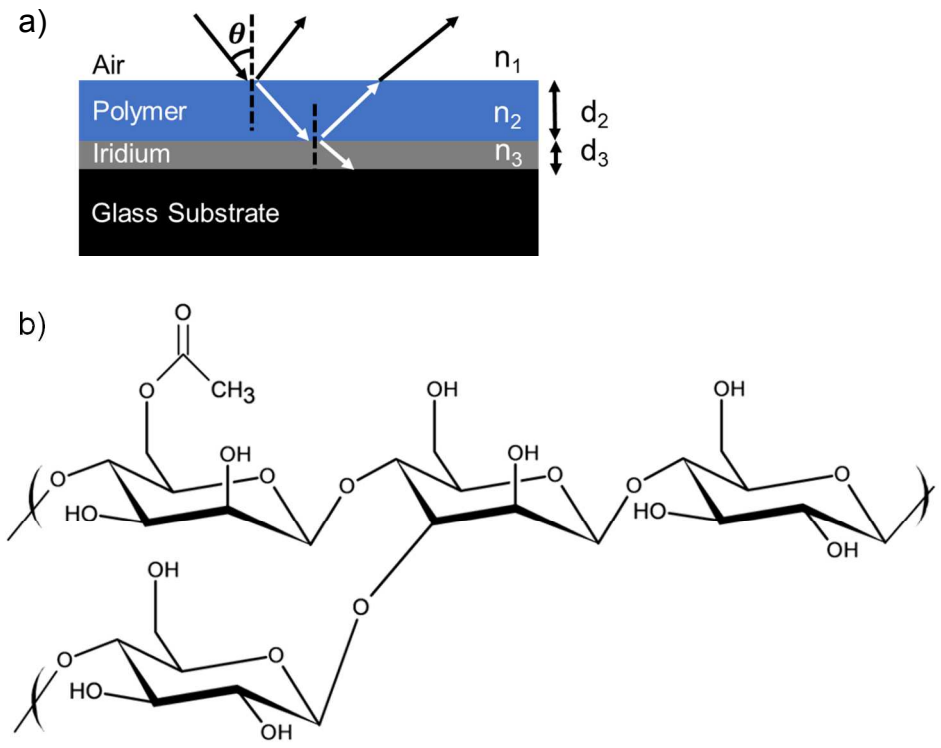

Figure 1. a) Responsive interference coloration sensor design developed from thin-film interference principle. b) Chemical structure of KGM.

This RIC sensor has been proven to have a response/recovery time of 0.6/3.5 seconds to water vapor from a distance of ~0.2 mm from the source.[1] The fast response/recovery times and high sensitivity to RH makes this sensor an excellent candidate to monitor soil moisture and human breath. Three variations of the RIC sensor were used throughout this study: KGM I, KGM II, and KGM III (Figure 2). The colorations of KGM are controlled by thickness in sensor preparation to exhibit first- or second-order interference at 33% RH based on the Michel-Lévy interference color chart.[3]

To determine soil moisture content, the RIC sensor is applied to the surface of watered soil to detect the soil surface humidity. As water is released upwards from the

soil by evaporation, the RIC sensor tracks water vapor trends over time. To monitor breathing, the RIC sensor is applied to the inside of an oxygen mask to detect breath humidity. Also, the sensor's response to the humidity caused by exhales and inhales can be tracked to show breath cycles and determine respiratory rate.

a) b) c)

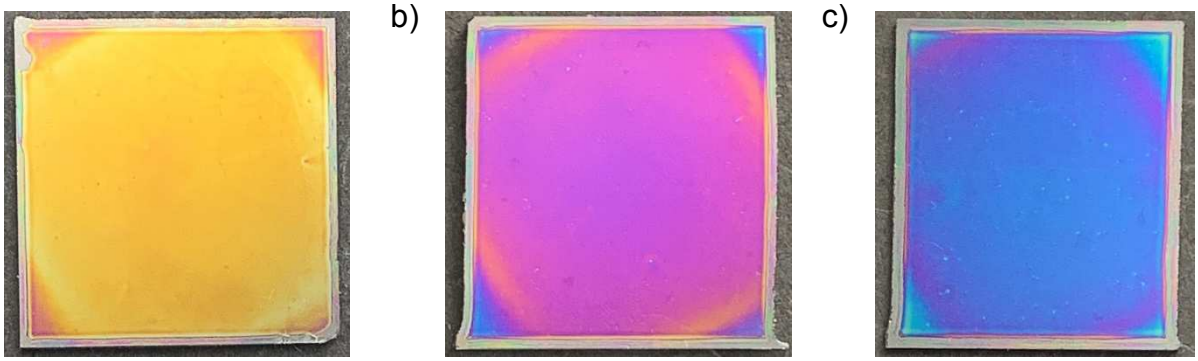

Figure 2. Variations of the RIC sensor at 33% RH. a) KGM I, exhibiting 1st order coloration. b) KGM II, exhibiting 2nd order coloration c) KGM III, exhibiting 2nd order coloration.

Chapter 1: Soil Moisture Sensor

1.1 Background

1.1.1 Soil Moisture Content

Soil moisture content, also known as soil water content, refers to the amount of water present in soil.[4] Water is not only essential for plant life, but is also responsible for the transport of nutrients from the soil to plant roots. The water level in soil can be broken up into three thresholds: saturation, field capacity, and permanent wilting point.[4] These thresholds differ depending on the soil's composition. Soil saturation is when all pores between soil particles have been filled with water and plant roots do not need to exert much energy to take up water. Because there is an overabundance of water in the soil at this threshold, some water is lost to runoff or leaching. At field capacity, most water has drained by gravitational pull and only capillary water remains. Plants need to exert slightly more force to take up water through the roots in this threshold. When soil reaches a permanent wilting point, the only water which remains is attracted so tightly to soil particles that it is impossible for plants to exert enough force to uptake water. The most plant available water is held at the water contents between field capacity and permanent wilting point.

1.1.2 Commercial Soil Moisture Sensors

In order to optimize efficiency and conserve resources, soil moisture sensors are needed to measure and/or track water content of soil. These sensors are used in farming, gardening, or tending to house plants. Soil moisture sensors fall into two categories: water tension sensors and electromagnetic sensors.

Water tension sensors, also called tensiometers, measure the attraction of water to soil particles.[5] A mechanical tensiometer (Figure 1.1 a) operates with a porous tip and water-filled vertical tube that is inserted into soil. The soil draws water down the tube and out the tip, creating a vacuum.[5] Dry soil will result greater suction than wet soils, which is measured in pounds per square inch or centibars. An electronic tensiometer (Figure 1.1 b) is a solid state electrical resistance sensor that measures the resistance in soil and estimates water potential to read like a mechanical tensiometer. [6]

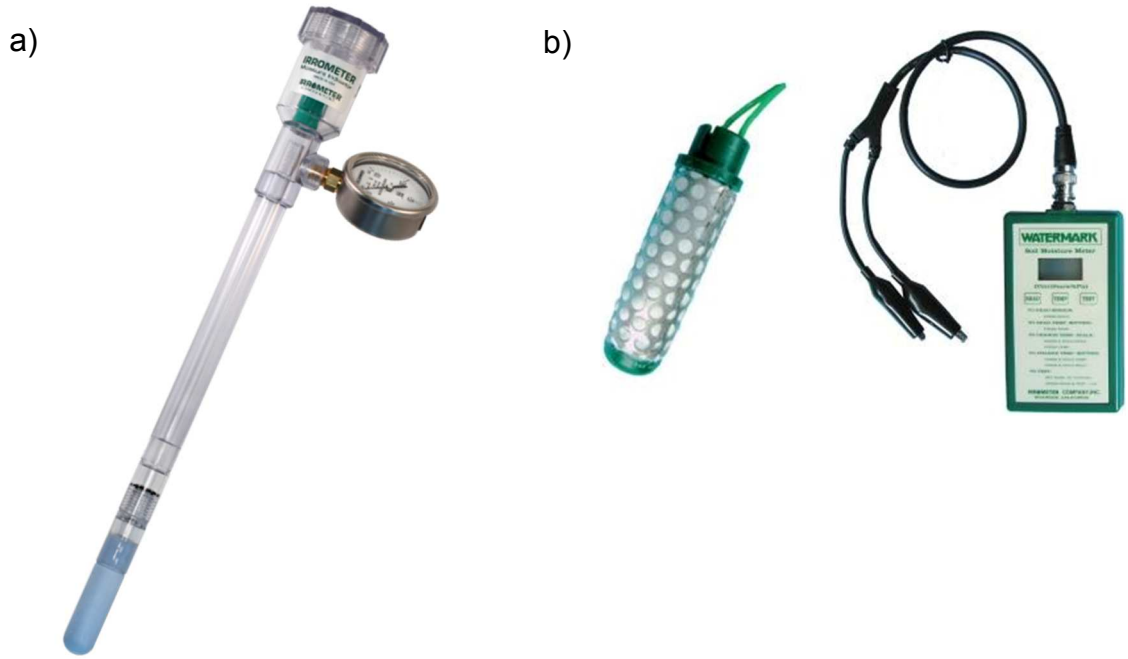

Figure 1.1. Commercially available soil water tension sensors. a) Mechanical tensiometer (IRROMETER® Tensiometer). b) Electronic tensiometer (IRROMETER® WATERMARK Sensor).

Electromagnetic sensors are popular soil moisture sensors as they read soil moisture instantly. They are either resistance, capacitance, or time domain reflectometry (TDR) sensors. Resistance sensors are not research grade[7] and are commonly used for house plants or home gardens (Figure 1.2 a). The main issue with

these sensors is how strongly dissolved salts can affect the resistance or conductivity reading. It is common to see these basic sensors change moisture readings when the soil is already past its wilting point. Because water is a poor conductor, these sensors are not sensitive to small changes in soil water content; they will only distinguish between a fully saturated soil and a bone-dry soil. Additionally, the sensor probes will become damaged if left in soil for more than a few minutes, which adds to their unreliability.

On the other hand, capacitance and TDR sensors are much more reliable to measure water content in soil. These sensors instantly measure the dielectric permittivity of the soil.[5] The capacitance sensor (Figure 1.2 b) estimates water content by measuring the charge in soil. However, since the rods are oppositely charged, soil salinity can have a large effect on the reading.[8] The TDR sensor is more effective in measuring soil moisture regardless of soil salinity (Figure 1.2 c). This is due to its ability to transmit a range of frequencies that, when high enough, can reduce effects from soil salinity.[8]

Figure 1.2. Commercially available electromagnetic soil moisture sensors. a) Resistance sensor (Amazon Soil Moisture Meter). b) Capacitance sensor (General® Moisture Meter). c) TDR sensor (FieldScout® TDR Moisture Meter).

1.1.3 Soil Moisture Sensors with Responsive Interference Coloration

In this study, responsive interference coloration is applied to the measurement of soil moisture. When soil is wet, water is not only held between pores of the soil but also is released upwards through evaporation.[9] In this study, we determine the relationship between soil surface relative humidity and soil moisture content by applying KGM's hydrogel properties in response to watered soil. Water levels from permanent wilting point up to saturation are studied to determine the sensor's feasibility and sensitivity.

1.2 Experimental

1.2.1 Materials

KGM was purchased from NOW Foods. Glass microslides (1 mm thick) were purchased from Corning. KGM solution was prepared with deionized water (0.6 wt%) and stored at room temperature. Loam soil was purchased from VWR International, LLC. A digital humidity sensor (AcuRite 01083M Pro Accuracy Temperature and Humidity Monitor) was purchased from Amazon and calibrated with saturated NaCl solution. PYREX dishes (100 x 50 mm and 125 x 65 mm) were purchased from Corning. Glass covers (100 x 1 mm and 125 x 1 mm) and hollow cylindrical glass stands (2.8 x 1.9 cm) were created by the glass shop.

1.2.2 Preparation of Responsive Interference Coloration Sensors

Glass substrates, used for low cost and convenience, were sputter coated with 3.0 nm of iridium (high-purity iridium target from Ted Pella, Inc.) using a sputter coating system (model K150X, Quorum Emitech). Then, KGM solution (~300 μL) was deposited on the Ir-glass substrate and spin coating was carried out at three spinning rates (300, 500, 1000 – 2000 rpm) for 334 seconds using a spin coater (model P6700, Specialty

Coating Systems, Inc.). Three distinct colors were created: 1st order yellow, 2nd order purple, and 2nd order blue by using final spin rates of 2000, 1800, and 1500 rpm, respectively. 1st order yellow was KGM I, 2nd order purple was KGM II, and 2nd order blue was KGM III. Sensors were stored at room temperature.

1.2.3 Preparation of Soil Samples

Loam soil was oven dried at 105°C for 24 hours to obtain constant mass, then allowed to cool to room temperature. The cooled, oven-dried loam soil was then added to the according container. For horizontal testing with multiple sensors and a commercial sensor (Figure 1.3 b), a larger PYREX 125 x 65 glass container was filled with 400.0 g soil. For horizontal testing with a sensor(s) without a commercial sensor, a smaller PYREX 100 x 50 glass container was filled with 300.0 g soil (Figure 1.3 c and d). Each soil-filled container was then placed in a temperature and humidity-stable room for 24 hours to equilibrate with the environment. After this period, water was added according to the goal volumetric water content (VWC). Then, the PYREX 125 x 65 soil was packed to 3.4 cm and the PYREX 100 x 50 was packed to 4.1 cm in height to ensure 1.0 g/cm^3 density throughout. The container was quickly covered with a glass top and secured with parafilm. This was allowed to equilibrate with the room temperature for 6 hours so fogging of the glass top could be avoided.

For vertical testing, the PYREX 100 x 50 glass container was filled with 369.3 g soil. For vertical tests, water was added according to the goal VWC and sat for 20 minutes without a covering to allow the soil to soak in the water.

In all cases, the goal VWC was calculated with Equation 2:

$$\theta_V = \frac{V_W}{V_S} = \frac{{}^{m_W}/_{\rho_W}}{{}^{m_S}/_{\rho_S}} = \frac{m_W}{m_S} = \frac{m_{SW} - m_S}{m_S} \quad (2)$$

where θ_V is the VWC, V_W is the volume of water, V_S is the volume of soil, m_W is the mass of water, m_S is the mass of soil, and m_{SW} is the mass of wet soil. The density of water and density of soil, ρ_W and ρ_S, respectively, are both 1.0 g/cm^3. For loam soil, the permanent wilting point is found at ~10% VWC, field capacity at ~30% VWC, and saturation at ~40% VWC.[3] This study utilized 10, 20, 30, and 40% volumetric water capacities to study the effectiveness of the KGM soil moisture sensor.

1.2.4 Horizontal Soil Tests

After 6 hours of the covered soil container equilibrating with room temperature, sensors were placed directly on the soil according to the layouts presented in Figure 1.3. The trilayer composition of the RIC is shown in Figure 1.3. To study the feasibility of the soil moisture sensor, two RIC sensors and a commercial humidity sensor were placed atop glass stands 2.0 mm high on the soil (Figure 1.3 b). The glass top and parafilm were immediately replaced to hold the soil at a stable VWC. Photos of the RIC sensors were taken immediately at time 0 and again every minute until 5 minutes, then every 5 minutes until the final 60 or 80 minutes. At every photo collection, the commercial sensor's temperature and RH were recorded.

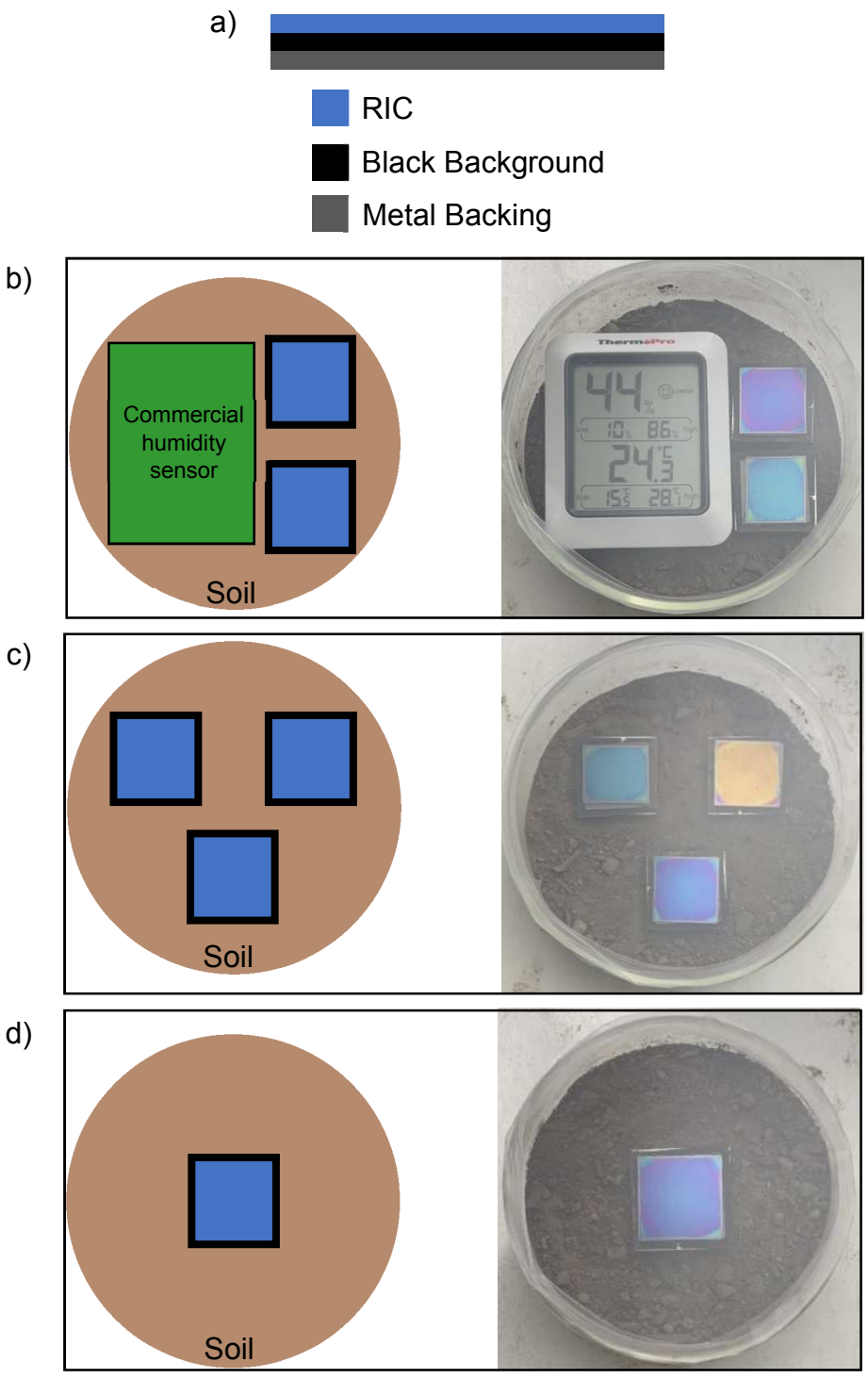

Figure 1.3. a) Trilayer sensor composition. b) Horizontal set-up to test feasibility: diagram and photo. c) Horizontal set-up to test sensitivity: three sensors diagram and photo. d) Horizontal set-up to test sensitivity: one sensor diagram and photo. Each set-up included a stand which raised the sensor 2.0 mm from the soil surface.

To study the sensitivity of the RIC, three sensors were placed atop glass stands 2.0 mm high on the soil without the commercial sensor (Figure 1.3 c). The extended time period of the sensitivity experiment would be damaging to the commercial sensor's electronic components. After sensor placement, the glass top was immediately replaced and secured with parafilm to hold the soil at a stable VWC. Photos of the RIC sensors were taken immediately at time 0 and again every 5 minutes until 180 minutes. At every interval, the reflectance spectroscopy of the RIC sensors was also recorded (Figure 1.4).

a)

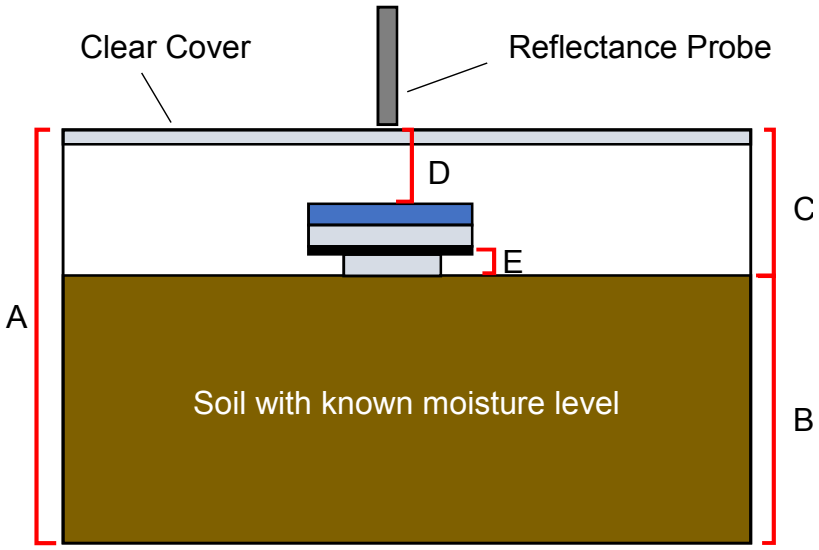

b)

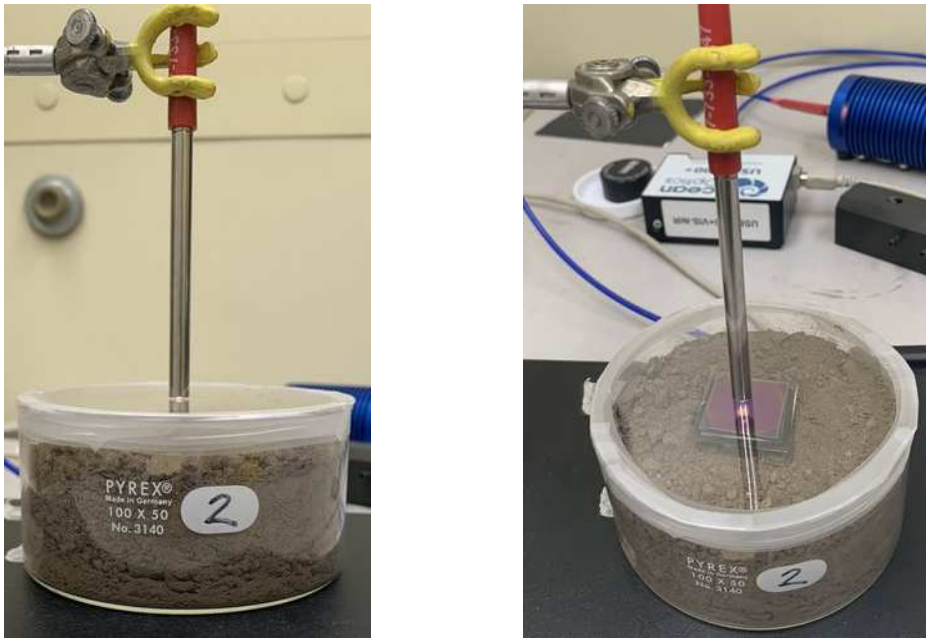

Figure 1.4. a) Diagram of reflectance spectroscopy set-up. Distances labeled are: A = 5 cm; B = 4.1 cm; C = 0.9 cm; D = 0.88 cm; E = 2.0 mm. Reflectance probe sits just above surface of the cover at a 90° angle to the sensor. b) Photos of reflectance spectroscopy set-up.

1.2.5 Vertical Soil Tests

After 20 minutes of allowing the soil to soak in water, the RIC sensor (same composition as in Figure 1.3 a) was inserted vertically into the center of the soil. The

sensor was pushed down into the soil until it reached 1.0 cm of depth (Figure 1.5). A two-minute video of the RIC was immediately recorded upon placement of RIC. This video ensured documentation of dynamic color changes on the KGM. The sensor remained in the soil for a total of seven days with two videos recorded a day: morning and afternoon. At the conclusion of the seven days, the RIC was removed, and the container was weighed to determine final soil VWC.

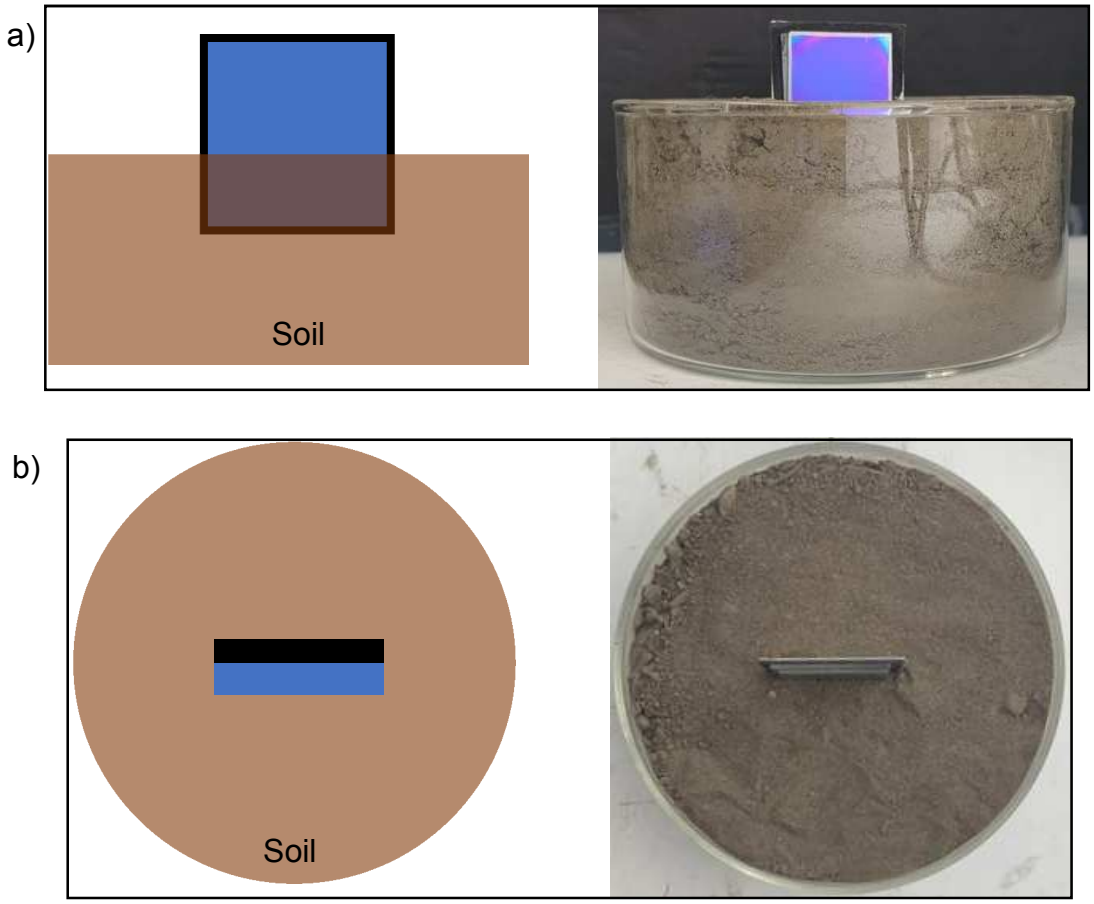

Figure 1.5. a) Diagram and photo of sensor pushed into soil at a 0° viewing angle. b) Diagram and photo of sensor pushed into soil at a 90° viewing angle.

In order to quantify the visual differences in KGM sensors over time in soil and relate soil moisture with the front line, the water vapor front line was tracked through video and photo analysis. In each of the 14 two-minute videos, an image was extracted at the moment of the most color change on each KGM sensor. Then, the height of the front line was approximated using the control KGM as a guide. Since the front line is a gradient of color, the top of the most easily viewed color change was designated as the front line. Figure 1.6 shows an example of this digital front line determination method using KGM I.

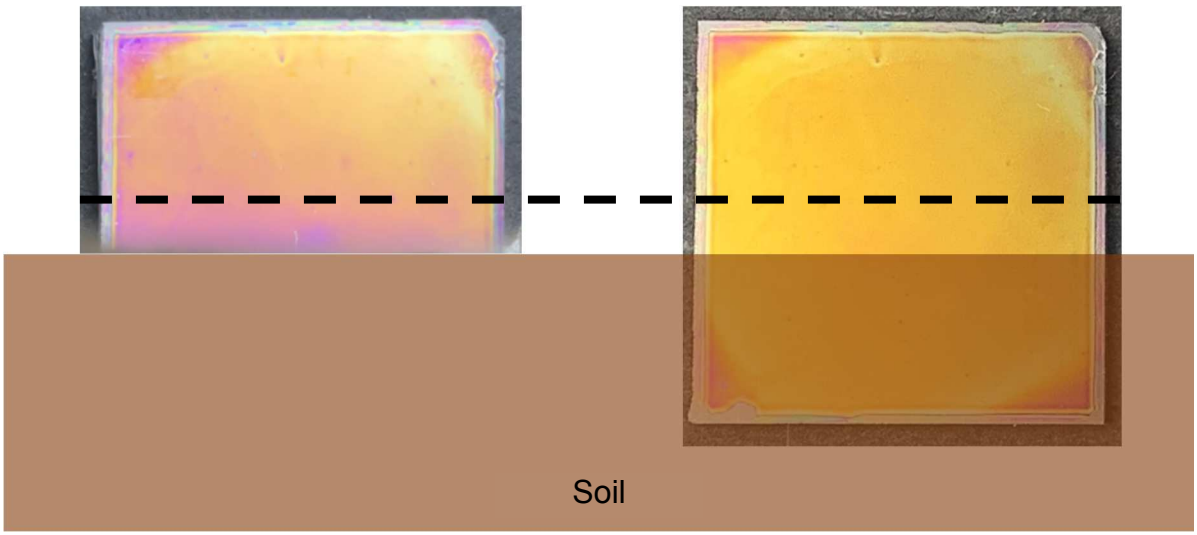

Figure 1.6. Example front line analysis with KGM I in 40% VWC at 96 hours (left) and control KGM in 24% RH (right). After scaling up the height to actual size of sensor, the front line was approximated at 0.33 cm.

1.3 Results and Discussion

1.3.1 Horizontal Set-Up Feasibility

The RIC sensor quickly changed in color immediately upon placement in the soil chamber. After 60 minutes placement on soil, each sensor was seen to have shifted to about 94% RH (Figure 1.7 and 1.8) according to Momtaz and Chen's KGM sensor array at various RH levels.[1] The commercial humidity sensor tracked humidity much slower than the sensor and was only able to reach 83% RH in the chamber after 60 minutes. After lengthening the experiment, it was seen that the KGM sensors were indeed able to reach 100% RH (Figure 1.9 and 1.10) after 24 hours of placement in soil according to Momtaz and Chen's KGM sensor array at various RH levels.[1] These studies showed that the KGM sensors were able to react to soil moisture's water vapor and a large range of RH could be reported. With these positive results, the sensitivity of the KGM sensors to different water contents in soil was studied next.

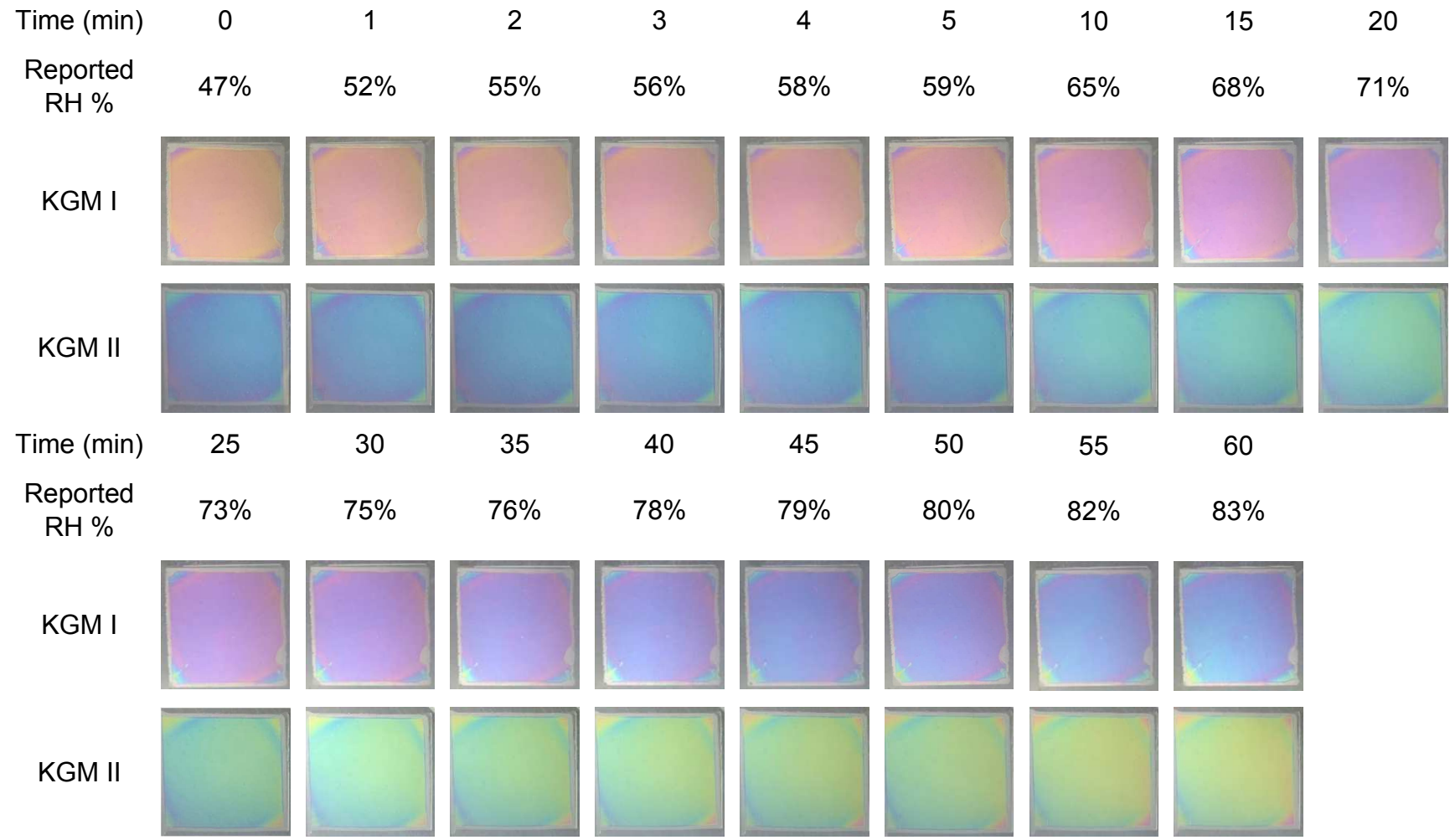

Figure 1.7. KGM I and II in 125 x 65 PYREX soil chamber with 30% VWC. The commercial humidity sensor in the chamber recorded temperature and RH.

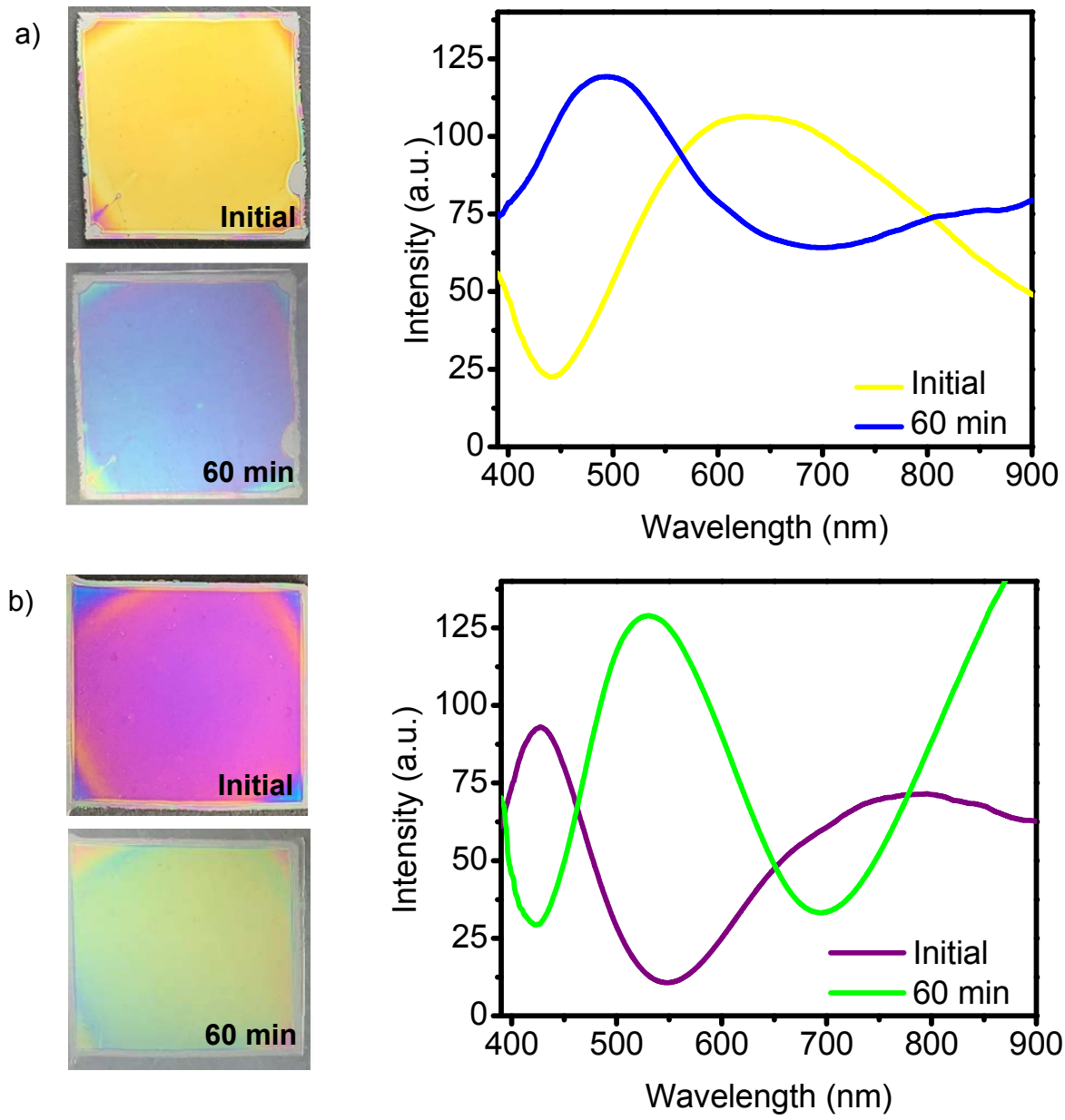

Figure 1.8. KGM reflectance spectroscopy and corresponding photos of KGM I (a) and KGM II (b) before and after 60 min insertion in chamber.

	Order of Interference	Initial	60 min
KGM I	1st	633	-
	2nd	-	494
KGM II	1st	790	-
	2nd	427	530

Table 1.1. Reflection peak wavelengths (nm) for KGM I and II after 60 minutes in soil chamber.

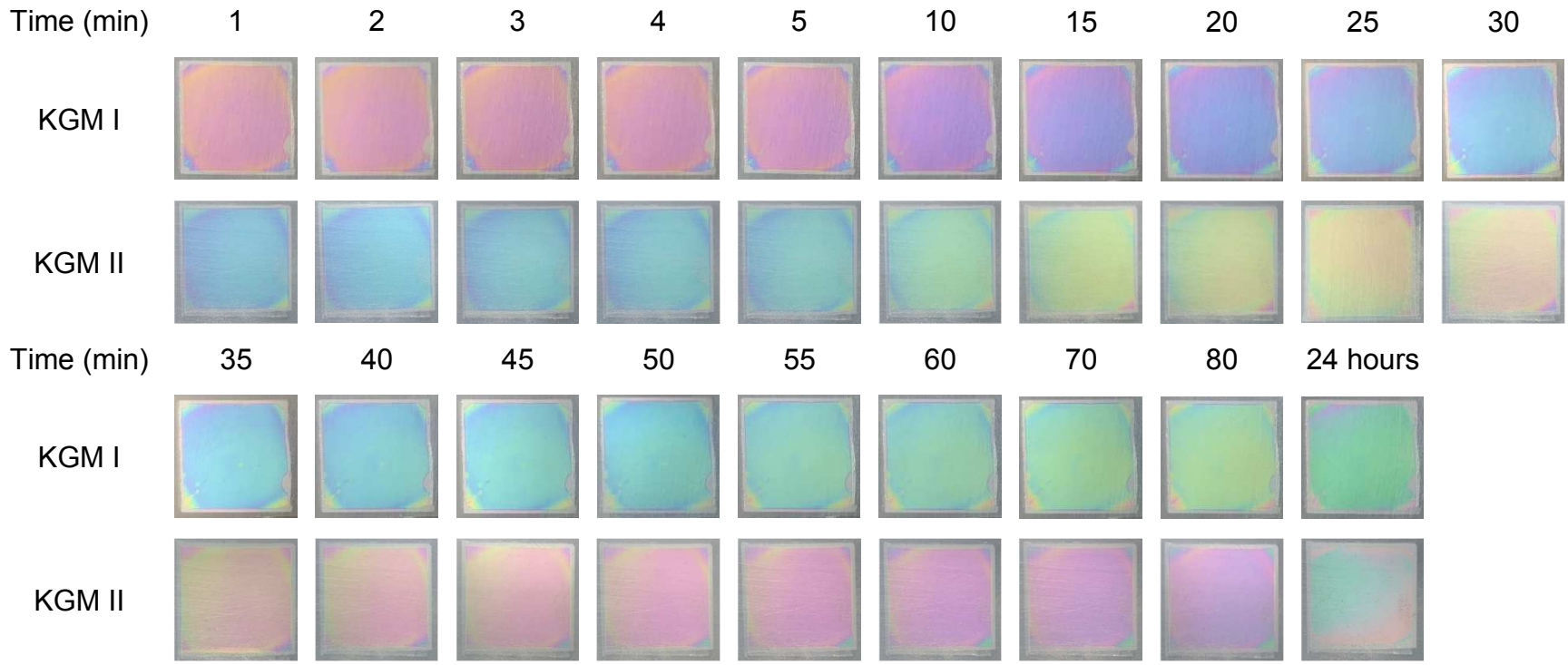

Figure 1.9. KGM I and II in 100 x 50 PYREX soil chamber with 30% VWC.

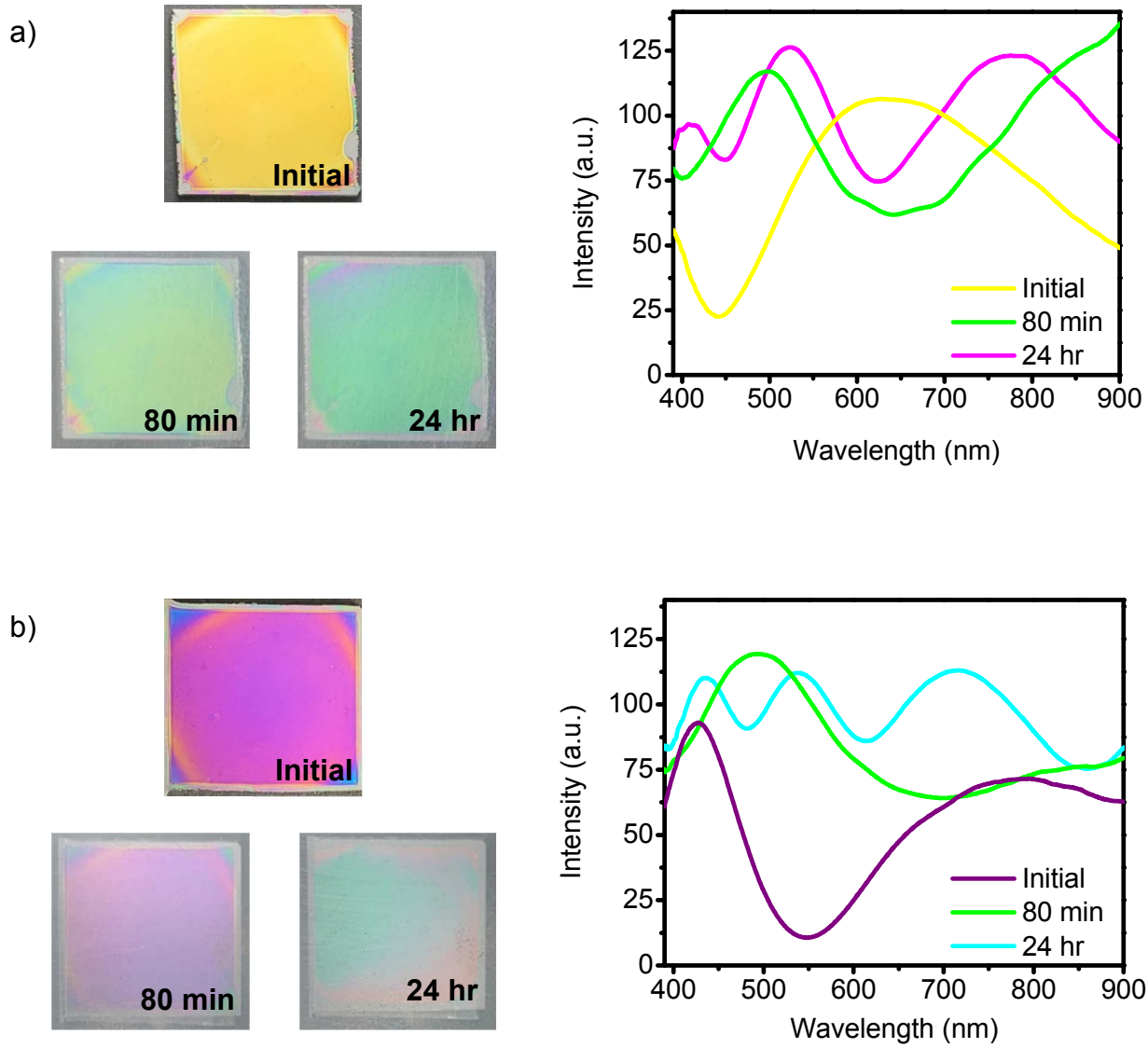

Figure 1.10. KGM reflectance spectroscopy and corresponding photos of KGM I (a) and KGM II (b) before, after 60 min, and after 14 min insertion in chamber.

	Order of Interference	Initial	80 min	24 hr
KGM I	1st	633	-	-
	2nd	-	497	780
	3rd	-	-	523
	4th	-	-	409
KGM II	1st	790	-	-
	2nd	427	493	-
	3rd	-	-	716
	4th	-	-	538
	5th	-	-	435

Table 1.2 Reflection peak wavelengths (nm) for KGM I and II after 80 minutes and 24 hours in soil chamber.

1.3.2 Horizontal Set-Up Sensitivity

KGM I, II, and III in the 100 x 50 PYREX soil chamber were able to distinguish between 20% and 30% VWC (Figures 1.11 and 1.15). However, the close proximity of the KGM sensors hindered their sensitivity to the water vapor. This caused gradients to occur on the KGM surfaces as water vapor was not evaporating evenly around the multiple sensors. The sensors reported a very slight change between 20% and 30% VWC when comparing the reflectance wavelength peaks (Tables 1.3 and 1.4).

To eliminate the sensor gradients, KGM I was studied in 10% VWC and 30% VWC soil chambers for 180 minutes (Figure 1.19). However, this sensor was not able to distinguish between 10% and 30% VWC when comparing the reflectance wavelength peaks (Table 1.5). This was due to the horizontal orientation of the sensor and its distance from the soil surface. If the sensor was raised higher than 2 mm, there was not adequate room for air and humidity flow in the soil chamber for good response from the

KGM sensor. If the sensor was lowered directly onto the soil surface, the soil water would evaporate unevenly as some would be trapped under the sensor. A sensor directly on the soil would change the chamber's air relative humidity and result in an inaccurate reading from the KGM sensor. To eliminate these issues from the orientation of the sensor, the vertical set-up was studied next.

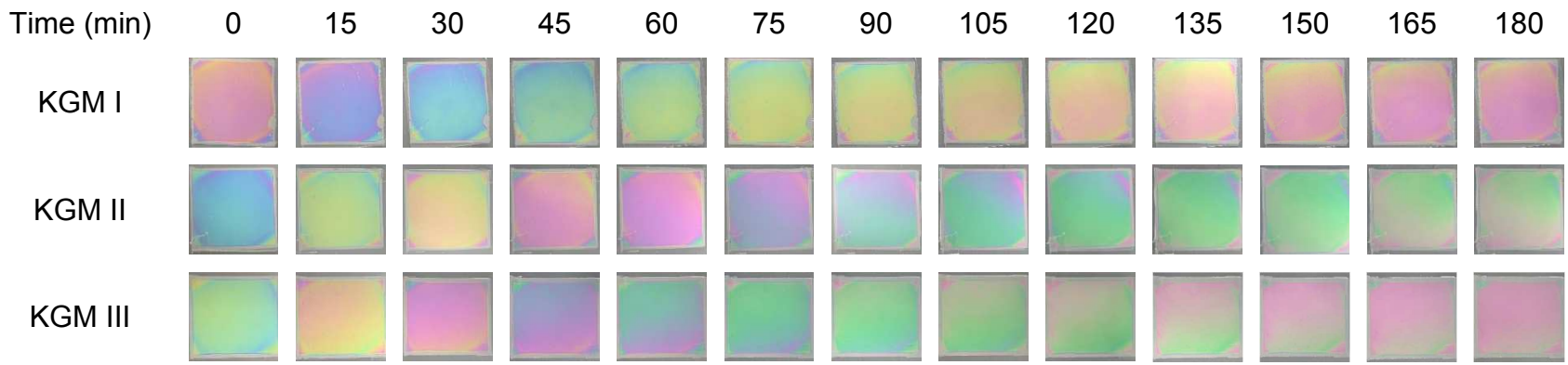

Figure 1.11. KGM I, II and III in 100 x 50 PYREX soil chamber with 20% VWC.

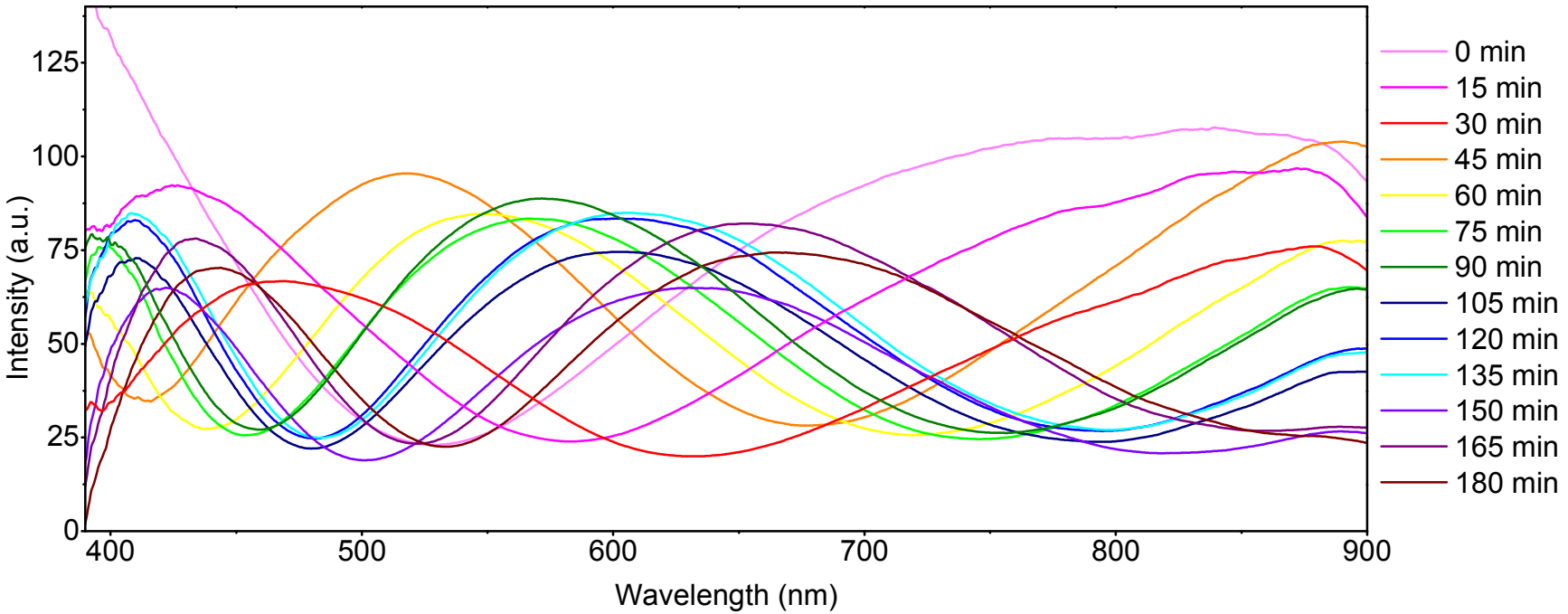

Figure 1.12. KGM I reflectance spectra in 20% VWC soil chamber.

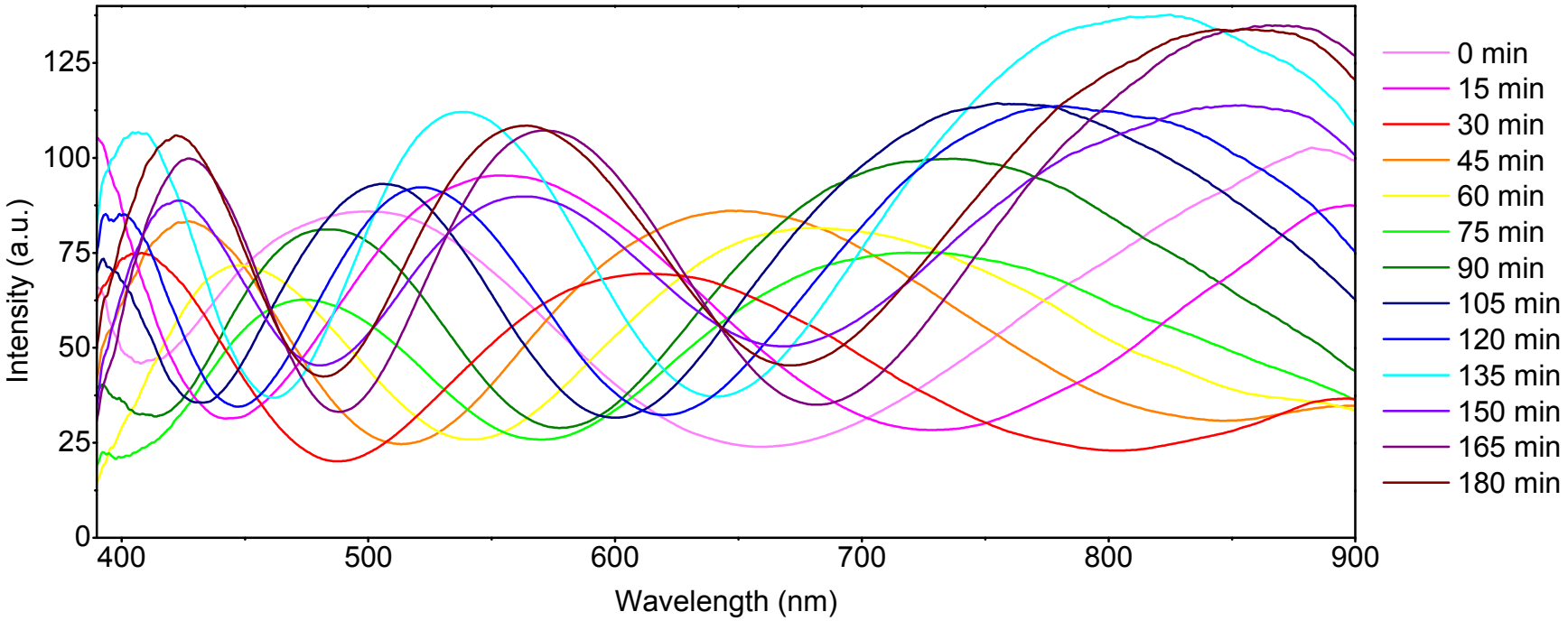

Figure 1.13. KGM II reflectance spectra in 20% VWC soil chamber.

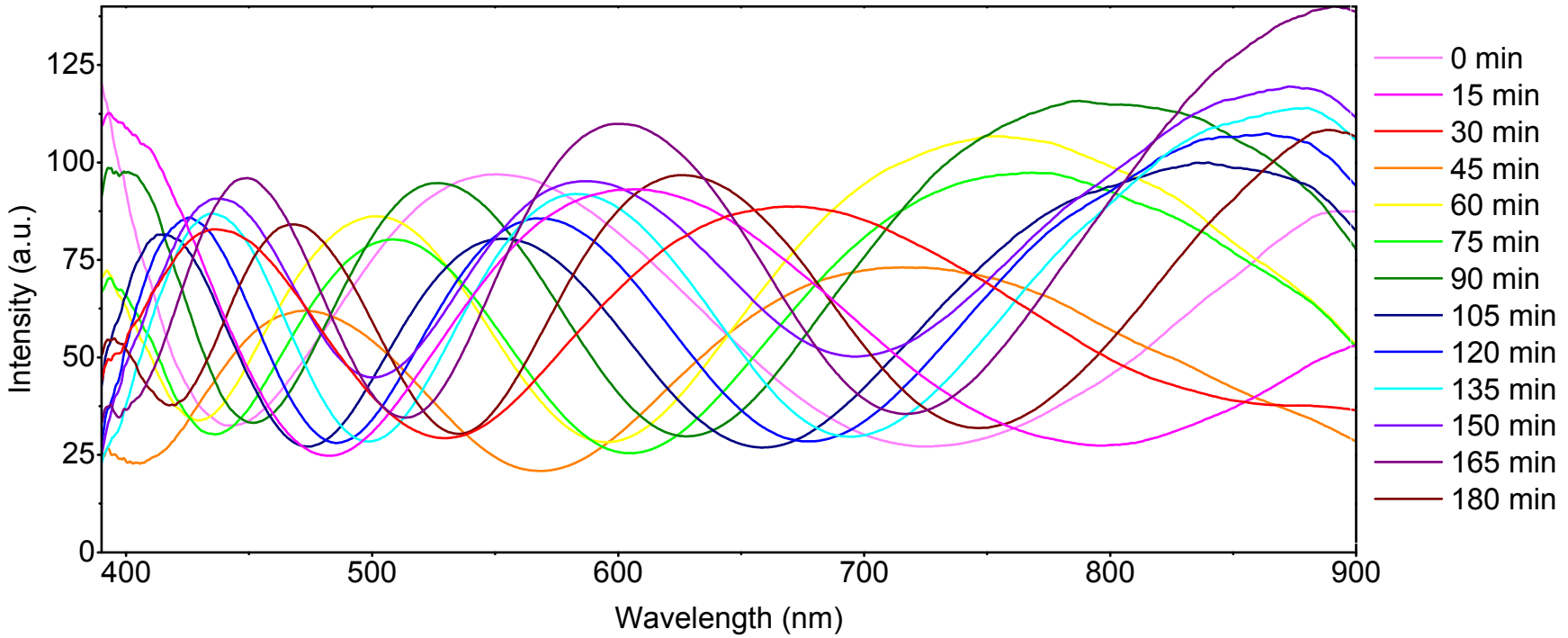

Figure 1.14. KGM III reflectance spectra in 20% VWC soil chamber.

	Order of Interference	0 min	15 min	30 min	45 min	60 min	75 min	90 min	105 min	120 min	135 min	150 min	165 min	180 min
KGM I	1st	828	-	-	-	-	-	-	-	-	-	-	-	-
	2nd	-	426	468	518	548	567	573	602	603	607	633	653	665
	3rd	-	-	-	-	-	398	398	411	411	409	422	433	443
KGM II	2nd	498	554	614	650	680	723	734	760	793	821	854	868	857
	3rd	-	-	408	426	448	474	483	506	522	537	563	571	563
	4th	-	-	-	-	-	-	-	-	401	406	423	427	423
KGM III	2nd	549	605	669	716	753	765	794	840	-	-	-	-	-
	3rd	-	-	437	472	501	508	526	553	569	583	587	600	626
	4th	-	-	-	-	-	-	398	416	426	435	438	488	468

Table 1.3. Reflection peak wavelengths (nm) for KGM I, II, and III during exposure to 20% VWC soil chamber.

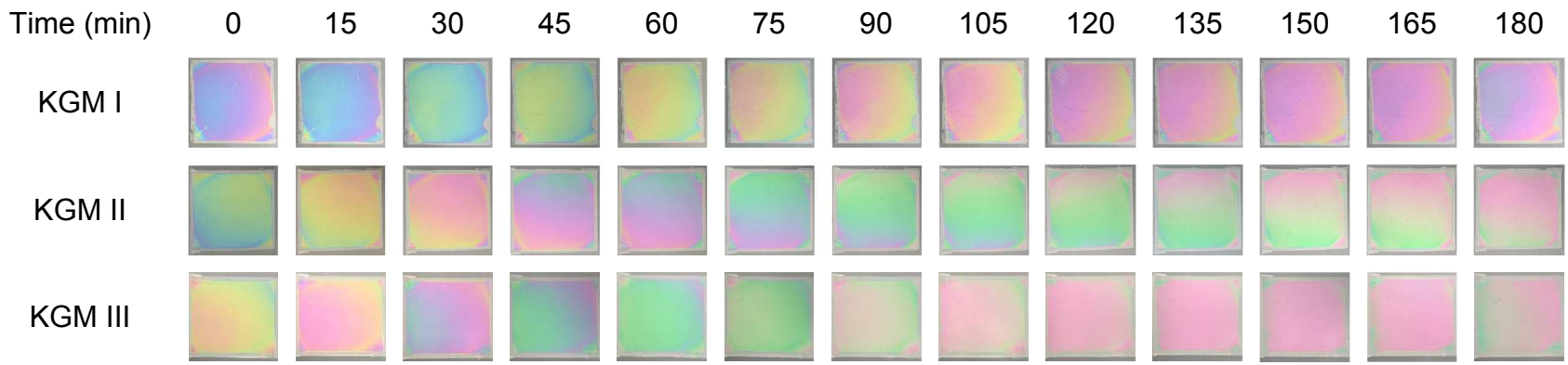

Figure 1.15. KGM I, II and III in 100 x 50 PYREX soil chamber with 30% VWC.

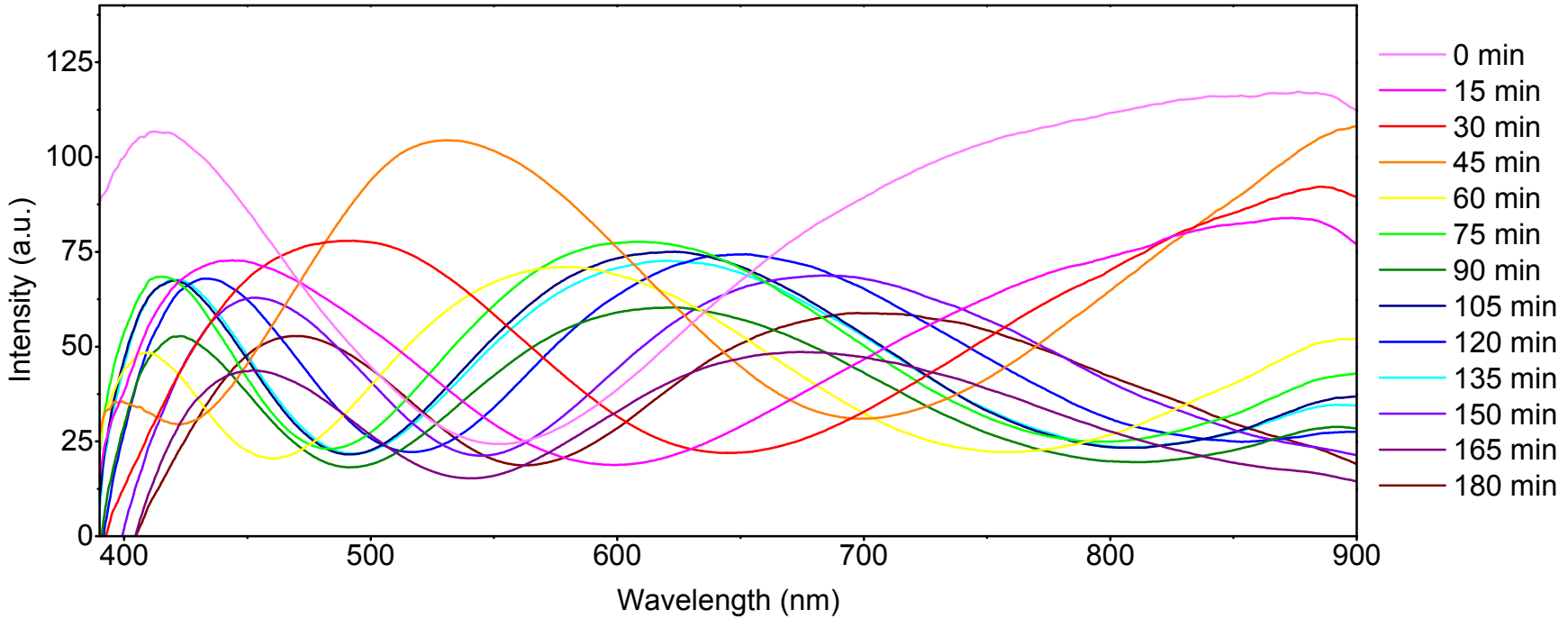

Figure 1.16. KGM I reflectance spectra in 30% VWC soil chamber.

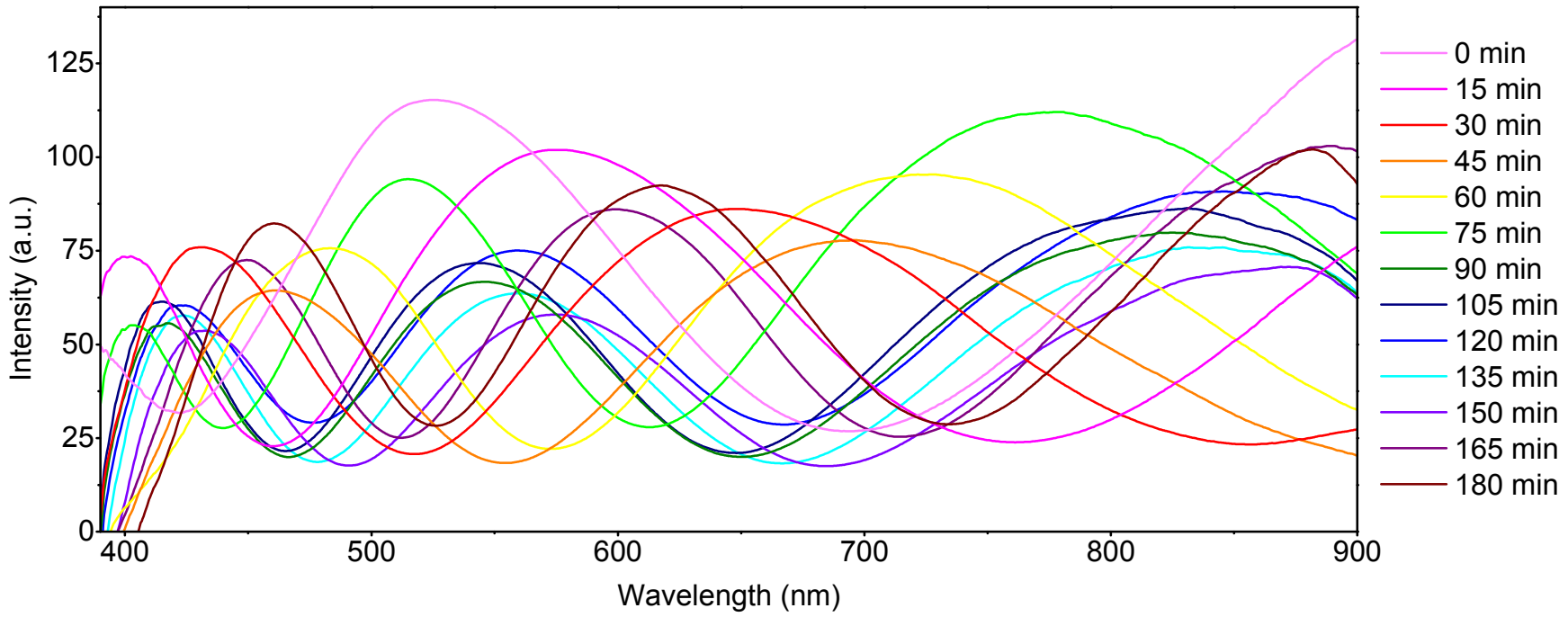

Figure 1.17. KGM II reflectance spectra in 30% VWC soil chamber.

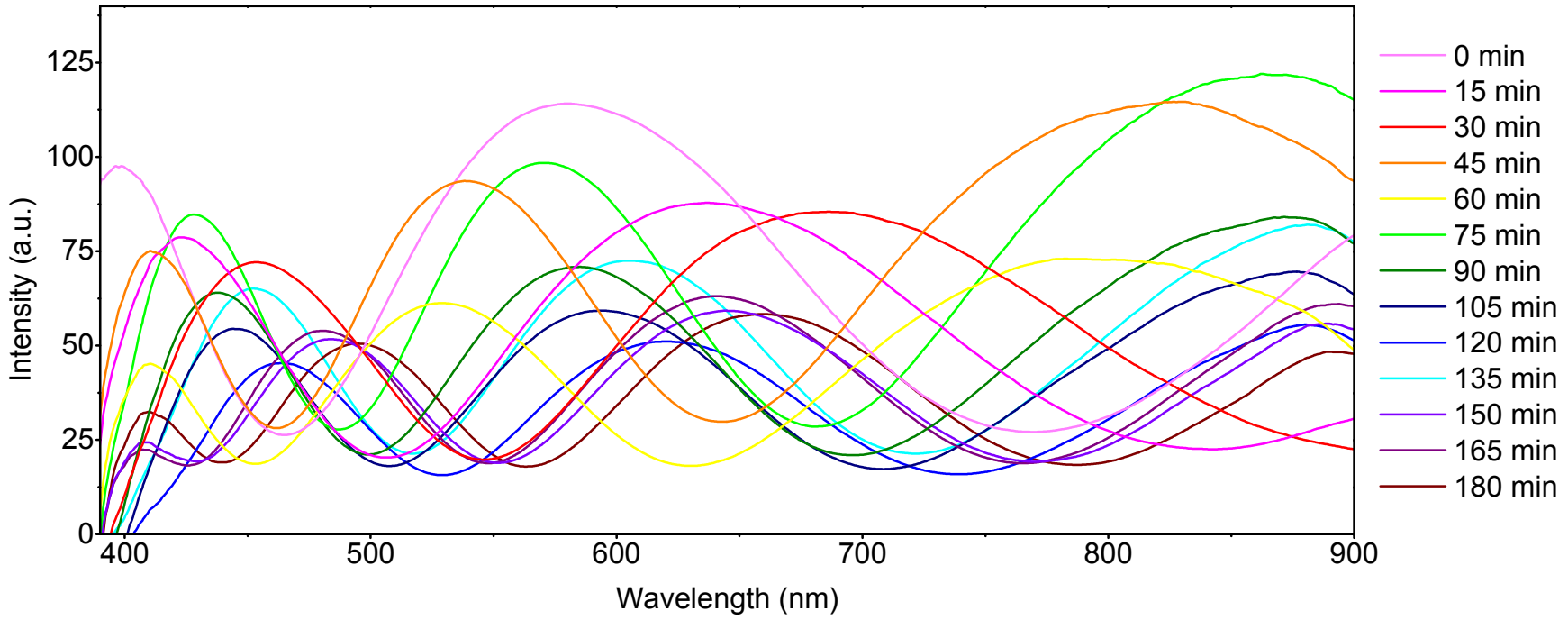

Figure 1.18. KGM III reflectance spectra in 30% VWC soil chamber.

	Order of Interference	0 min	15 min	30 min	45 min	60 min	75 min	90 min	105 min	120 min	135 min	150 min	165 min	180 min
KGM I	2nd	414	444	493	531	579	609	620	621	651	622	683	675	702
	3rd	-	-	-	-	409	415	422	420	434	421	453	452	470
KGM II	2nd	526	575	651	695	721	778	829	827	853	842	-	-	-
	3rd	-	-	431	461	483	516	546	544	560	560	575	600	618
	4th	-	-	-	-	-	404	417	415	423	424	432	449	460
KGM III	2nd	580	637	687	828	804	865	-	-	-	-	-	-	-
	3rd	399	423	454	539	530	571	584	595	621	606	646	641	660
	4th	-	-	-	411	411	429	438	445	464	453	484	480	495
	5th	-	-	-	-	-	-	-	-	-	-	-	-	410

Table 1.4. Reflection peak wavelengths (nm) for KGM I, II, and III during exposure to 30% VWC soil chamber.

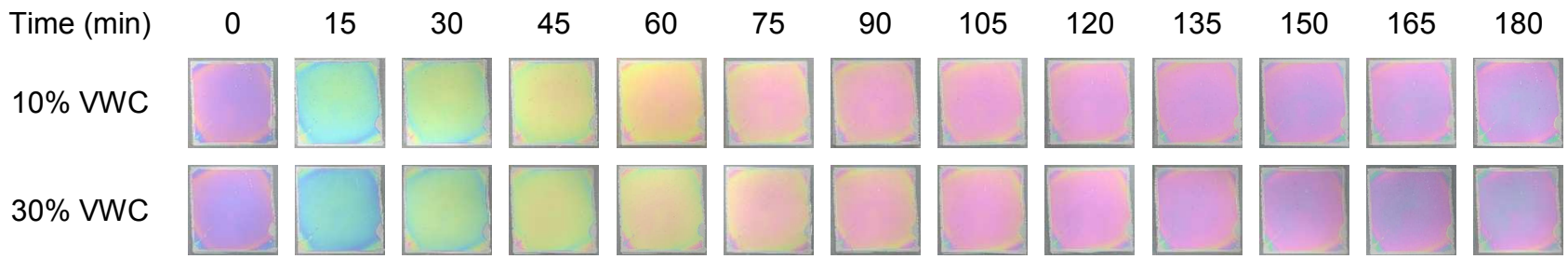

Figure 1.19. KGM I in 100 x 50 PYREX soil chambers of 10% and 30% VWC.

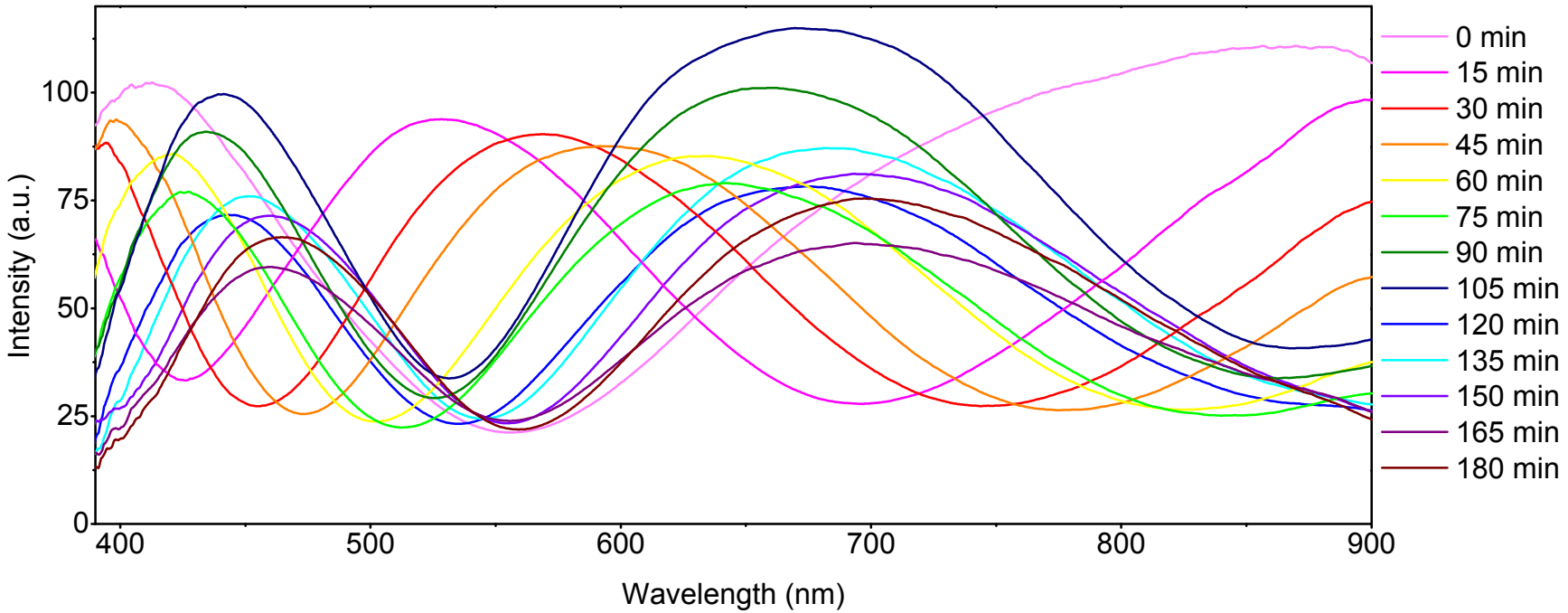

Figure 1.20. KGM I reflectance spectra in 10% VWC soil chamber.

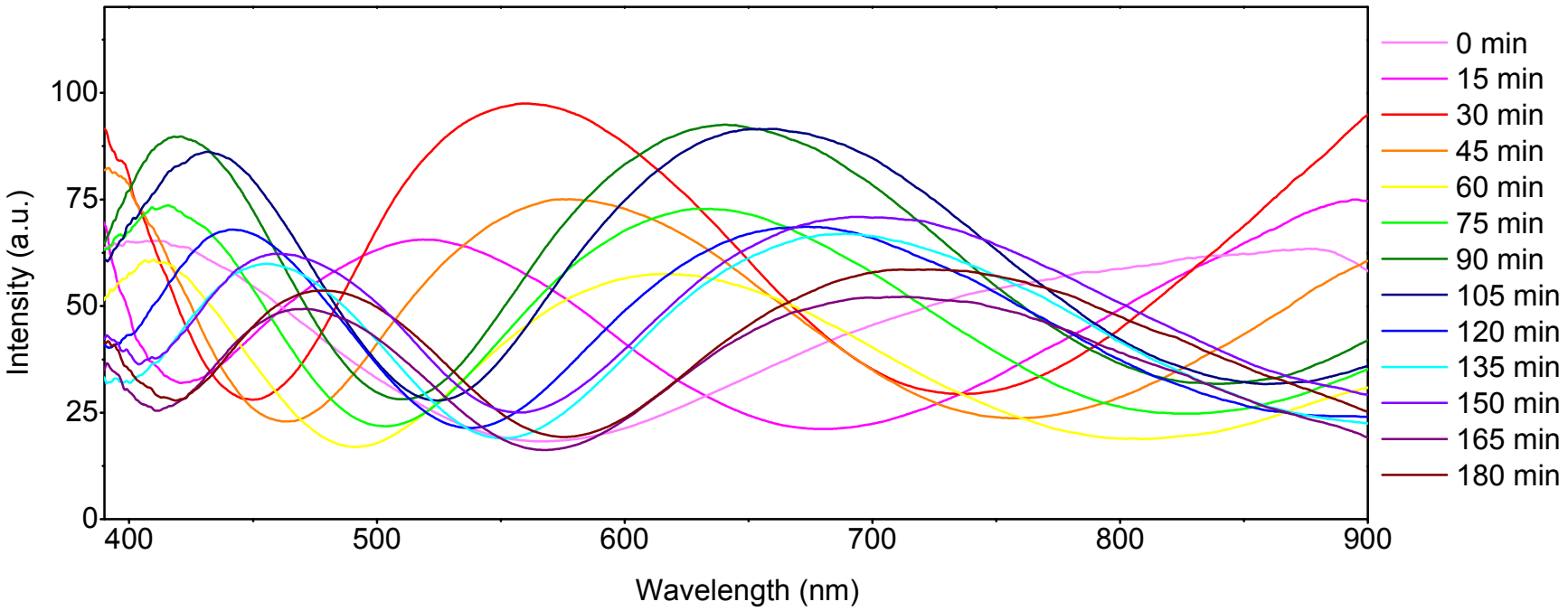

Figure 1.21. KGM I reflectance spectra in 30% VWC soil chamber.

	Order of Interference	0 min	15 min	30 min	45 min	60 min	75 min	90 min	105 min	120 min	135 min	150 min	165 min	180 min
10% VWC	2nd	412	528	568	597	634	644	660	671	675	686	697	698	701
	3rd	-	-	-	399	420	427	435	441	443	452	460	462	464
30% VWC	2nd	409	520	560	579	617	633	641	659	672	689	697	712	720
	3rd	-	-	-	-	411	415	420	431	443	456	461	471	479

Table 1.5. Reflection peak wavelengths (nm) for KGM I during exposure to 10% and 30% VWC soil chambers.

1.3.3 Vertical Set-Up

To simulate at-home pots of soil and increase the sensitivity of the KGM sensor, the orientation of the sensor was changed to vertical. This set-up of the soil sensor was able to distinguish between 10, 20, 30, and 40% VWC over time. Any moisture in the soil was represented as a colorful dynamic water vapor front line on the KGM sensor. Front line readings at time 0 hours are indistinguishable from each other as the soil had only been sitting with water for 20 minutes (Figures 1.22, 1.24, and 1.26). But over time, the sensors proved to be sensitive to different VWC's.

To relate the front line to estimated VWC at the time of data collection, the front line and estimated VWC over time must be compared. By doing so, the KGM will be able to report the wilting point of the soil (~10% VWC) to signal that the soil needs watering. Tables 1.9. 1.11, and 1.13 summarize the lowest estimated average VWC per KGM sensor by way of front line height.

KGM I showed a decrease in front line over time (Figure 1.22). However, the sensor at 20% VWC is an outlier from the rest of the soil samples. This sensor tracked a front line even after 30% VWC soil sensor was reporting none. This outlier may be due to higher room humidity at the time of data collection (Table 1.6). Setting up all four soil samples to run simultaneously will most likely eliminate this outlier. As seen in Figure 1.23 b and c, the soil sample water contents and masses decreased in a linear fashion. This shows that the slight difference in room humidity did not affect the soil water evaporation. Therefore, the KGM sensor's high sensitivity to different RH's would be the reason for the outlier. Another possibility for the outlier could root from the length of video taken. Since only two minutes of video were recorded, perhaps a higher front line

was missed in 30% VWC. To eliminate this possibility, videos of length 5 minutes could be recorded to allow for more time to identify the highest front line.

KGM II had much higher front lines over time when compared to KGM I and KGM III (Figure 1.24). In particular, 10, 30, and 40% VWC include the highest front lines. This can be related back to the room's relative humidity during data collection (Table 1.8). It is seen that up until hour 53, the RH for 10, 30, and 40% VWC was considerably higher than that of 20% VWC. Again, running all samples simultaneously may remove this effect. However, an at-home scenario will not have steady humidity. KGM I and II have shown that the vertical set-up may not be the most reliable for soil moisture measurements over time. Since ambient humidity affects data collection, isolating the KGM to the soil surface humidity with a small chamber around the sensor may eliminate this effect. Then, the KGM sensors would be able to exclusively measure soil surface humidity in a way that is more applicable to at-home use.

KGM III is an excellent example of how to use front line determination to follow the soil moisture level over time (Figure 1.26). The four soil samples were able to run simultaneously over time, and the front line height is related directly to the soil moisture (Figure 1.27 a). At 24 hours, the 10 and 20% VWC samples were distinguished from the rest. At 48 hours, the 30 and 40% VWC samples reported differing front lines. In relating the front line to estimated VWC at the time of data collection (Table 1.13), this sensor illustrated the best direct relationship.

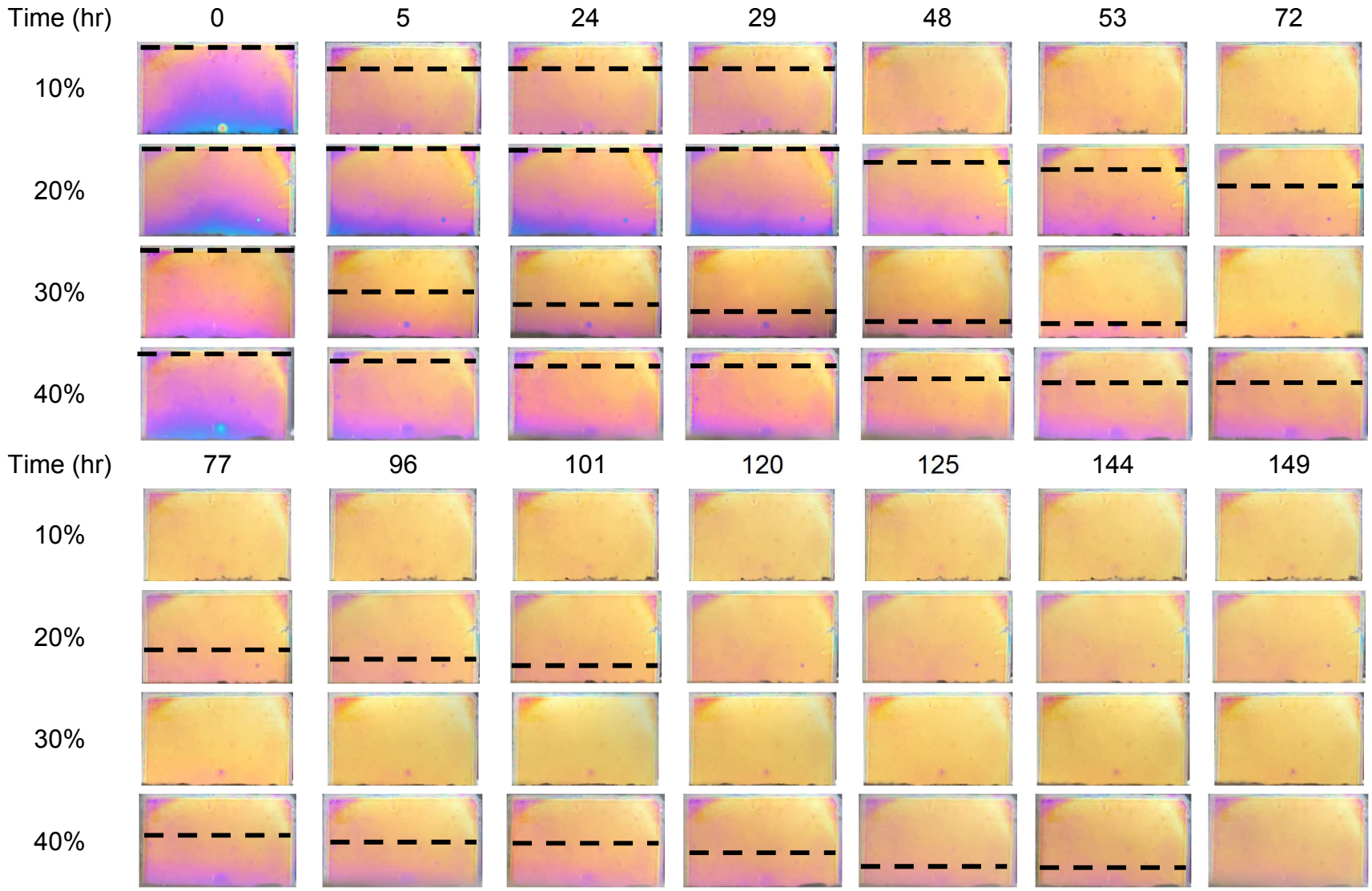

Figure 1.22. KGM I vertical in soil of 10-40% VWC. Front line is labeled with dashed line.

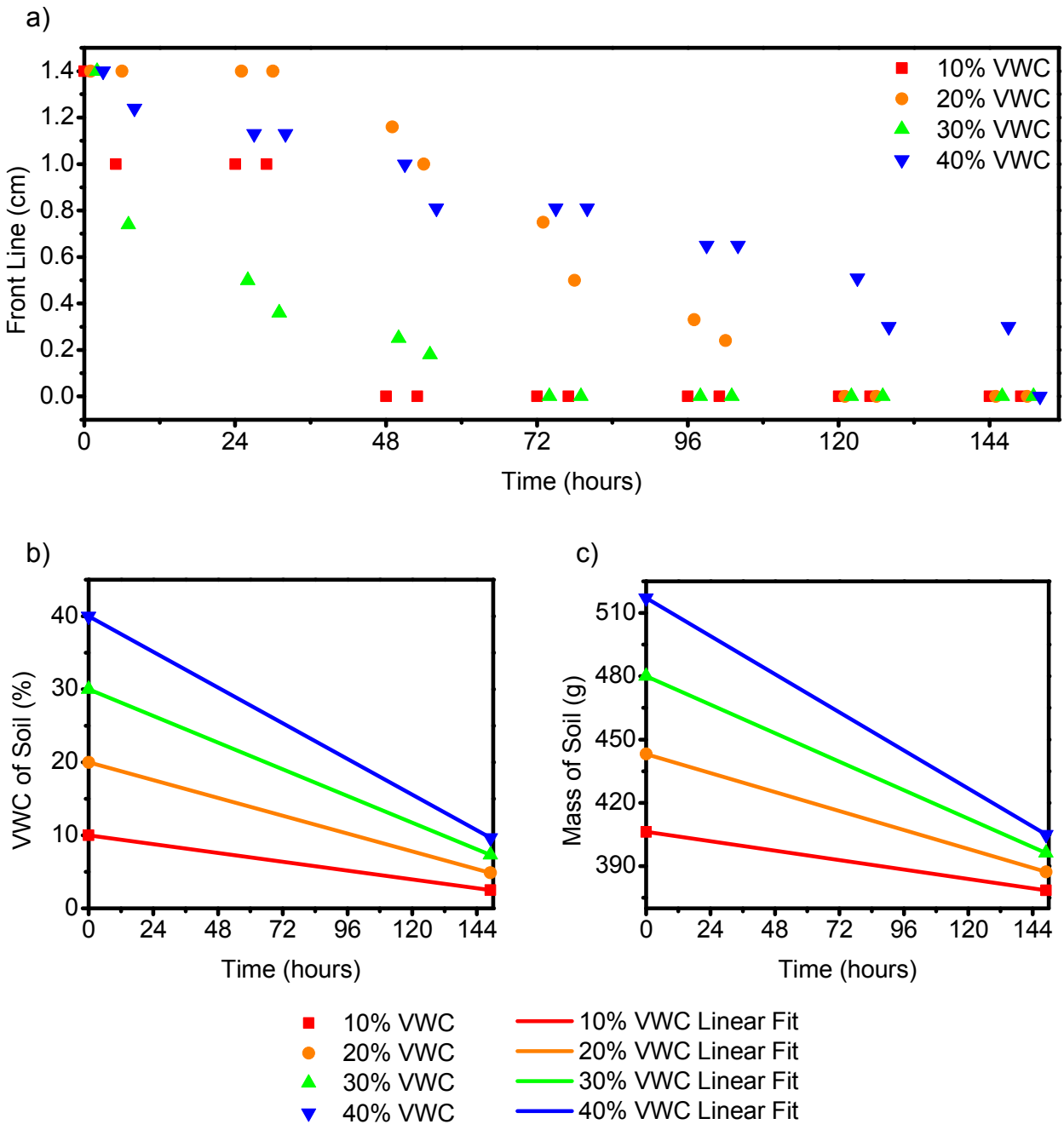

Figure 1.23. a) Front line of the KGM I sensor gradient over time. b) VWC of the soil over time. Measurements taken at time 0 and 149 hours. c) Mass of the soil over time. Measurements taken at time 0 and 149 hours.

	10%, 30%, 40% VWC		20% VWC	
Time (hr)	Temperature (°C)	RH%	Temperature (°C)	RH%
0	23.2	14	23.1	21
5	23.4	14	22.8	19
24	23.8	17	22.9	27
29	24.0	17	22.9	28
48	23.9	17	23.2	23
53	24.0	17	23.3	23
72	22.8	14	23.2	17
77	22.9	14	23.2	17
96	22.5	17	23.6	17
101	22.9	14	23.1	17
120	23.1	14	22.9	17
125	23.5	17	22.9	17
144	24.3	17	23.8	17
149	24.5	17	24.0	17

Table 1.6. Room temperature and relative humidity over time for KGM I vertical soil studies.

Sample	Time (hr)	Front Line (cm)	Average Front Line (cm)	Estimated VWC%	Average Estimated VWC%
10% VWC	5	1.0	0.94	10	21
20% VWC	53	1.0		15	
30% VWC	5	0.74		30	
40% VWC	48	1.0		30	

Table 1.7. Average front line of KGM I in loam soil between wilting point and field capacity.

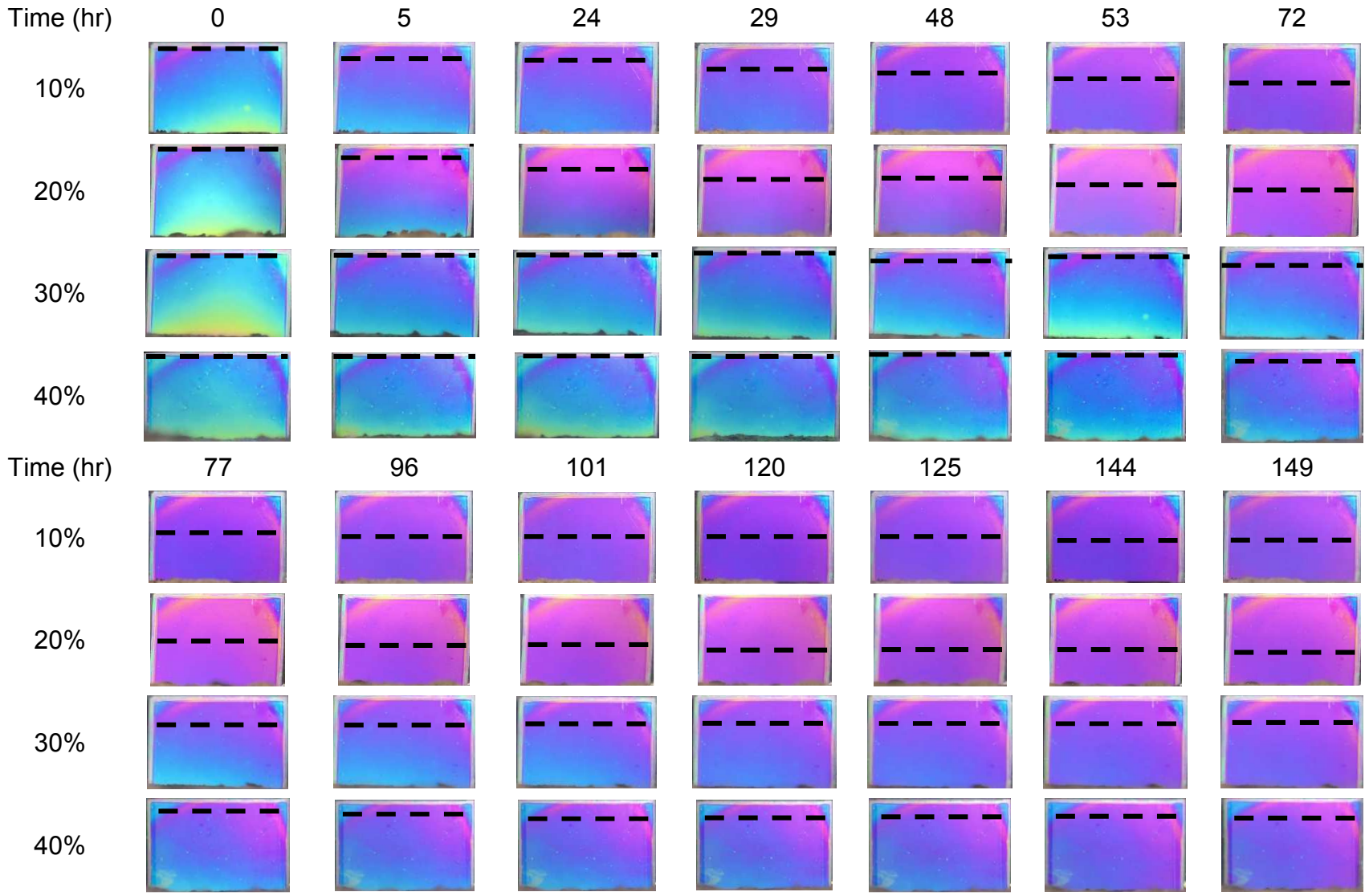

Figure 1.24. KGM II vertical in soil of 10-40% VWC. Front line is labeled with dashed line.

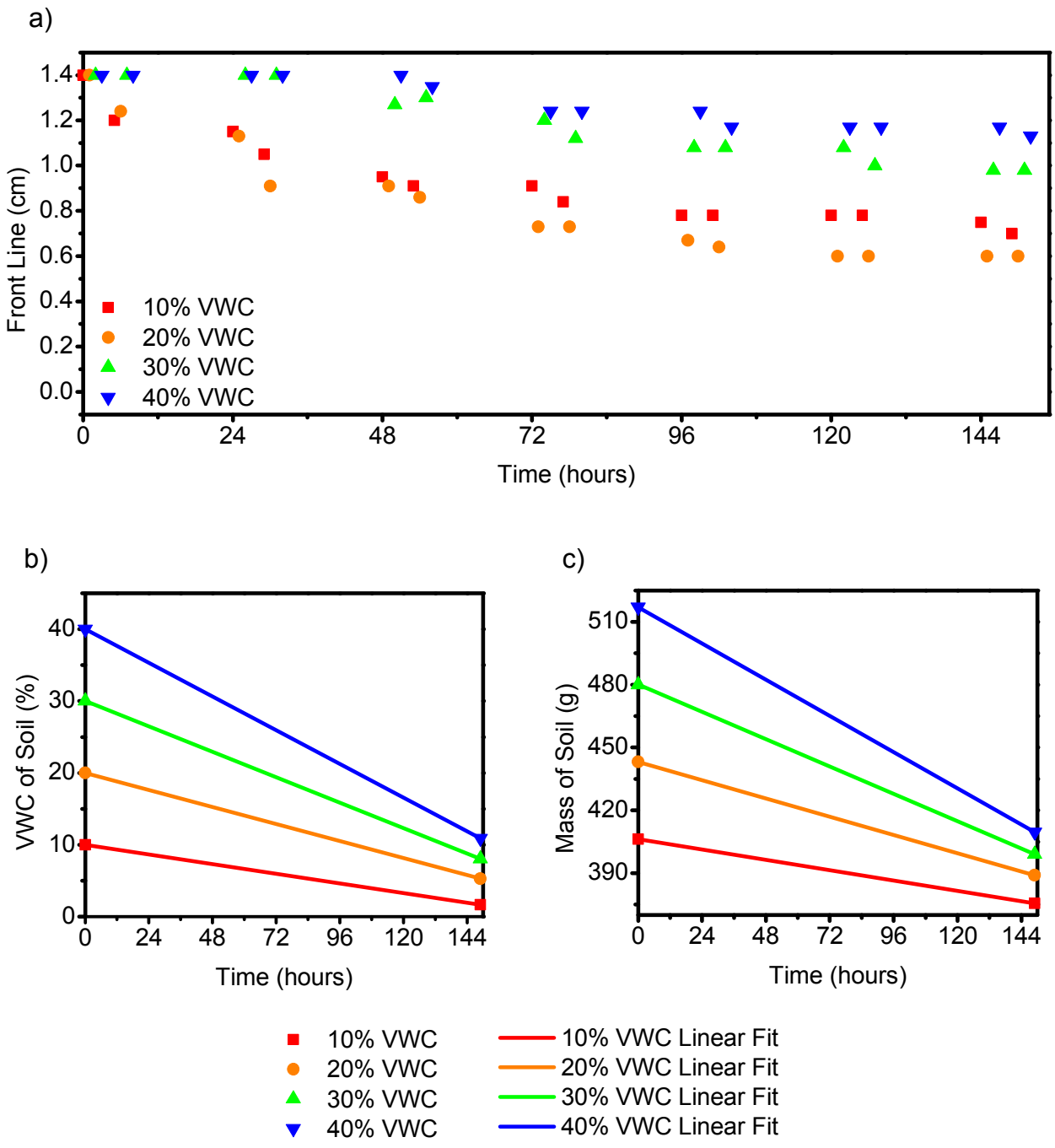

Figure 1.25. a) Front line of the KGM II sensor gradient over time. b) VWC of the soil over time. Measurements taken at time 0 and 149 hours. c) Mass of the soil over time. Measurements taken at time 0 and 149 hours.

	10%, 30%, 40% VWC		20% VWC	
Time (hr)	Temperature (°C)	RH%	Temperature (°C)	RH%
0	23.1	21	23.2	14
5	22.8	19	23.4	14
24	22.9	27	23.8	17
29	22.9	28	24.0	17
48	23.2	23	23.9	17
53	23.3	23	24.0	17
72	23.2	17	22.8	14
77	23.2	17	22.9	14
96	23.6	17	22.5	17
101	23.1	17	22.9	14
120	22.9	17	23.1	14
125	22.9	17	23.5	17
144	23.8	17	24.3	17
149	24.0	17	24.5	17

Table 1.8. Room temperature and relative humidity over time for KGM II vertical soil studies.

Sample	Time (hr)	Front Line (cm)	Average Front Line (cm)	Estimated VWC%	Average Estimated VWC%
10% VWC	29	1.05	1.11	9	14
20% VWC	24	1.13		17	
30% VWC	77	1.12		19	
40% VWC	149	1.13		11	

Table 1.9. Average front line of KGM II just above loam soil wilting point.

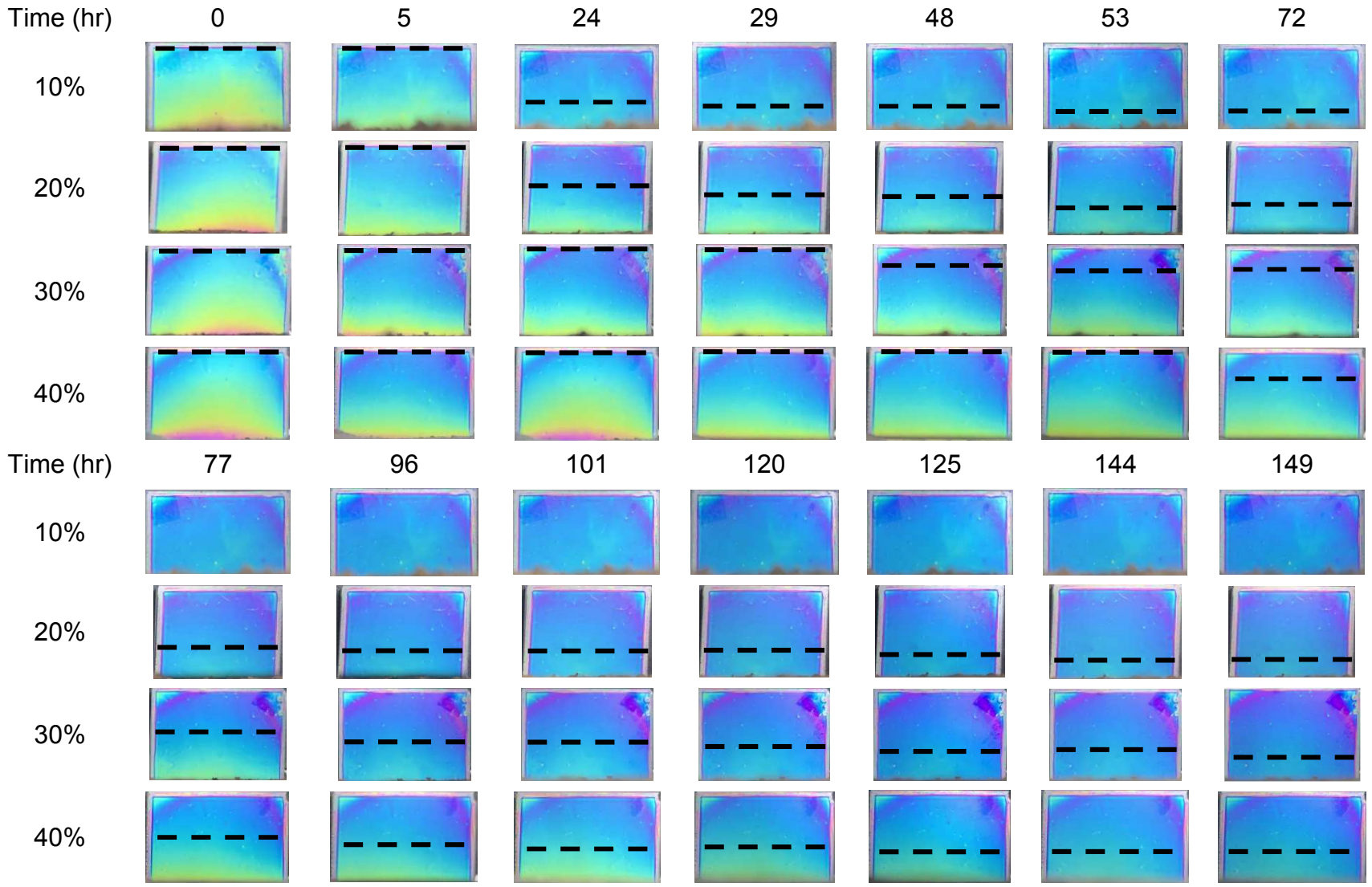

Figure 1.26. KGM III vertical in soil of 10-40% VWC. Front line is labeled with dashed line.

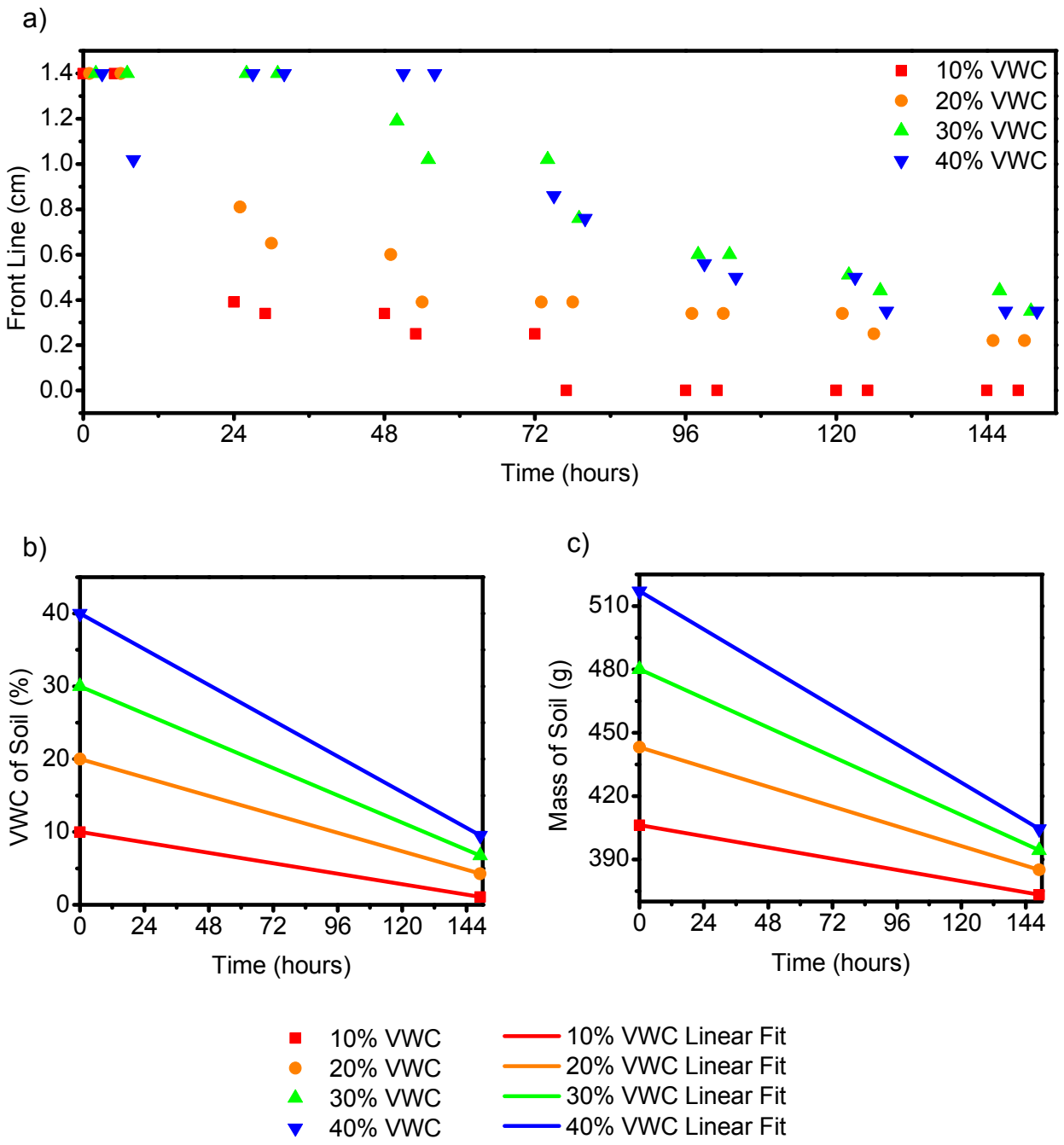

Figure 1.27. a) Front line of the KGM III sensor gradient over time. b) VWC of the soil over time. Measurements taken at time 0 and 149 hours. c) Mass of the soil over time. Measurements taken at time 0 and 149 hours.

	10%, 20%, 30%, 40% VWC	
Time (hr)	Temperature (°C)	RH%
0	25.8	17
5	25.3	17
24	25.1	17
29	24.9	17
48	24.3	17
53	24.1	18
72	24.1	17
77	24.1	17
96	24.7	17
101	23.5	17
120	23.4	17
125	23.2	17
144	23.2	17
149	23.0	17

Table 1.10. Room temperature and relative humidity over time for KGM III vertical soil studies.

Sample	Time (hr)	Front Line (cm)	Average Front Line (cm)	Estimated VWC%	Average Estimated VWC%
10% VWC	25.8	0.40	0.40	8	11.5
20% VWC	25.3	0.39		14	
30% VWC	25.1	0.44		10	
40% VWC	24.9	0.35		14	

Table 1.11. Average front line of KGM III at loam soil wilting point.

1.4 Conclusion

The vertical responsive interference coloration sensor with KGM is effective in detecting and monitoring soil moisture levels over time, easily seen with KGM III results. The KGM sensors are good competition for low-cost soil moisture sensors used with indoor plants because of their sensitive response to moisture changes in soil and ability to remain placed in soil long term. By simply viewing the RIC sensor each day and estimating the water vapor front line, the user will not only understand the moisture content of the soil, but also if it needs watering. The KGM sensors have each shown to have a unique front line height at which they measure loam soil wilting point. This height will inform the user of when to water before the soil has become too dry, therefore reducing the stress on the plant. Since the soil water's evaporation is not uniform, a 1-2 minute viewing window is best to determine the RIC sensor's most dramatic color change and highest front line. To eliminate room ambient humidity impact on the KGM sensor, a small chamber around the sensor should be investigated and implemented.

In future studies, soil composition effect may be analyzed. Loam soil used in this study is most common with house plants and has both moderate water capacity and soil particle size. Although soil type effects soil moisture capacity, it is not expected to effect the efficiency of the RIC soil moisture sensor. Calibration may be needed for different soil types (10% VWC is permanent wilting point for loam soils but field capacity for sandy soils[3]), but the sensor's effectiveness would not be altered. For any soil sample at the highest water content, the RIC sensor will be the most colorful with the highest front line when compared to the soil's lowest water content. In addition to soil composition effect, the reproducibility of the vertical soil sensor must be explored. It has

proven to be sensitive to different VWC's, but continuing studies will further confirm the positive results from vertical set-up studies.

Chapter 2: Breath Monitor

2.1 Background

2.1.1 Breath Characteristics

Breathing patterns and respiratory rate are vital signs measured in healthcare environments and can tell much about a person's health. Respiratory rate can detect crucial changes in health status and has been found to give more information than heart rate when detecting changes in critically ill patients.[10] The respiratory rate is measured by counting the number of breaths for one minute to determine the patient's breath per minute (bpm).[11] One breath is comprised of one inhale and one exhale. A typical breathing rate of an adult is about 12-18 bpm.[11] The exhale of a breath has previously been assumed to reach 100% RH. However, breath analysis has shown the typical exhale to fall short of 100% RH and only reach about 89-97% RH.[12]

2.1.2 Current Relative Humidity Breath Monitors

Typical sensors for breath monitoring in clinical practice analyze the composition of exhaled gases and high relative humidity from 89-97% when measuring respiratory rate.[13] Few sensors have been developed which focus solely on the humidity level of the exhale instead of the gas composition of the exhale breath. Breath humidity monitoring is important to be able to reveal dehydration status in an individual.[14] Current developments are electronic-based sensors which measure voltage and/or current in the exhaled breath to determine breathing pattern and exhaled RH. Duan et al.[15] developed a paper-based humidity sensor with aluminum wire electrodes to measure voltage signal from humid air through conduction. This sensor was placed in a 3M

9001V mask within 2 cm of the mouth and most sensitive to high RH ranges (72.0-91.5%). But with slow response and recovery speeds, the sensor seems to be appropriate only for slow breath rates in a relaxed body state.

Yan et al.[16] developed a humidity sensor composed of supramolecular ionic material on Au electrodes for respiration monitoring. Holding the sensor 4 cm from the mouth, current was recorded from breathing and related back to corresponding RH values. The sensor exhibited fast response times of less than 1 second but only reported RH values within the range of 0-86% from nose and mouth breathing.

A humidity sensor comprised of silicon nanocrystal film with Ti and Au electrodes to measure current as a result of human breath was developed by Kano et al.[17] This sensor performed within the RH range of 8-83% during water vapor tests. Holding the sensor 20 cm from the mouth, exhales were recorded intermittently, only reaching the range of 34-39% RH. This allowed for visualizations of exhales by current vs. time, but not at accurate human exhale humidity levels.

Mogera et al.[14] developed supramolecular nanofibers to determine RH intensity and human breath patterning by measured current. The sensor was applied to human breath in an oxygen mask 3.5 cm from the nose and could easily track fast or slow breath. The average RH recorded for an inhale was 20.2% and for an exhale 88.8%. Tracking faster breathing rates is essential for health purposes, but the narrow RH range the sensor performed at falls short of what is necessary of a breath sensor.

Many other breath sensors have been applied to various scenarios with differing breathing rates.[18,19,20,21] Scenarios studied include breath from physical activity, asthma, respiratory arrest, deep breathing, sleep, and breath from a smoker and an ill person.

These sensors reported response/recovery times of approximately 1 second each with the goal to measure respiratory rate and depth. Although the sensors responded quickly to various breath rates and illustrate the breath rate and depth, the RH of the breath during these scenarios was not observed.

2.1.3 Breath Monitors with Responsive Interference Coloration

The challenge of a breath monitor is to distinguish between different breath states, as different body states and health conditions lead to changes in the breath pattern.[19] In our breath monitoring study with an RIC sensor, we apply a normal breath state while sitting, standing, after a 12 hour fast, and after vigorous exercise. Responsive interference coloration is applied to determine the breathing pattern, respiratory rate, and relative humidity by facile colorimetric analysis. These variables are determined by simply viewing the sensor during a 60 second period. This easy access makes the RIC breath monitor an excellent candidate for at-home use.

2.2 Experimental

2.2.1 Materials

Responsive interference coloration sensors with konjac glucomannan were prepared as stated previously in Section 1.2.2. An oxygen mask (Salter Labs Adult Elongated Mask) was purchased from Amazon. Double- and single-sided 3M Scotch Tape was purchased from Amazon.

2.2.2 Breathing Tests

First, a control experiment was performed with no sensor in the oxygen mask. The oxygen mask was donned while sitting and video was recorded for two minutes

while breathing though the nose. The left side of the mask was focused on as it is the same side the sensor would be placed (Figure 2.1).

Then, the RIC sensor was added to the mask to observe its response to different breathing scenarios. To ensure best reflection, the sensor was secured with double sided tape on a square of black paper, then inserted into the oxygen mask. The sensor was taped to the inside of the left side with space between the wall of the mask and front of the RIC to allow for air flow, about 5 cm from the nose (Figure 2.1 a).

a) b)

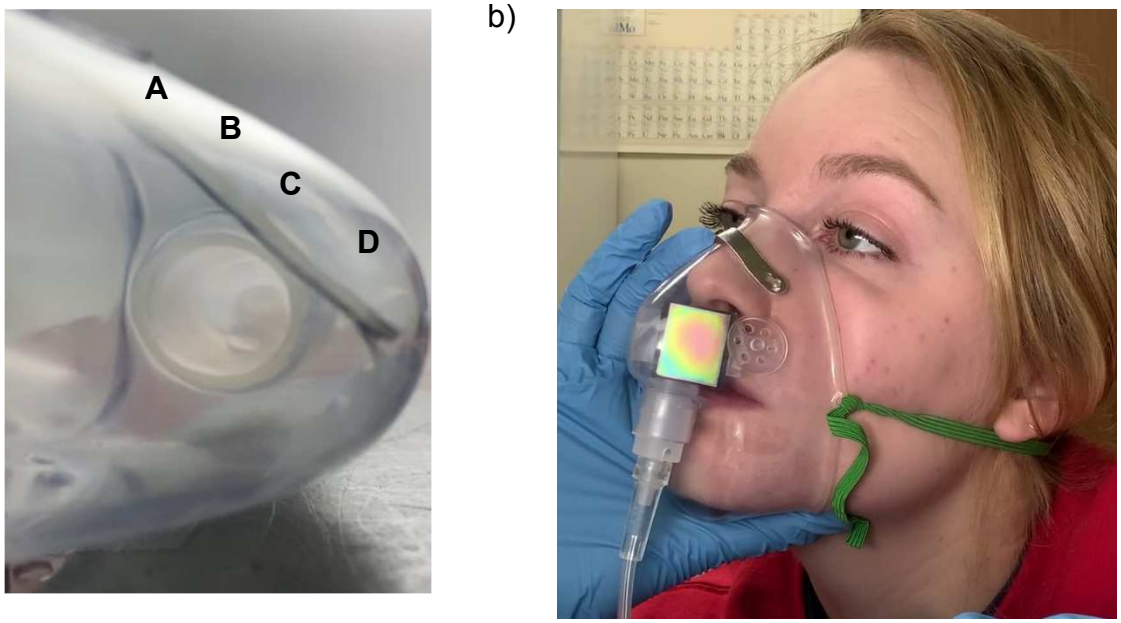

Figure 2.1. a) Sensor placement in oxygen mask. Distances from the mask are marked as follows: A = 0.0 mm. B = 1.0 mm. C = 2.0 mm. D = 3.0 mm. b) Image of oxygen mask with adhered sensor on the face. Sensor is about 5 cm from the nose.

While wearing the oxygen mask, video was recorded with an iPhone XR for 1-2 minutes with KGM I, II, and III in four different scenarios. These tests consisted of breathing through the nose while sitting, standing, after a 12 hour fast, and after exercising. In the sitting scenario, the “back side” and “front side” of the sensor were

tested to determine best placement for good RH determination (Figure 2.2). This position would determine if the KGM polymer needed closer contact with the humidity source (nose). The color observed on the “back side” is the compliment of the “front side” as seen on the color wheel in Figure 2.2 e. All other scenarios were performed using the “front side” of the sensor.

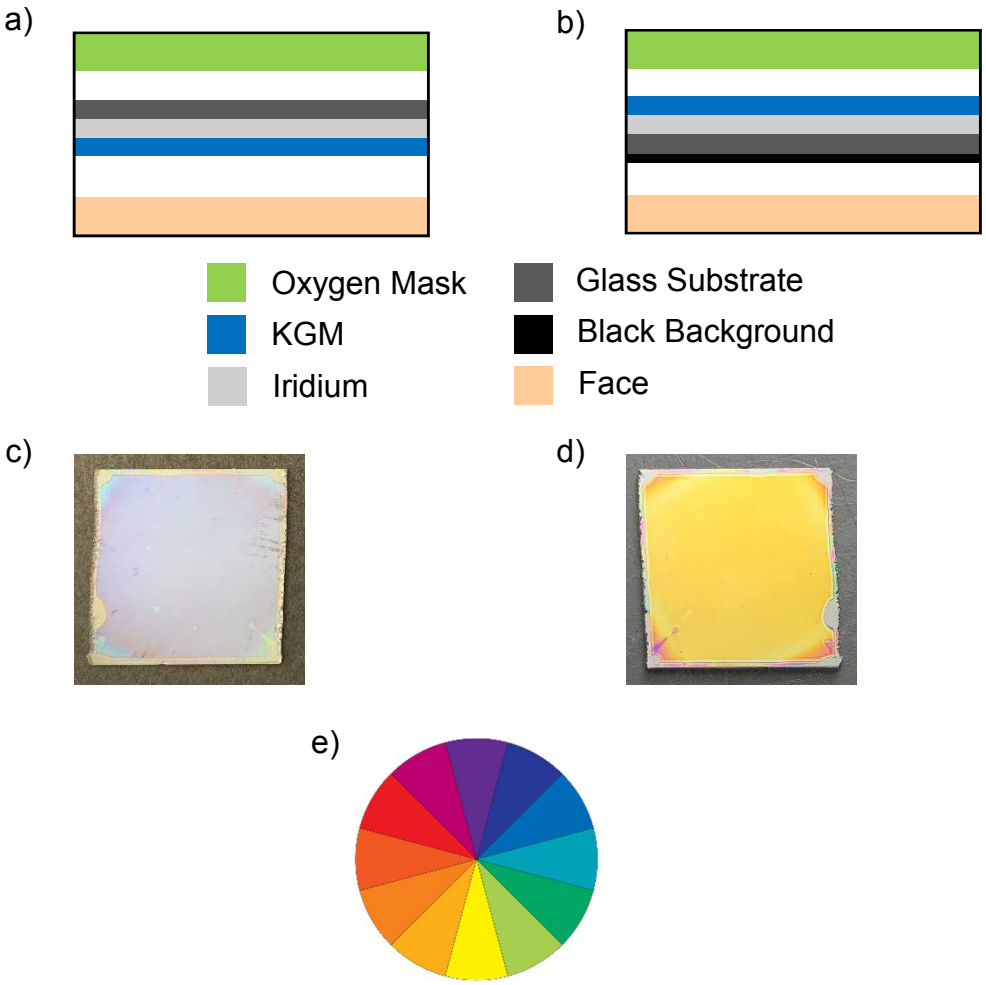

Figure 2.2. Schematic representations of sensor in oxygen mask with a) back side facing viewer and b) front side facing viewer. c) Photograph of the back side of KGM I facing viewer. d) Photograph of the front side of KGM I facing viewer. e) Standard color wheel. Every color has its compliment across from it on the wheel.

The fasting scenario was performed sitting. No food or water had been consumed during a 12 hour fast, including overnight. The exercising scenario involved jogging in place for five minutes, then immediately donning the mask with sensor to record breathing while standing. After the recording of a scenario, each video was cropped to zoom in on the RIC to watch its pattern and color changes.

2.2.3 Reflectance Spectroscopy for Color Confirmation

Reflectance spectroscopy was performed with a fiber optic spectrometer (USB2000+, Ocean Optics) with incident light perpendicular to the RIC while wearing the mask sitting down. Dynamic reflection spectra were acquired continuously with the interval time of 10 ms. Spectra were recorded through three breath cycles.

2.2.4 RGB Analysis with MATLAB

MATLAB was used to analyze each video and extract the RGB values from each frame. To prepare a video for RGB analysis, the view was cropped to zoom into a 1 x 1 square in the center of the RIC sensor. The main flow of the code is outlined in Figure 2.3. Using the video's frames per second (fps) value, the resulting data was converted to RGB value vs. time (seconds). MATLAB analysis reported RGB values every 30 ms.

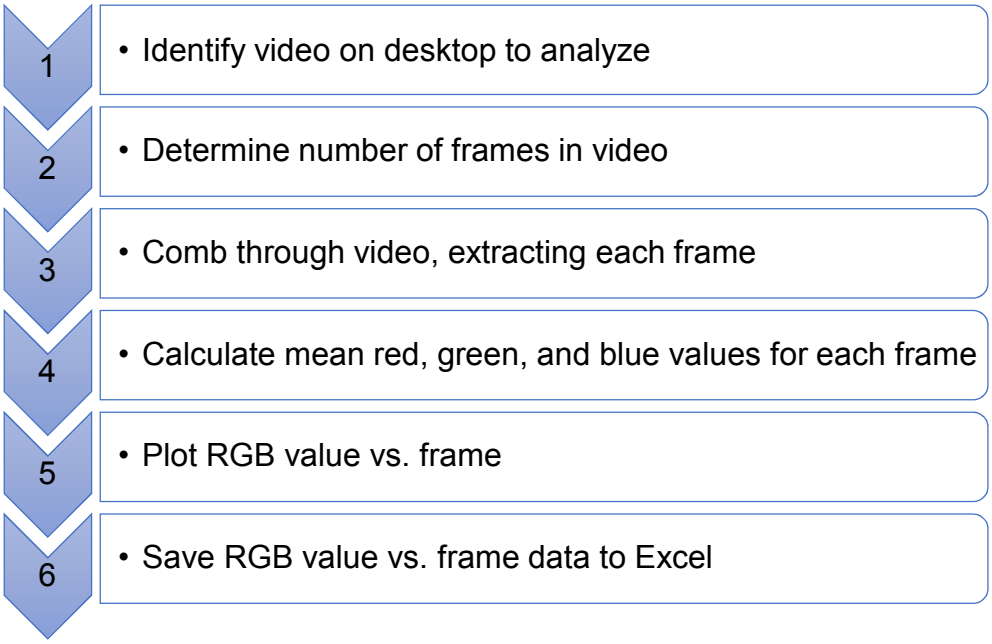

Figure 2.3. Outline of MATLAB code to extract RGB values of each frame in a breathing video.

2.2.5 Determination of Relative Humidity and Breathing Pattern

The breathing cycle videos were analyzed two different ways to understand the RH of the breath. First, the videos were analyzed qualitatively. The peak inhales and exhales were compared to a KGM sensor array from Momtaz and Chen[1] (Figure 2.4 a). This method determined a range of RH from breath monitoring. When the back side of the KGM sensor was analyzed, the compliment color for each peak inhale and exhale were determined (Figure 2.5). If spectroscopy was performed during the breath monitoring scenario, the reflectance wavelength data was also consulted to determine RH.

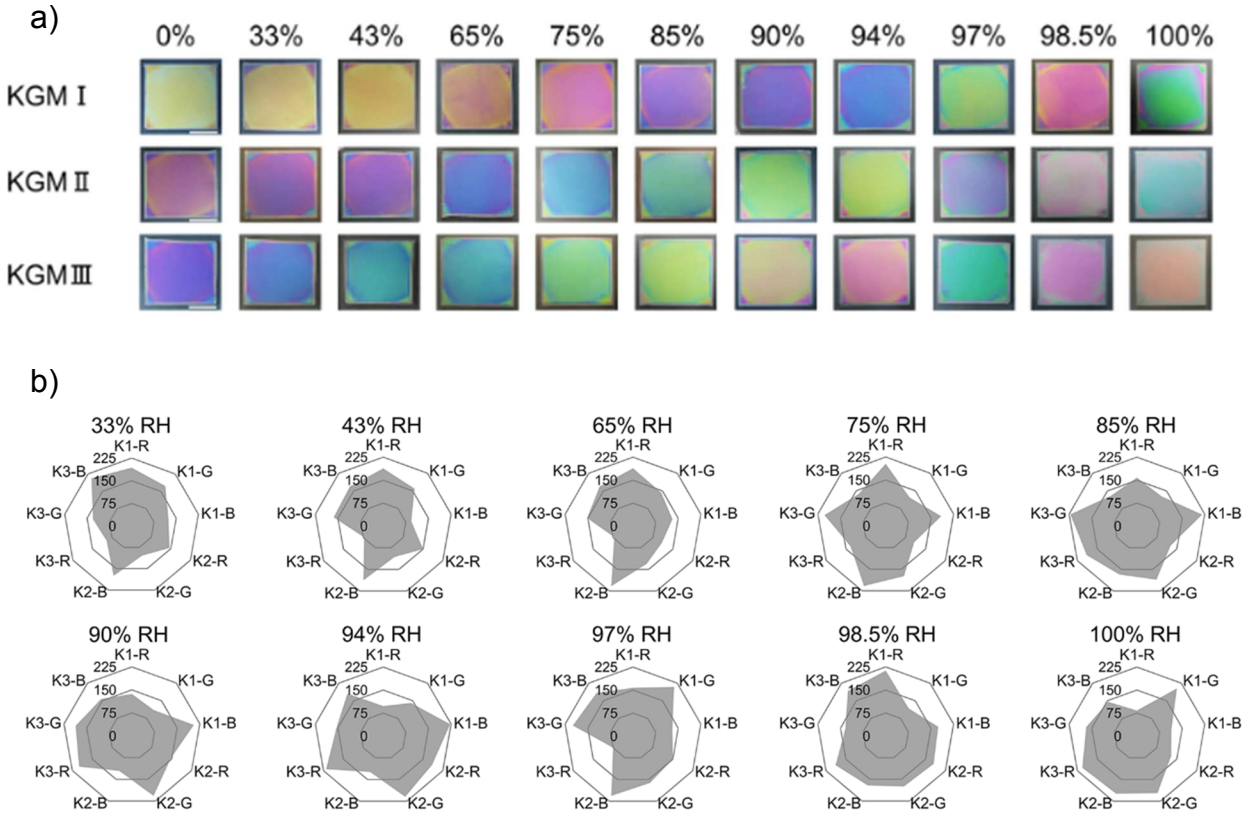

Figure 2.4. Excerpts from Momtaz and Chen,[1] used to compare with RIC data. a) KGM I, II, and III sensor arrays at various RH. b) RGB radar plots of KGM I, II, and III at various RH.

Second, radar plots were created with the RGB data of KGM I, II, and III. The resulting radar plots were referenced with KGM I, II, and III radar plots from Momtaz and Chen[1] (Figure 2.4 b). This method confirmed the RH ranges that had been deduced from previous analysis.

In order to determine the breathing pattern of every scenario, the RGB plots were analyzed. With consultation from the parent video, the peak inhales and exhales were determined. Then, the number of breaths were counted within the 60-second RGB vs.

time plot. This analysis provided the breaths per minute and average breath cycle duration.

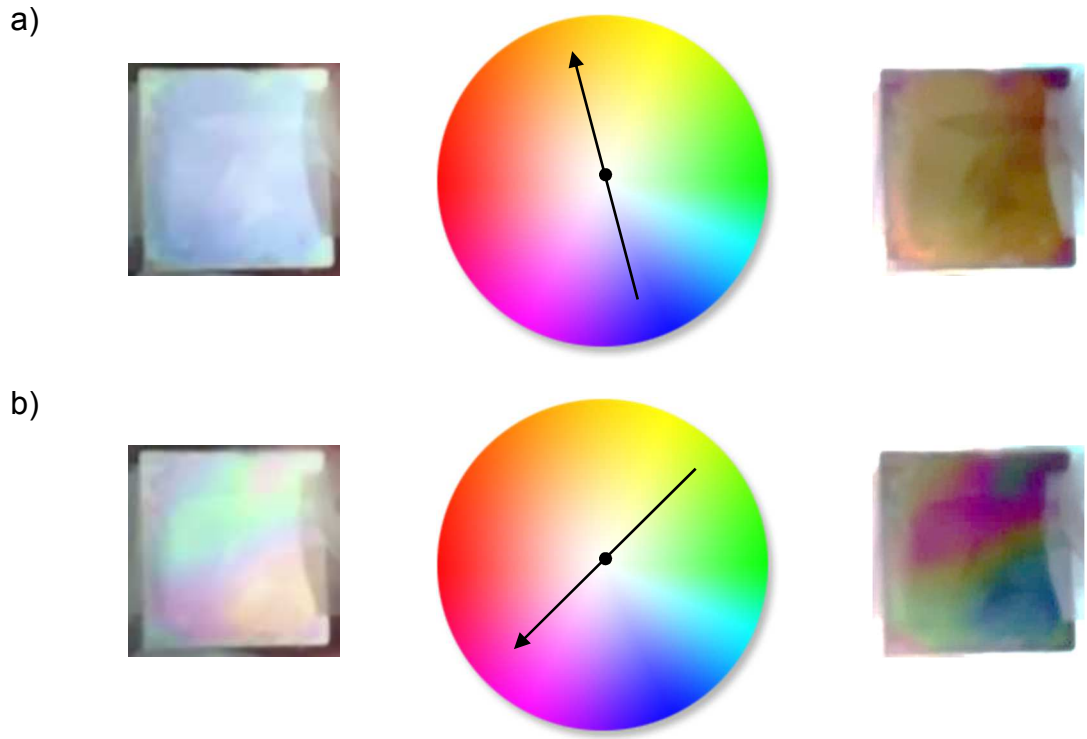

Figure 2.5. Method to determine actual KGM color when viewing the back side of the sensor. a) KGM I inhale photo (left) and inverted color photo (right). b) KGM I exhale photo (left) and inverted color photo (right). Color wheel arrows point to the compliment colors.

2.3 Results and Discussion

2.3.1 Control Experiment

The control experiment proved that the oxygen mask alone is not sufficient to determine breath cycles. As seen in Figure 2.6, an exhale does not cause much fogging from humidity. This makes an inhale and exhale visually indistinguishable from each

other. Therefore, an RIC sensor placed in the oxygen mask is needed to monitor breath cycles and humidity level.

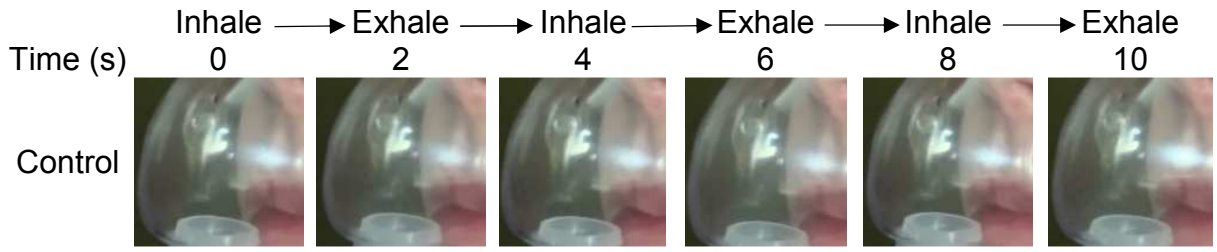

Figure 2.6. Oxygen mask without RIC sensor. Performed breathing through the nose in the sitting position.

2.3.2 Sitting: Back Side of Sensor

The back side of the RIC sensor was not successful at determining the RH of breath while sitting and breathing through the nose. This is because the glass substrate is reflective to light, as seen in the composition of the RIC sensor in Figure 2.2. The KGM polymer is not the top layer seen by the camera, which makes the observed color weak. After identifying the compliment colors of the peak inhales and exhales using a color wheel, the KGM sensor array at various RH[1] was used to visually determine the RH of the sitting scenario. Each sensor recorded an inhale of 33% RH and an exhale of 97% RH. Visually determining the RH of the back side of the RIC sensor would be difficult for at-home use because of the weak colors and the need to invert what is seen to understand the actual humidity level.

KGM I's back side cycled from a blue to a yellow color; opposite from what is seen from the front side results. However, during one exhale, the color changes from blue to yellow to red, then undergoes further color change to purple, to green and to

another red (Figure 2.7 a). This repeating of colors twice in each exhale pattern resulted in a shaky RGB plot with a few extra peaks during an exhale interval. Figure 2.8 a, b, and c all represent this unstable color change within each exhale interval.

To determine breath cycles and bpm, video analysis was used in tandem with the RGB plots to ensure the correct peaks were labeled. KGM I recorded 11 bpm with an average of 5.2 seconds for a breath cycle. Without the inhale and exhale intervals noted on KGM I's RGB plots the breath pattern could not be understood, making KGM I's back side a poor candidate for a facile breath monitoring device.

KGM II's back side was similar to KGM I as it also cycled through colors twice during one exhale interval. Besides making visual analysis difficult, the RGB plots are affected, too, and are difficult to read without notations. The color change from yellow-green to red, then to purple and to yellow caused peaks in between each exhale interval (Figure 2.9). These extra peaks made it necessary for video analysis to be used in tandem again with RGB plots to determine breath cycles. KGM II recorded 16 bpm with an average cycle of 3.6 seconds. As with KGM I, KGM II's back side is a poor candidate for a breath monitoring device because of the repeating of colors which lead to difficulty assigning breath cycles both visually and in RGB analysis.

KGM III's back side exhibited behavior resembling that of KGM I and II. During an exhale, KGM III cycled from yellow to red, then to purple and to another yellow (Figure 2.10). These repeating colors also revealed themselves as peaks within each exhale interval, making the breath cycles difficult to identify without video analysis accompanying the RGB plots. After the combination of the two analysis methods, it was determined that KGM III tracked 15 bpm with an average breath cycle of 4.0 seconds.

As with the latter two sensors, KGM III's back side RIC sensor is unfit to be a breath monitoring device because of repeating colors.

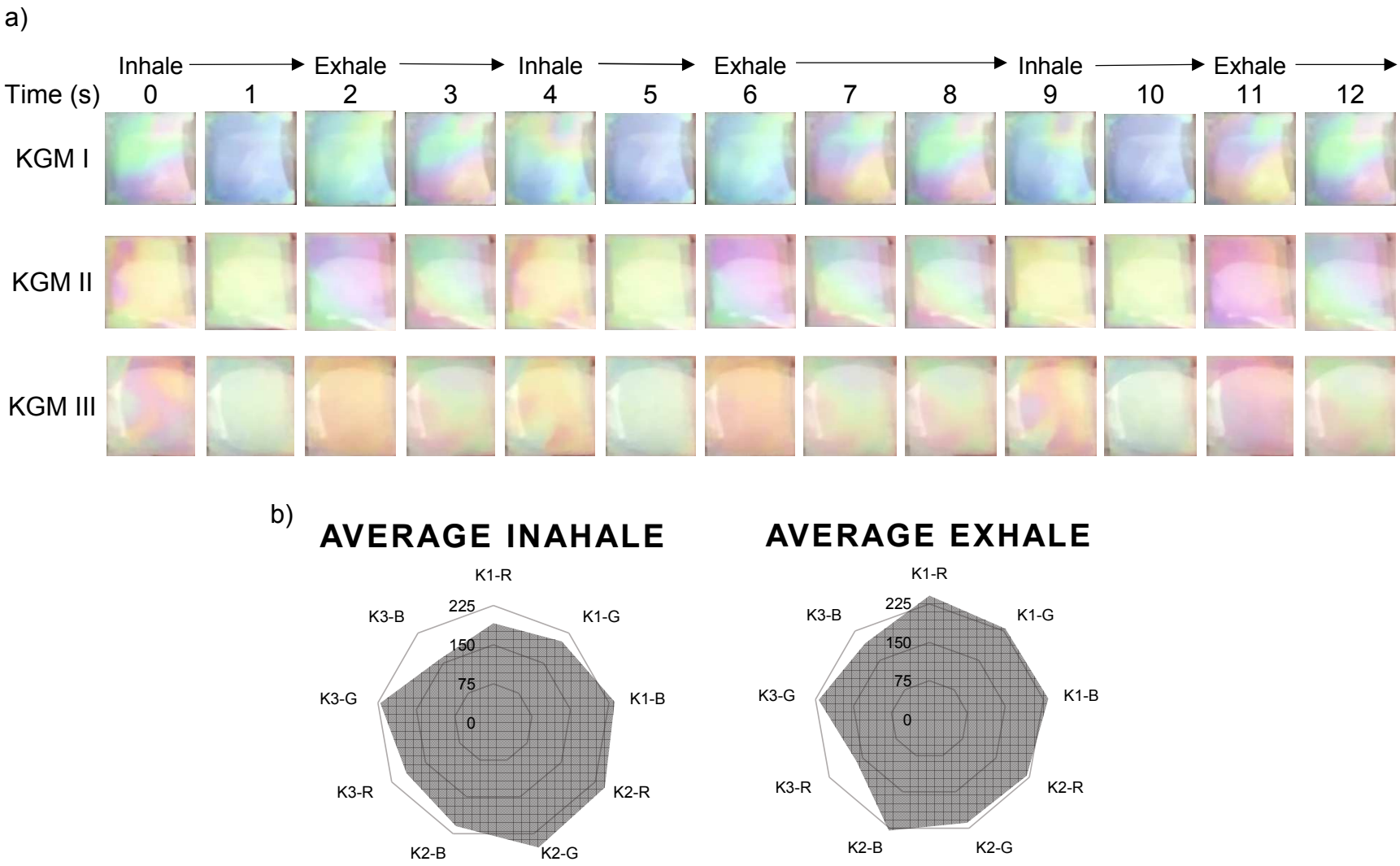

Figure 2.7. a) Colorimetric responses of the back side of KGM humidity sensors with sitting condition, breathing through the nose. The breathing cycles for KGM I, II, and III have been aligned to compare exhale and inhale colorations. b) Radar plots of the back side of KGM I, II, and III for the sitting scenario.

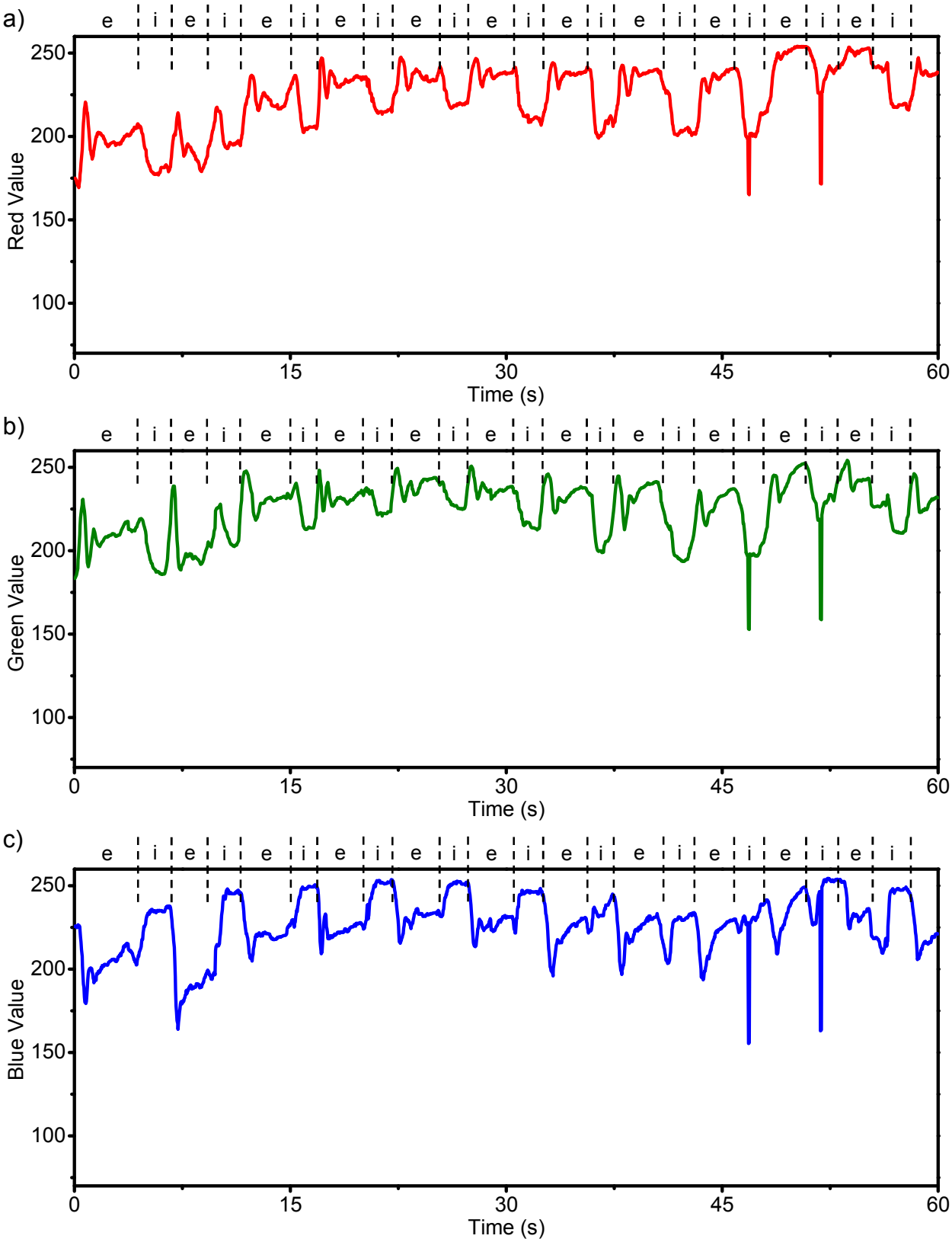

Figure 2.8. Back side of KGM I RGB plots vs. time for the sitting scenario. a) Red values, b) green values, c) blue values. Exhales are denoted as “e”, inhales as “i”.

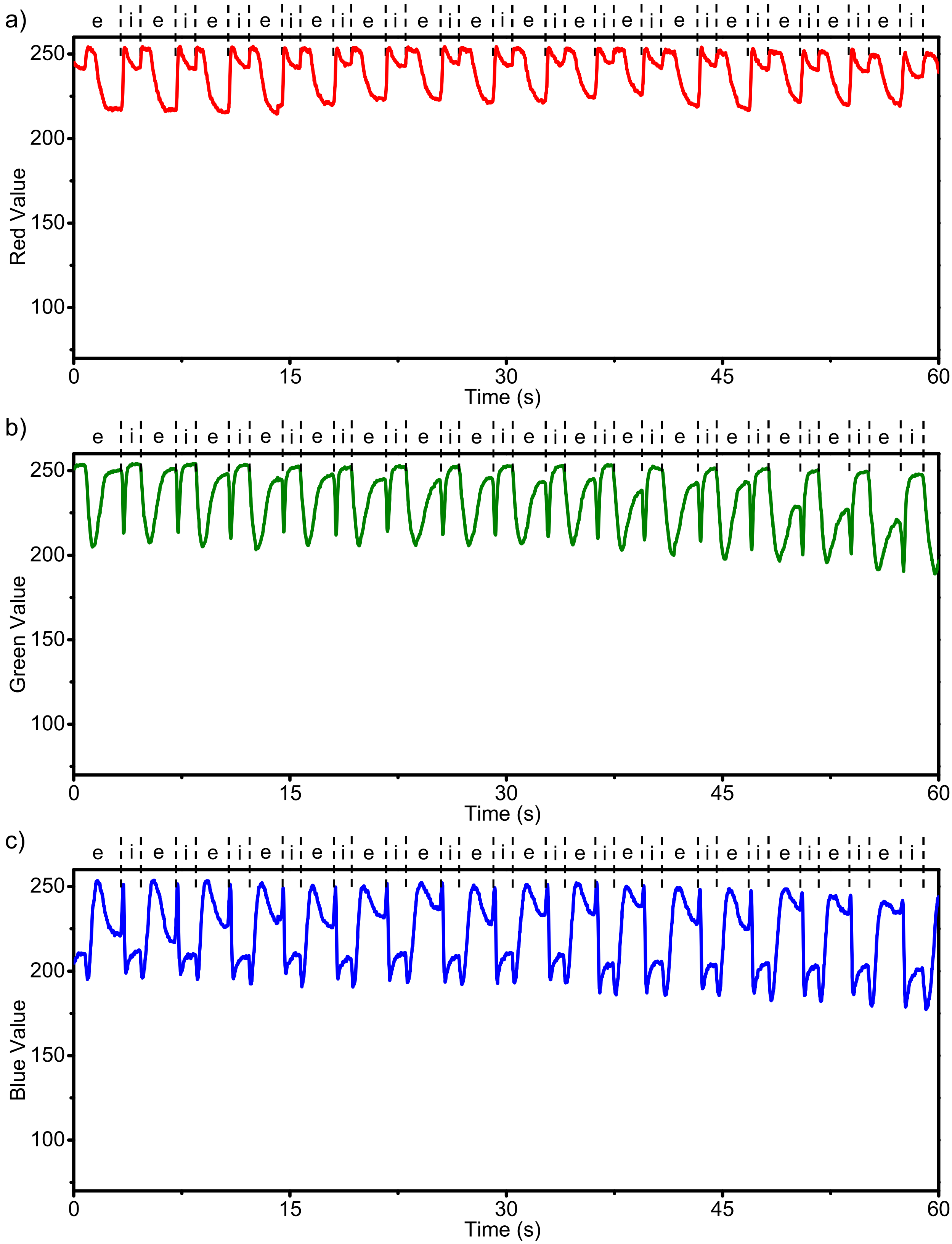

Figure 2.9. Back side of KGM II RGB plots vs. time for the sitting scenario. a) Red values, b) green values, c) blue values. Exhales are denoted as “e”, inhales as “i”.

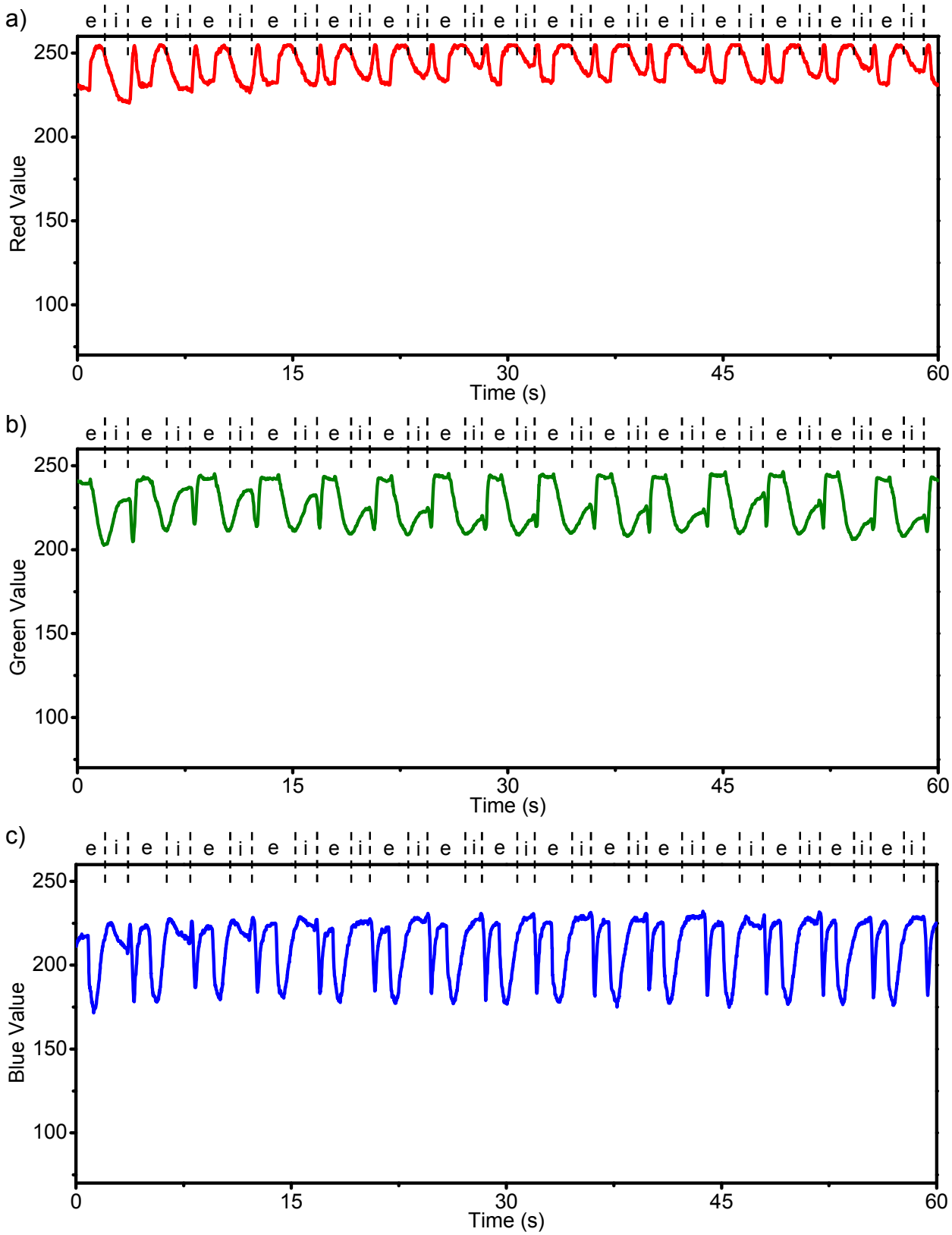

Figure 2.10. Back side of KGM III RGB plots vs. time for the sitting scenario. a) Red values, b) green values, c) blue values. Exhales are denoted as “e”, inhales as “i”.

2.3.3 Sitting: Front Side of Sensor

The RIC sensor responded very quickly and efficiently to breathing through the nose. After comparison with the KGM sensor array at various RH[1], KGM I, II, and III are in 33% RH at peak inhale. At peak exhale, KGM I reported about 94-97% RH while KGM II and III reported 94% RH. Since KGM I's exhale color is a cyan, it quite possibly is exactly in the middle of the blue 94% RH and the green 97% RH on the array. With this assumption, KGM I reached about 95.5% RH, very similar to KGM II and III.

The radar plots are in good agreement with 43% RH at peak inhale and 90-94% RH at peak exhale (Figure 2.11 b). Since the radar plots do not exactly resemble the reference plots (2.4 b), this method of RH determination is best to only estimate the inhale and exhale levels.

With reflectance spectroscopy to confirm sensor color, KGM I, II, and III are seen in second-order interference (Figure 2.12). Reflectance spectroscopy confirmed that the KGM colors follow the same pattern as in the sensor array[1] when exposed to humidity from the breath (2.4 a).

Considering both visual and radar plot analysis, the overall average RH of an inhale through the nose in the sitting position is 35.5%. The overall average RH of an exhale through the nose in the sitting position is 94.7%.

The RGB plots (Figures 2.13 – 2.15) illustrate breathing cycles very well. Plots without double peaks (as seen in Figure 2.13 b) are best to view breath rate and pattern. These double peaks found in many RGB plots of the KGM front side were determined to be the intermediate color between inhale and exhale presenting itself. For this reason, not every RGB plot is best at representing breathing cycles. The most

informative and easy-to-read RGB plots are those which include an increase for the inhale interval and a decrease for the exhale interval, or vice vera, without intermediate color peaks (as seen in Figure 2.13 a). The plateaus found in many RGB plots (as seen in Figure 2.13 a) were determined to be respiratory pauses. These pauses occur naturally in breathing at the end of an inhale and/or exhale and can stand out more during slow breathing rates.[10]

For KGM I, the red plot shows breath cycles by increasing values during an inhale and decreasing values during an exhale (Figure 2.13 a). This is because the inhale (or lowest RH) color for KGM I is a yellow, reaching a ~125 red value. This color has much more red hue than the exhale (highest RH) color for KGM I, which is a cyan, reaching a ~250 red value. Oppositely, the blue RGB plot shows inhales at low blue values (~100) and exhales at high blue values (~250) (Figure 2.13 c). KGM I's green RGB plot includes an extra peak within the inhale and exhale intervals which track an intermediate color of purple during the breath cycle (Figure 2.13 b). The inhales are seen at ~210 and exhales at ~230. The intermediate purple presents itself as a peak at ~130 which borders the inhale intervals. As the green plot increases in time, the green value of the exhale decreases. This is indicative of the breath humidity decreasing slightly as it experiences a shift towards the blue color of 94% RH. The RGB plots overall tracked 14 bpm with KGM I with an average breath cycle of 4.3 seconds.

KGM II's RGB plots are similar to KGM I in that a transition color can be seen on the red and blue plots within inhale and exhale intervals. On the red plot, these peaks are caused by the transition color of blue, which border the inhale intervals (Figure 2.14 a). The inhale has a red value of ~160, the exhale has a red value of ~ 220, and the

blue transition color stands out with a value of ~ 75. This transition peak is not seen in the green plot for KGM II, making it much easier to see breath cycles (Figure 2.14 b). The plot increases during exhale intervals and decreases during inhale intervals. When studying the blue plot, extra peaks are seen bordering the inhale intervals (Figure 2.14 c). These peaks are also caused by the blue transition color as it contains the most blue value at ~240. With these high values, it stands out from the inhale's ~210 and the exhale's ~125. Overall, KGM II tracked 15 bpm with an average breath cycle of 3.9 seconds, very similar to what KGM I tracked.

KGM III has RGB plots most similar to KGM II because they both tracked a higher RH% than KGM I did for this scenario. Because of this wider range of colors, transition color peaks are seen again, in this case within green and blue plots. The green plot for KGM III includes peaks which border the inhale intervals, much like what was seen in KGM II's blue plot (Figure 2.15 b). These high peaks at ~200 belong to a green transition color which occurs between the inhale (~160) and exhale (~140). The transition color peaks occur on the blue plot as well at values of ~120 (Figure 2.15 c). The red plot for KGM III is the most simple plot to view breath cycling as there are no transition color peaks visible (Figure 2.15 a). Inhales are shown as decreasing intervals and exhales are shown as increasing intervals. It is seen that 12 bpm were recorded with an average breath cycle of 4.9 seconds.

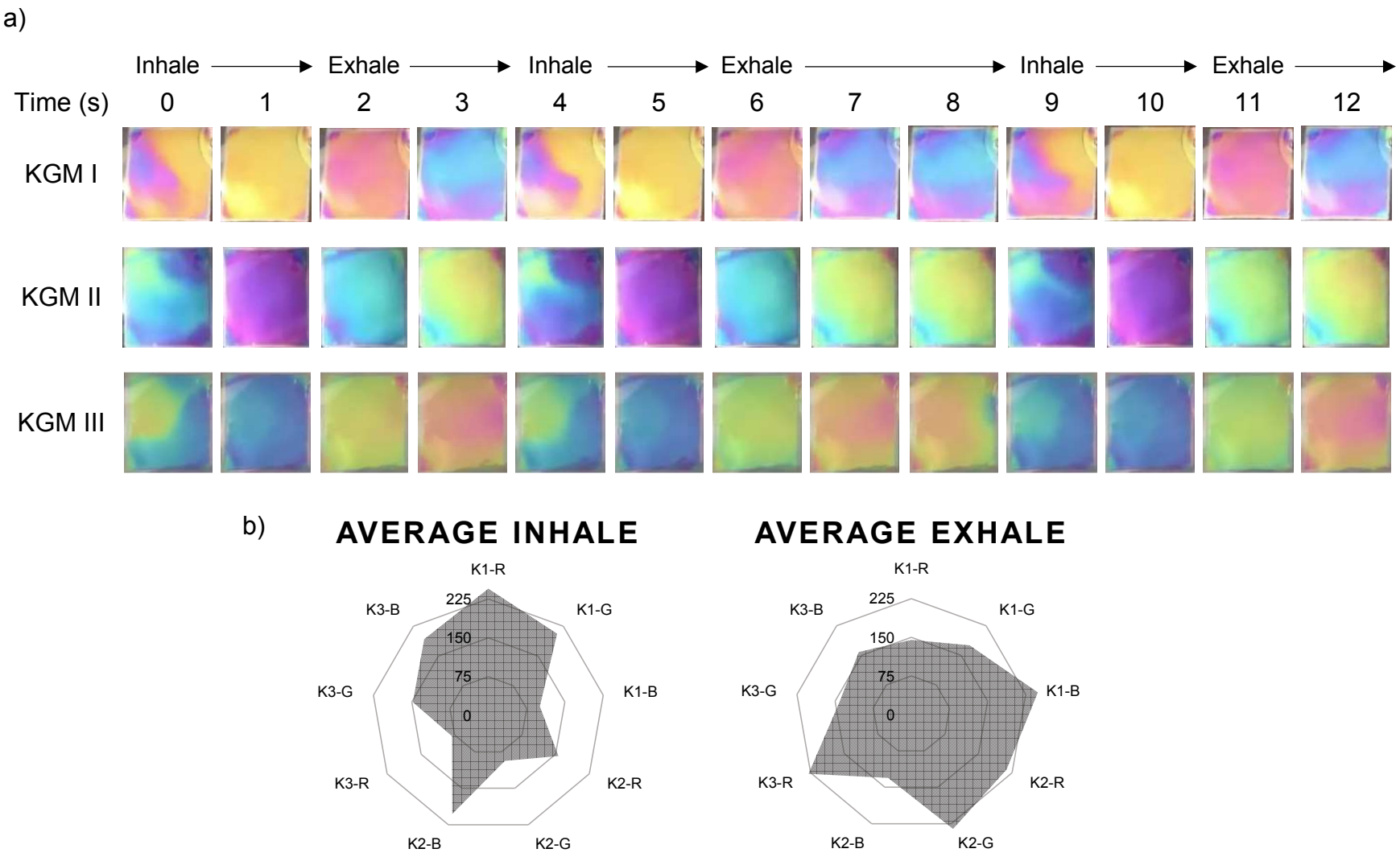

Figure 2.11. a) Colorimetric responses of the front side of KGM humidity sensors with sitting condition, breathing through the nose. The breathing cycles for KGM I, II, and III have been aligned to compare exhale and inhale colorations. b) Radar plots of KGM I, II, and III for the sitting scenario.

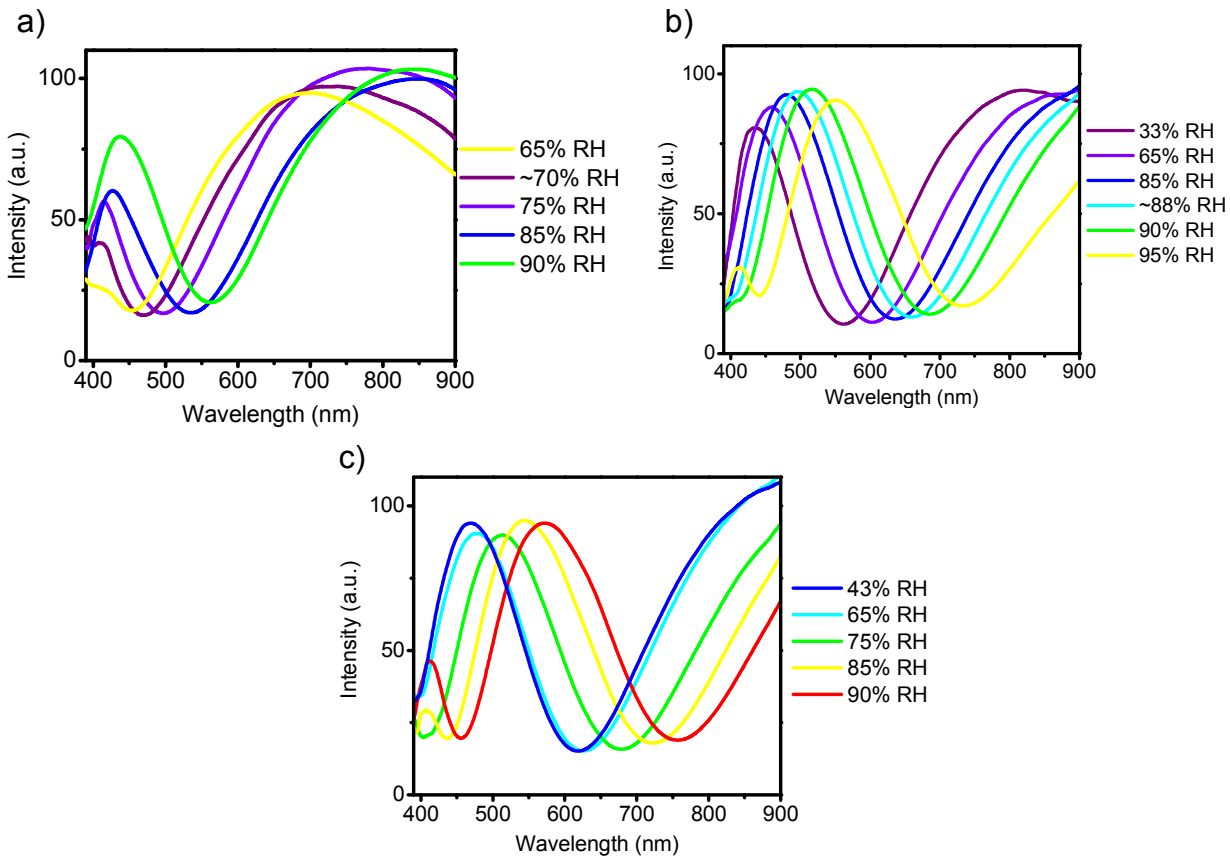

Figure 2.12. Reflectance spectroscopy tracking one exhale interval of a) KGM I, b) KGM II, c) KGM III.

	Order of Interference	33% RH	43% RH	65% RH	-	75% RH	85% RH	-	90% RH	94% RH
KGM I	1st	-	-	698	722	776	-	-	-	-
	2nd	-	-	414	411	415	427	-	434	
KGM II	1st	816	-	-	-	-	-	-	-	-
	2nd	434	-	459	-	-	480	496	517	551
KGM III	1st	-	-	-	-	-	-	-	-	-
	2nd	-	469	478	-	513	543	-	572	-
	3rd	-	-	-	-	-	407	-	412	-

Table 2.1. Reflection peak wavelengths (nm) for KGM I, II, and III at RH according to Momtaz and Chen.[1]

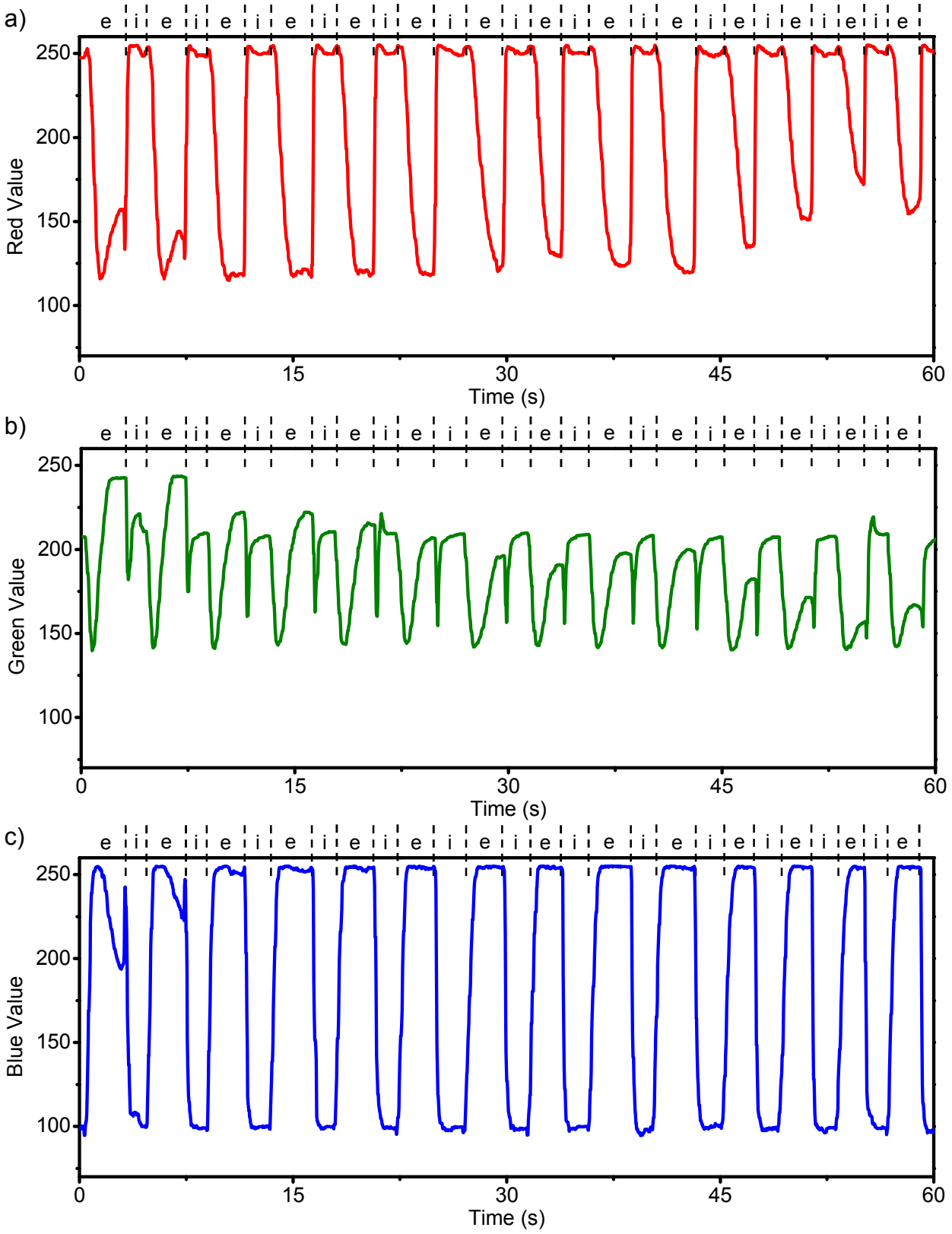

Figure 2.13. KGM I RGB plots vs. time for the sitting scenario. a) Red values, b) green values, c) blue values. Exhales are denoted as “e”, inhales as “i”.

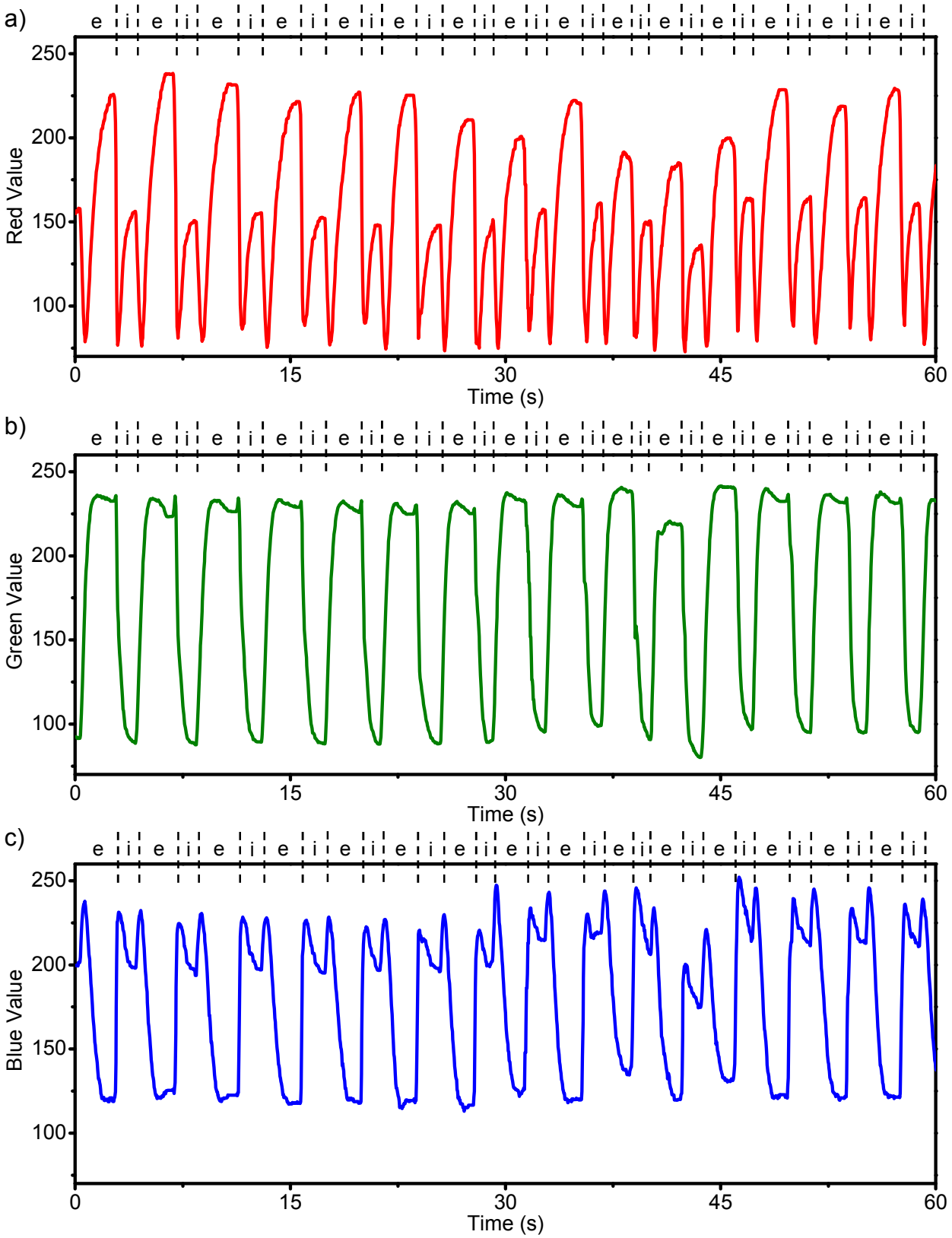

Figure 2.14. KGM II RGB plots vs. time for the sitting scenario. a) Red values, b) green values, c) blue values. Exhales are denoted as “e”, inhales as “i”.

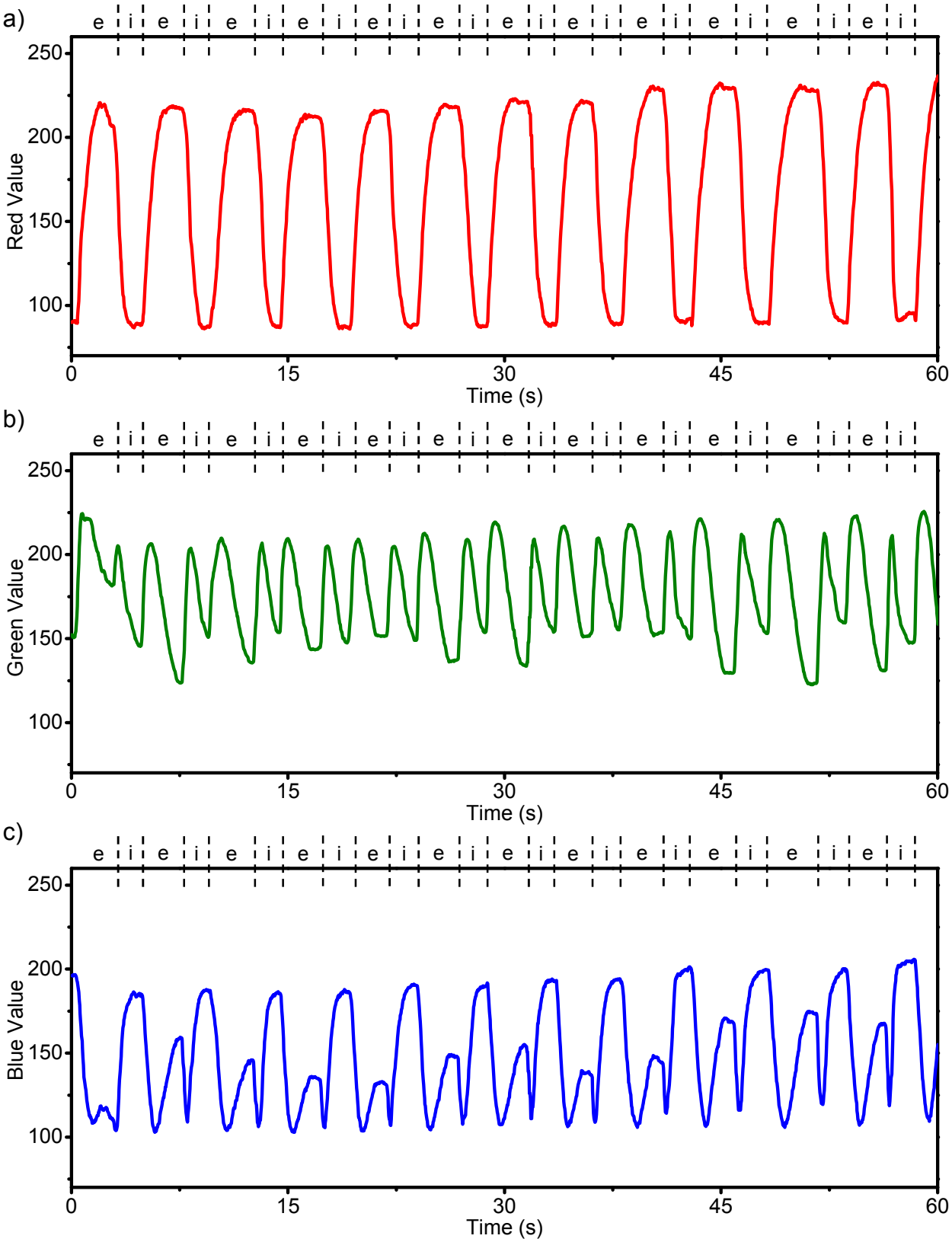

Figure 2.15. KGM III RGB plots vs. time for the sitting scenario. a) Red values, b) green values, c) blue values. Exhales are denoted as “e”, inhales as “i”.

2.3.4 Standing

The standing scenario resulted in about 2% higher relative humidity in exhales than the sitting scenario. This is to be expected as standing exerts more effort from the body than sitting, so breathing intensifies slightly. With higher exhale humidity, more colors are seen on the KGM sensor through a breath cycle, which leads to a higher possibility for multiple peaks in RGB plots.

After comparison with the KGM sensor array at various RH[1], KGM I, II, and III were determined to reach 33% RH at peak inhale. At peak exhale KGM I reaches 94%, KGM II reaches 98.5%, and KGM III reaches 97% RH. It is notable that KGM I's detected RH is lower than the other two sensors. In further scenario studies, KGM I has proven to reach higher RH levels, so this difference is not a defect of KGM I itself, but more likely a result of uneven breath during human testing. As described later, the respiratory rate tracked by KGM I was greater than what KGM II or III tracked. This faster rate of breathing may attribute to the lower RH as it is likely faster breath rate includes shallow breathing with low RH exhales.

The radar plots are in good agreement with 43% RH at peak inhale and 94-97% RH at peak exhale (Figure 2.16 b). Therefore, the overall average RH of an inhale through the nose in the standing position is 35.5%. The overall average RH of an exhale through the nose in the standing position is 96.3%, almost 2% higher than the average RH while sitting (94.7%).

KGM I has clear RGB plots for this scenario most likely because fewer colors are represented in the humidity range of 33-94% RH. KGM I's red and green RGB plots both follow the trend of increasing color value during an inhale and decreasing for an exhale (Figure 2.17 a and b, respectively). KGM I's blue plot follows the opposite trend;

values increase during an exhale and decrease during an inhale (Figure 2.17 c). Each RGB plot shows KGM I's full 18 bpm with 3.2 average seconds per breath cycle. This higher rate of breathing may be caused by shallow breathing since no activity was performed to increase the breathing rate.

KGM II had many peaks in the RGB plots because the color tracks beyond second-order interference to fourth-order interference at its high RH of 98.5%. In the red plot, inhales reached ~150 and the exhales ~180 (Figure 2.18 a). Bordering the inhale intervals at ~120, a blue-green transition color is seen. Bordering the exhale peak, a red transition color is seen at ~210. The green plot only includes one transition color peak which borders the inhale intervals (Figure 2.18 b). This is a yellow transition color at ~190. Other than these transition peaks, the inhales are seen as decreasing intervals and the exhales are seen as increasing intervals. Lastly, the blue RGB plot for KGM II identified three transition color peaks along with the inhale and exhale peaks (Figure 2.18 c). The exhale is at ~200, then decreases to a transition green peak at ~160 as inhale begins. Then, a transition blue is seen at ~205 before reaching the inhale peak at ~195. When exhale begins again, a yellow transition peak is seen at ~210. These many transition peaks make each RGB plot very difficult to read, so video analysis was needed to confirm inhale and exhale intervals in each KGM II plot. The KGM II sensor recorded 14 bpm with an average breath cycle of 4.3 seconds.

The RGB plots for KGM III appear similar to the sitting scenario because the RH range was at 33-97%. The red plot is easiest to view breath cycles from because an exhale is shown as increasing red values and an inhale is shown as decreasing red values (Figure 2.19 a). There are a few transition color peaks scattered throughout: the

first three inhales have a peak at a green transition color at ~130-115 on its way to the inhale peak of ~80. The exhale interval also has a few transition colors seen throughout as a double peak instead of a plateau. These peaks indicate the transition color red at ~175 which borders the exhale peak of ~160. Not all exhale intervals include clear double peaks which shows the KGM sensor was just barely reaching 97% RH at times. The sensor may have been detecting breath RH just below 97% which resulted in the red plot's green transition peaks decreasing in value and creating a plateau for the exhale.

KGM III had a complex green RGB plot as well (Figure 2.19 b). However, it only contains one transition color peak. The green transition color peaks at ~175 and borders the inhale intervals. The blue RGB plot of KGM III resembles the sitting scenario, but with more peaks as the RH range was increased from 94% to 97% RH at peak exhale (Figure 2.19 c). During an exhale, transition green is seen at ~120 before hitting the final exhale peak of ~185. During an inhale, transition yellow is seen at ~140 before increasing again to ~185 for the final color of blue for KGM III inhale. The KGM III sensor detected 15 bpm with an average breath cycle of 3.9 seconds from the RGB plots, similar to what KGM II tracked.

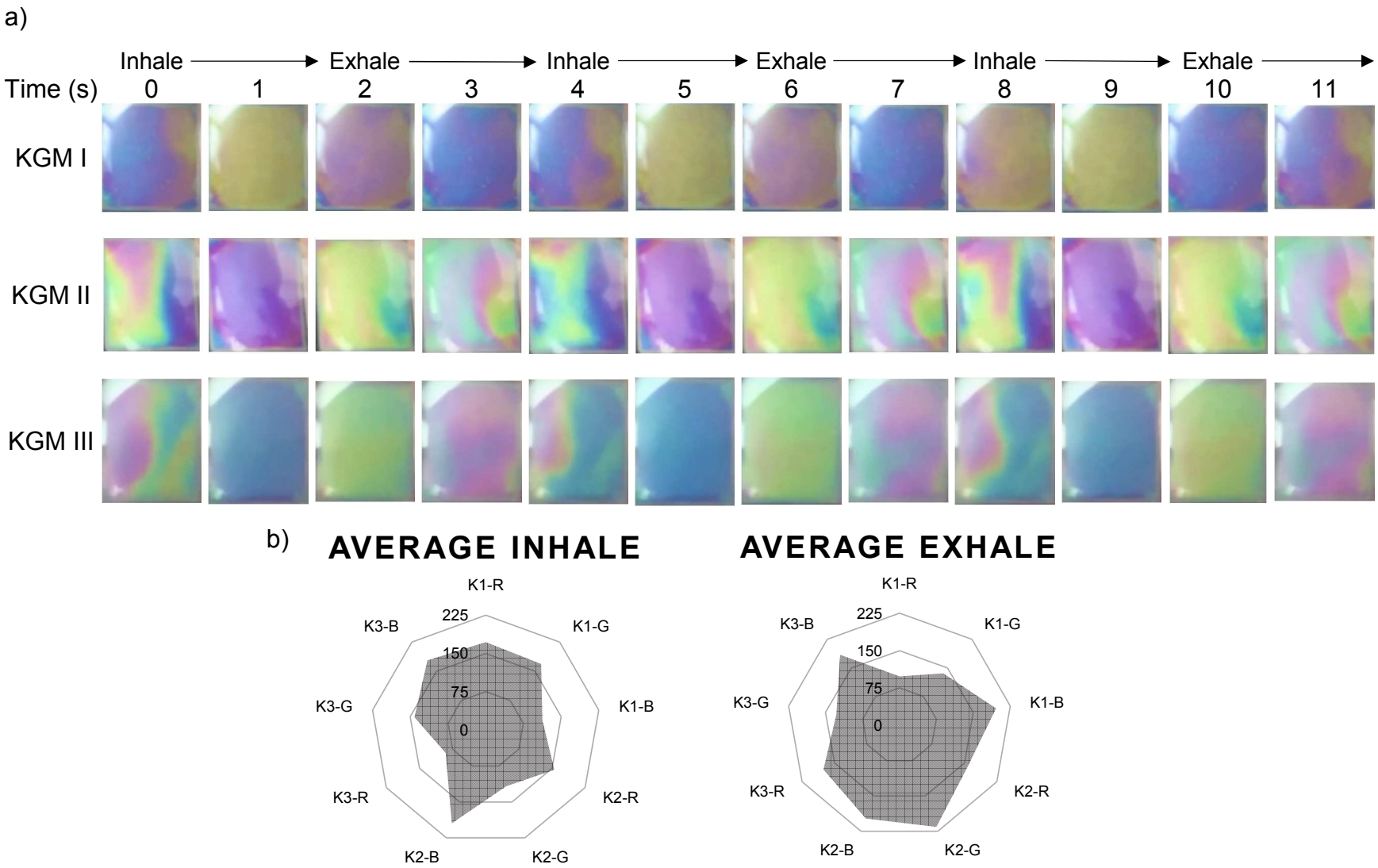

Figure 2.16. a) Colorimetric responses of KGM humidity sensors with standing condition, breathing through the nose. The breathing cycles for KGM I, II, and III have been aligned to compare exhale and inhale colorations. b) Radar plots of KGM I, II, and III for the standing scenario.

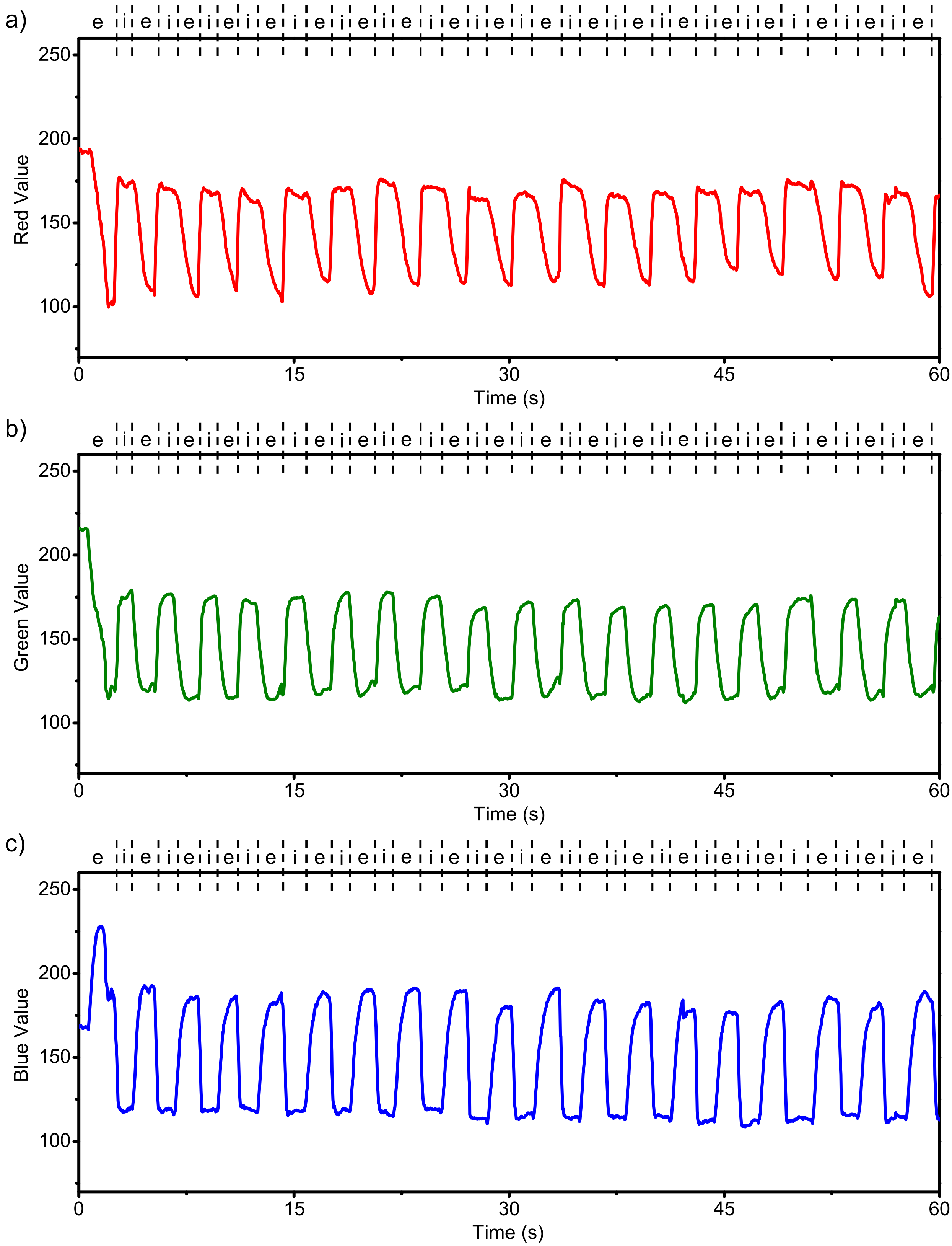

Figure 2.17. KGM I RGB plots vs. time for the standing scenario. a) Red values, b) green values, c) blue values. Exhales are denoted as “e”, inhales as “i”.

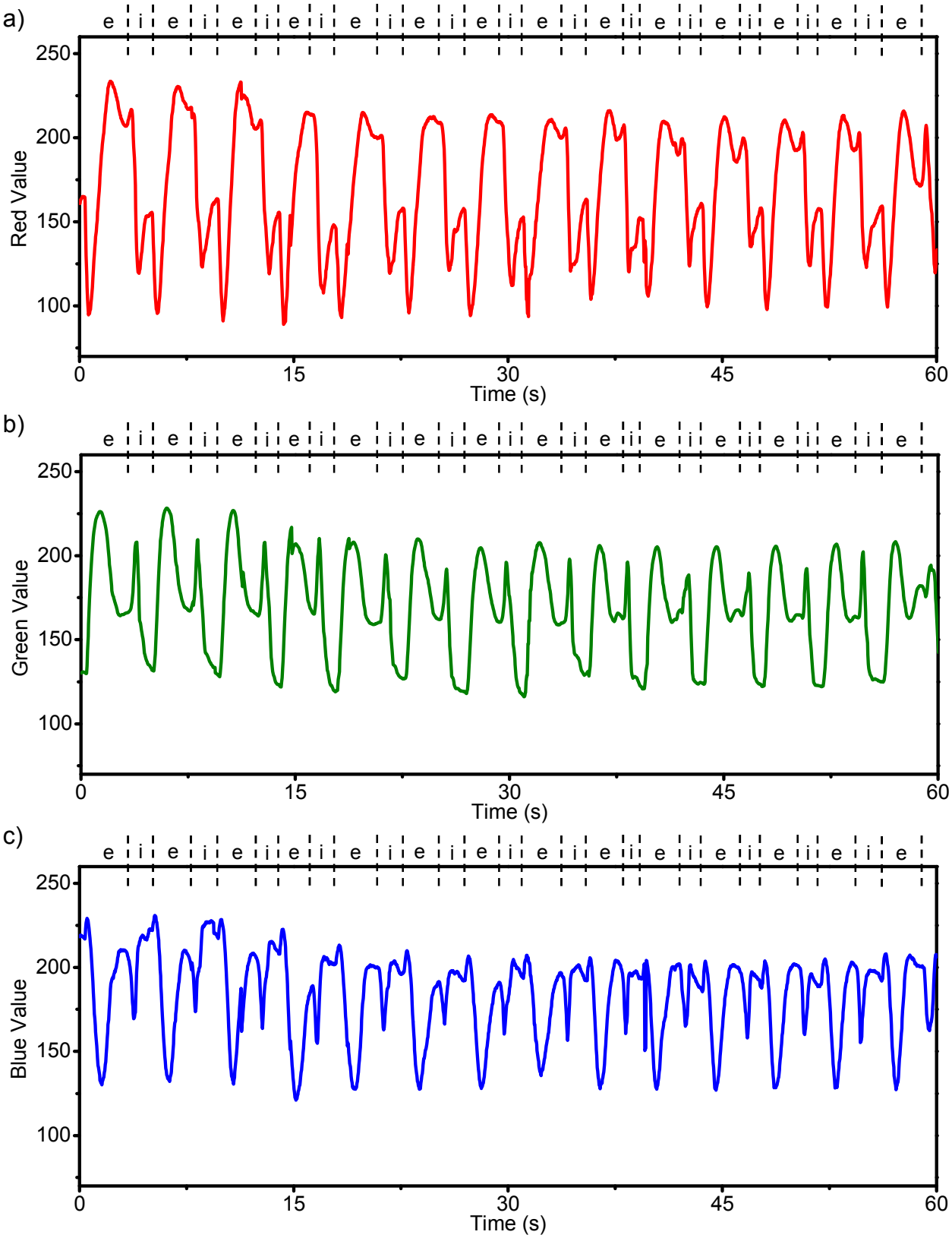

Figure 2.18. KGM II RGB plots vs. time for the standing scenario. a) Red values, b) green values, c) blue values. Exhales are denoted as “e”, inhales as “i”.

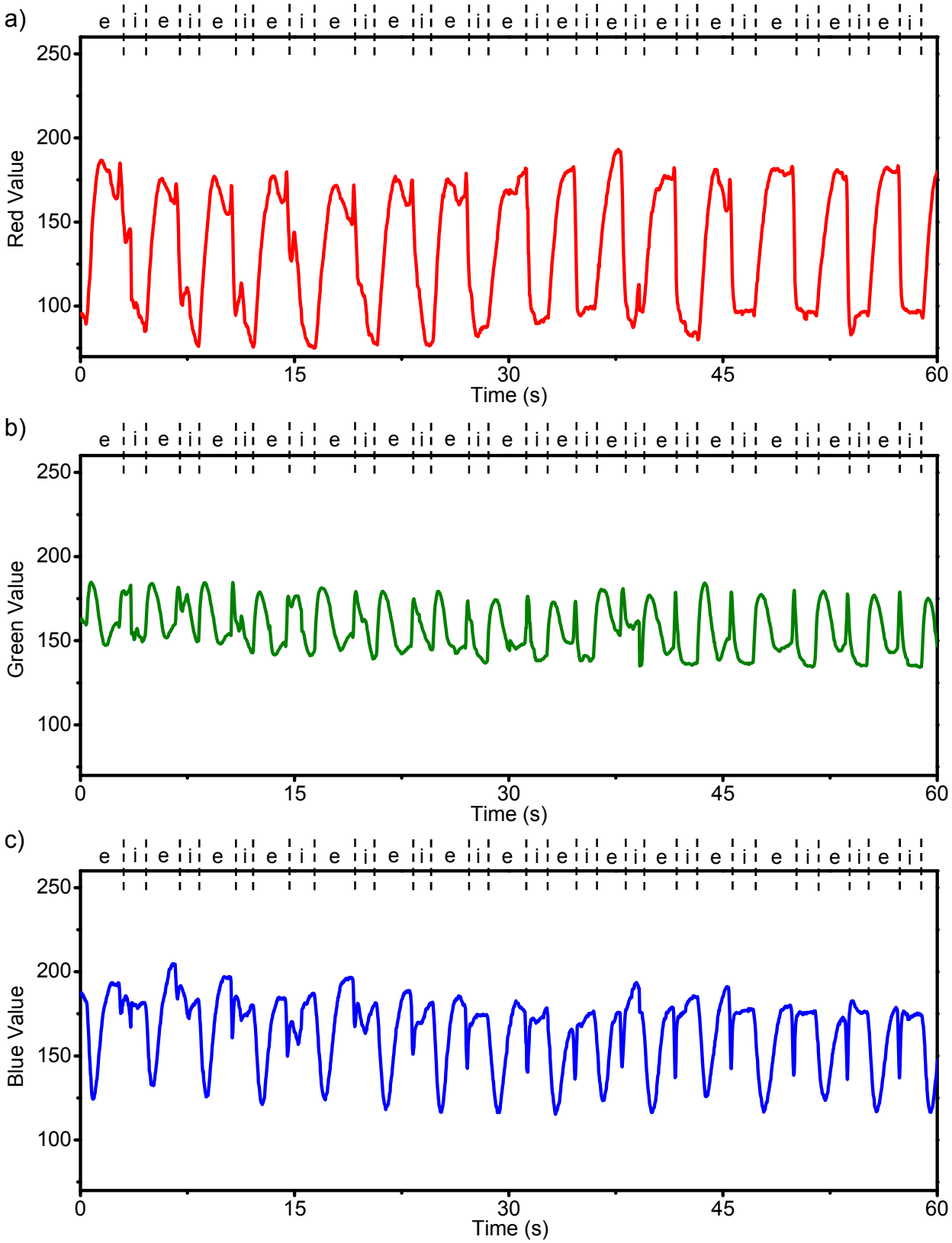

Figure 2.19. KGM III RGB plots vs. time for the standing scenario. a) Red values, b) green values, c) blue values. Exhales are denoted as “e”, inhales as “i”.

2.3.5 After 12 Hour Fast

The fasting scenario showed no significant difference in breath RH from the standard sitting position. However, the average respiratory rate was about 2 seconds faster than standard sitting. After comparison with the KGM sensor array at various RH[1], KGM I, II, and III are in 43% RH at peak inhale. At peak exhale KGM I reached 97%, KGM II reached about 94-97% RH, and KGM III reached 94% RH. With radar plot comparisons, the peak inhale is about 33% RH and the peak exhale is about 94% RH (Figure 2.20 b). This creates an average inhale RH in the fasting scenario to be 40.5% and the average exhale 95.1%. These values are very similar to the 35.5% RH inhale and 94.7% RH exhale averages of the standard sitting condition.

RGB plot analysis reflects the higher RH KGM I reached in this scenario by showing more peaks within the inhale or exhale intervals. The red plot increases with inhales and decreases with exhales with an extra peak in each interval (Figure 2.21 a). This belongs to a transition color blue of valued at ~145 that appears just before the final exhale peak at ~170, and again immediately after as inhale begins. Since the final exhale color is green on the RIC sensor, it is the highest point on the green RGB plot at ~225 (Figure 2.21 b). A transition red color appears before the peak exhale (~160) and a transition cyan color appears after the peak exhale (~170). This RGB plot shows the peak inhale at a higher green value of ~200. Unlike the red plot, this green plot shows inhale and exhale both as increasing intervals. This trend changes in KGM I's blue plot, as it represents inhales as decreasing intervals and exhales as increasing intervals (Figure 2.21 c). A transition blue color at ~210 is seen as a peak before and after the final exhale at ~165. The red and blue plots are much easier to understand breath rate

and pattern from because the inhales and exhales follow opposite trends. They show an average breath cycle of 3.4 seconds with 17 bpm.

Since KGM II reached about 95.5% RH, the RGB plots had few transition color peaks. In the red plot, a transition blue color is seen before and after the peak inhale (Figure 2.22 a). The inhales are at ~200 with the blue transition color at ~155. This red plot shows increasing intervals for both inhale and exhale. The green plot is opposite of the red; it shows decreasing intervals for both inhales and exhales (Figure 2.22 b). The inhale peak is shown at ~155, bordered by green transition colors at ~245. The exhale peak follows by dropping down to ~200-180. The blue plot is the only plot for KGM II that shows opposite intervals for inhales and exhales (Figure 2.22 c). The inhale is represented as an increase in blue value, peaking at ~210, and the exhale is represented as a decrease in blue value, dropping to ~170-190. This plot is also different from the red and green plots because there are two transition colors that appear. A blue-purple transition color at ~225 borders the inhale peak, and a yellow transition color at ~150 borders the exhale peak. Because two transition colors appear on the blue RGB plot for KGM II, it is not the best plot to understand breath information. The red and green plots are slightly easier to help visualize the inhale and exhale intervals. The average breath cycle of KGM II was 3.5 seconds with 17 bpm, almost exactly as KGM I had tracked.

KGM III tracked breath humidity up to 94% RH, so there were fewer transition colors seen in its RGB plots. The red RGB plot is the easiest to view breath cycles as there are no transition peaks (Figure 2.23 a). Inhale intervals are shown as decreasing in red value, and exhale intervals are shown as increasing in red value. In both the

green and blue RGB plots, one transition color can be seen. For the green plot, a transition green color is seen at ~240 which borders the inhale peaks of ~200 (Figure 2.23 b). Both the inhale and exhale intervals are decreasing in green value with the exhale reaching ~170. The blue RGB plot is opposite of the green as it shows inhale and exhale intervals both as increasing in blue value (Figure 2.23 c). The inhale reaches the highest blue value at ~225 which the exhale reaches slightly lower at ~190-200. Like the green plot, there is a transition color bordering the inhale in the blue plot. This is a yellow-green transition color at ~140-160. As was observed in the sitting and standing scenario, the red RGB plot for KGM III is most simple for viewing the breath cycle. 15 bpm were tracked at an average cycle of 3.8 seconds, similar to what KGM I and II had tracked.

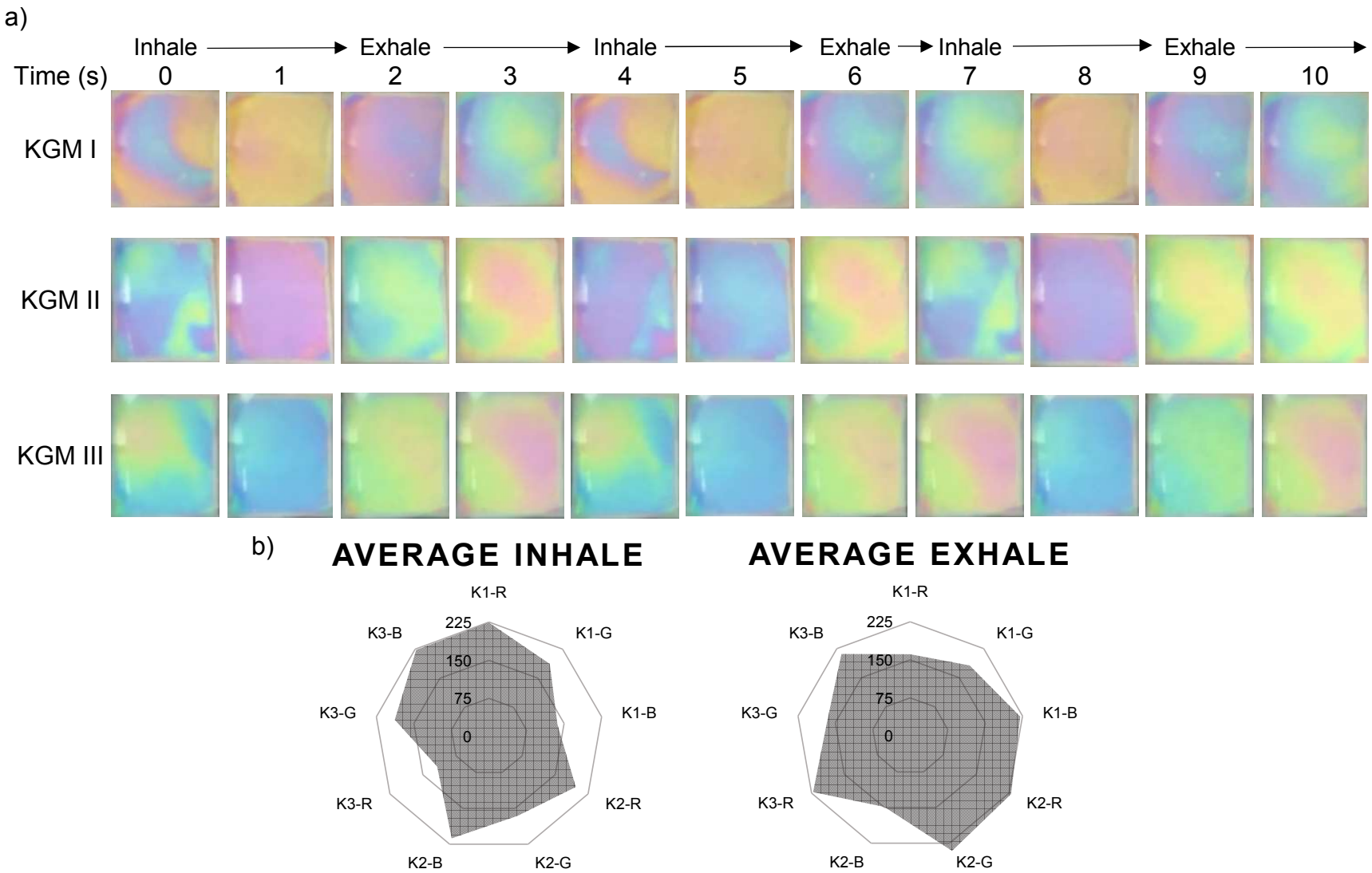

Figure 2.20. a) Colorimetric responses of KGM humidity sensors while sitting after 12 hour fast, breathing through the nose. The breathing cycles for KGM I, II, and III have been aligned to compare exhale and inhale colorations. b) Radar plots of KGM I, II, and III for the fasting scenario.

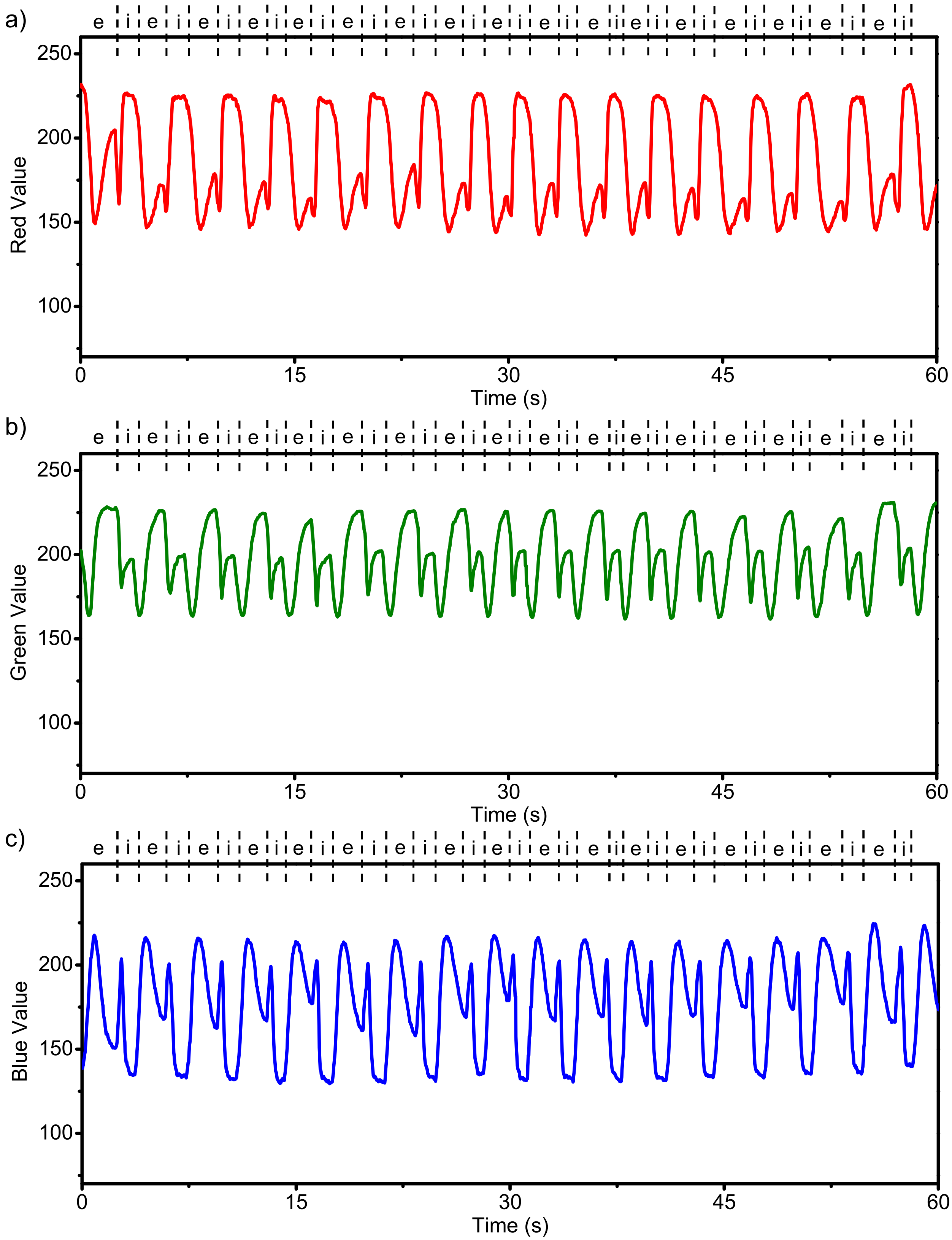

Figure 2.21. KGM I RGB plots vs. time for the fasting scenario. a) Red values, b) green values, c) blue values. Exhales are denoted as “e”, inhales as “i”.

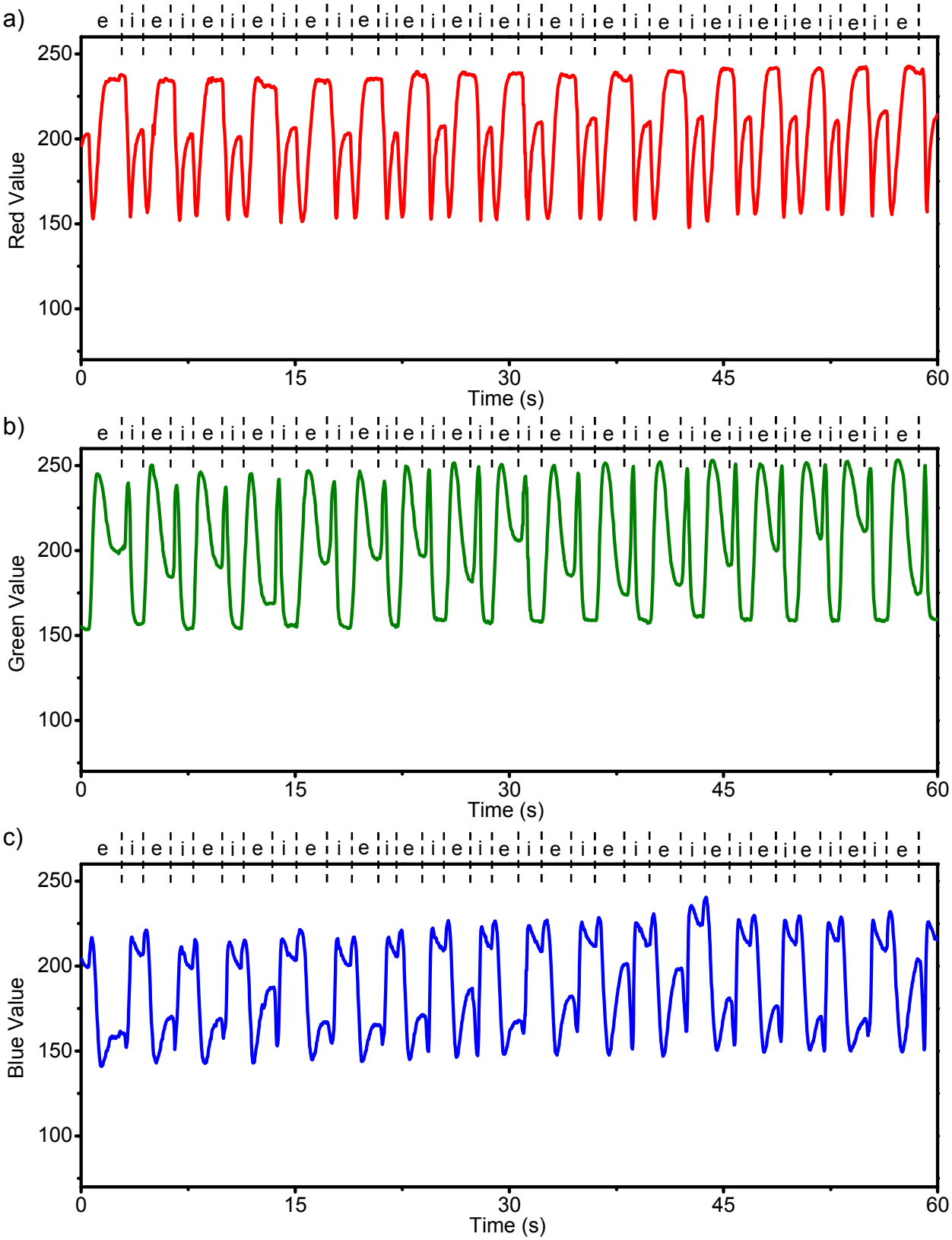

Figure 2.22. KGM II RGB plots vs. time for the fasting scenario. a) Red values, b) green values, c) blue values. Exhales are denoted as “e”, inhales as “i”.

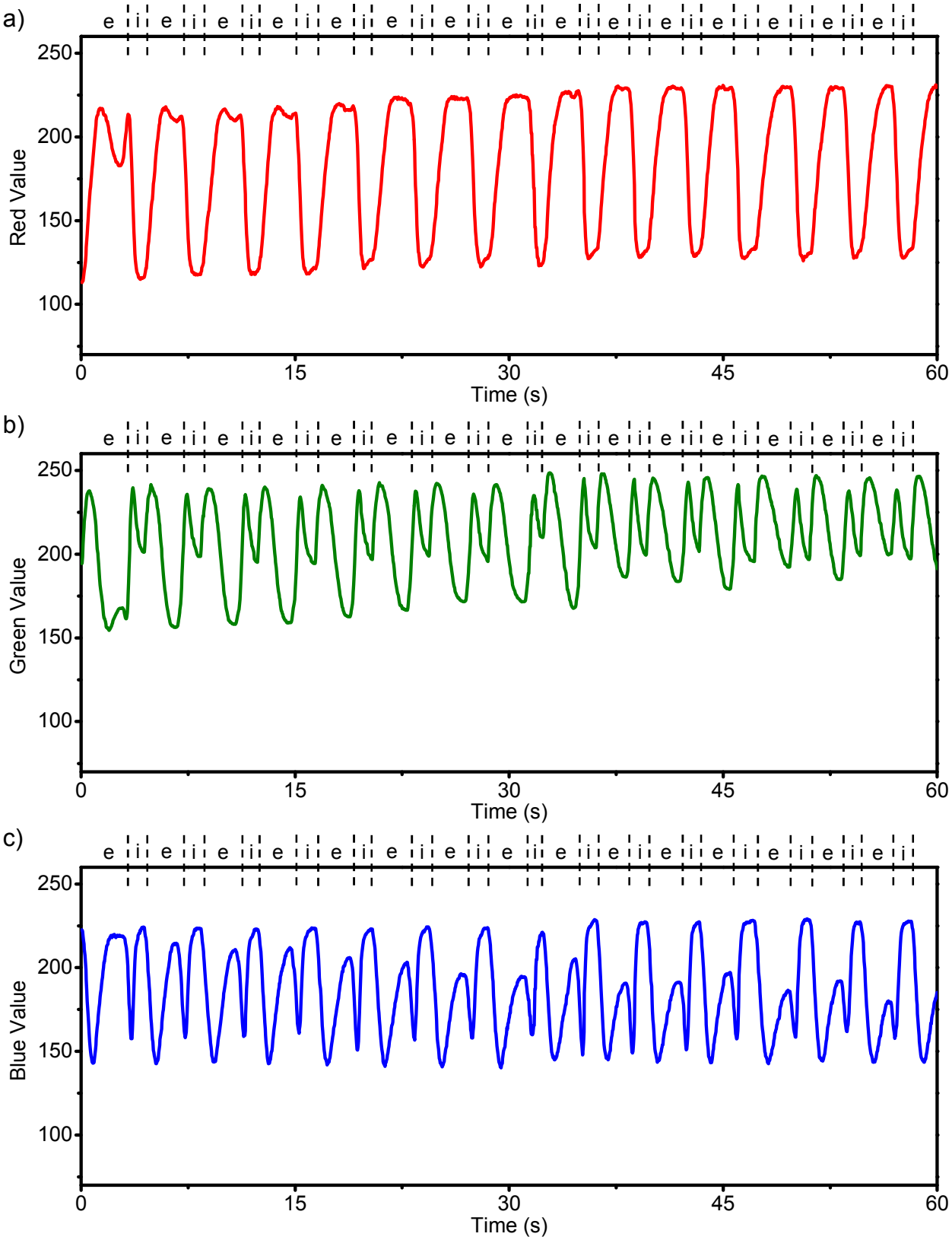

Figure 2.23. KGM III RGB plots vs. time for the fasting scenario. a) Red values, b) green values, c) blue values. Exhales are denoted as “e”, inhales as “i”.

2.3.6 After Exercise

The RIC sensor was able to track rapid respiratory rates while standing, immediately after exercising, at an RH up to 100%. After comparing with the KGM sensor array at various RH[1], the peak inhale of KGM I reached 43%, KGM II reached 65%, and KGM III reached 54% RH. The sensors all reached 100% RH at peak exhale (Figure 2.24 a). Radar plot comparisons agreed with 43% RH for peak inhale and 100% RH for peak exhale (Figure 2.24 b). The resulting average peak inhale is therefore 51.3% RH with average peak exhale 100% RH. The inhale humidity immediately after exercise is 15.8% higher than the standard standing condition and the exhale humidity 3.7% higher.

Since the humidity reached 100% RH, RGB plots had many transition color peaks. KGM II and III were not able to track a few breath cycles at the beginning of breath analysis after exercising as the sensors did not have time after an exhale to revert back to ambient humidity. In addition, there may be unintended effects from sweat caused by exercising. In order to improve the sensor's application to exercise scenarios, the distance between the sensor and the breath source should be increased. By increasing the distance, the RIC sensor will be able to reach ambient humidity faster to show more clear and distinct breath cycles.

KGM I's RGB plots tracked a wide range of humidity, 45-100%, which allowed for inhales and exhales to be more easily seen. However, since 100% RH is reached, the RGB plots do not resemble previous scenarios as more transition colors can be seen. In the red plot, the inhales and exhales both peak at ~170 (Figure 2.25 a). Two transition colors are seen in this plot: green and purple. The green transition color appears at the

lowest peaks on the red plot at ~80, right after peak inhales. The purple transition color appears after peak exhales at ~120-150. The green RGB plot includes one more transition color than the red plot (2.25 b). Bordering the exhale peak (~180), transition green/cyan is seen at ~220-200. Bordering the inhale peak (~185), transition purple at ~150 is seen on the left and transition blue at ~100 is seen on the right. The three transition colors on the green RGB plot for KGM I makes it difficult to analyze breath cycles without video analysis. The blue RGB plot for KGM I is the easiest to read as the exhale interval is overall increasing and the inhale interval is overall decreasing (Figure 2.25 c). The exhale peak is found at ~165 with a blue transition color bordering it at ~215. The inhale is clearly seen at the low value of ~110. After analysis, it is seen that KGM I achieved 22 bpm at an average breath cycle of 2.7 seconds. This is 4 breaths more than that of the standard standing condition, proving the RIC sensor can track breath cycles for increased respiratory rates at high RH.

KGM II had very noisy RGB plots, possibly caused by the sensor being slightly too close to the nose or from sweat after exercising. Immediately after exercise, the breath humidity is extremely high, and the sensor distance must be carefully monitored to ensure breath cycles can be viewed. As seen at the conclusion of the red and green plots, the sensor was finally able to revert back to inhale humidity to show clear breathing cycles. For the red RGB plot, the inhale intervals are shown as decreasing in red value and the exhale intervals are shown as increasing in red value (2.26 a). Before about 35 seconds, the inhale and exhale intervals are difficult to view without annotations. The same can be said about KGM II's green RGB plot; before 35 seconds, inhale and exhale intervals are difficult to view (2.26 b). Here, inhale intervals are shown

as overall decreasing in green value and exhale intervals are overall increasing in green value. There is a green transition color at ~160 bordering the exhale's ~140 and is best seen towards the end of the analysis. The blue plot for KGM II is the most difficult to view as many transition peaks appear (Figure 2.26 c). This is due to repetitive interference coloration of fourth-order and fifth-order interference seen when KGM II reaches maximum humidity levels. This repetitive coloration only occurs in KGM II and III when high RH is achieved because they move past fourth-order interference. KGM I stops at fourth-order interference coloration at 100% RH, so no repetitive colors occur. To determine breath cycle data of KGM II, video analysis was paired with RGB plot analysis. KGM II resulted in 22 bpm with an average breath cycle of 2.6 seconds, almost identical to what KGM I tracked.

For KGM III, the RGB plots, especially red, were able to show breath cycling much better than KGM II. Since the KGM III plots are not uniform as KGM I, the sensor could have been slightly too close to the nose or impacted by sweat formed by exercising. The red plot followed KGM III's usual trend of increasing in value for exhale intervals and decreasing in value for inhale intervals (Figure 2.27 a). Before 30 seconds elapsed, a few cycles show a red transition color at ~130 bordering the exhale peak of ~110. This red transition color is evidence of KGM III's movement past fourth-order coloration to reach fifth-order coloration. As breathing intensity decreased over time, this transition color peak decreased as well, indicating breath humidity slightly dropping below 100% RH. Unlike the red plot, KGM III's green plot is difficult to read without breath cycle annotations (2.27 b). The inhale peaks at ~125 and immediately decreases to ~105 because of a yellow transition color. Then, a green transition color peak is seen

at ~125. The exhale peak is reached next at a low green value of ~95. KGM III's blue plot is slightly easier to decipher compared to the green plot (2.27 c). Again, two different transition colors can be seen along with the exhale and inhale peaks. The highest peaks belong to the exhale at ~140 which are followed by a transition green color at ~100. Then, the inhale peak is seen at ~115, and another transition color, red, is seen at ~90. These RGB plots for KGM III tracked an average breath cycle of 2.6 seconds with 23 bpm, similar to what KGM I and II were able to track.

Every KGM sensor was able to track a rapid respiratory rate at high humidity levels. KGM I had the most success at translating breath cycles into RGB plots as its high humidity only reaches fourth-order interference coloration. As seen with KGM II and III at maximum humidity levels, moving past fourth-order coloration resulted in more transition color peaks as color repetition began.

a)

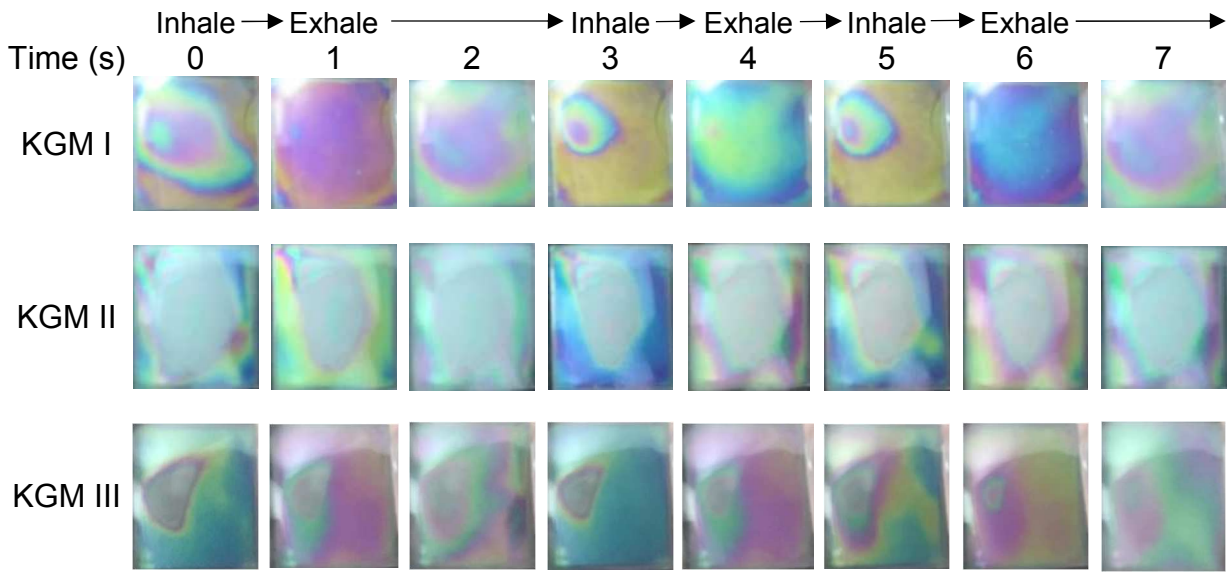

b)

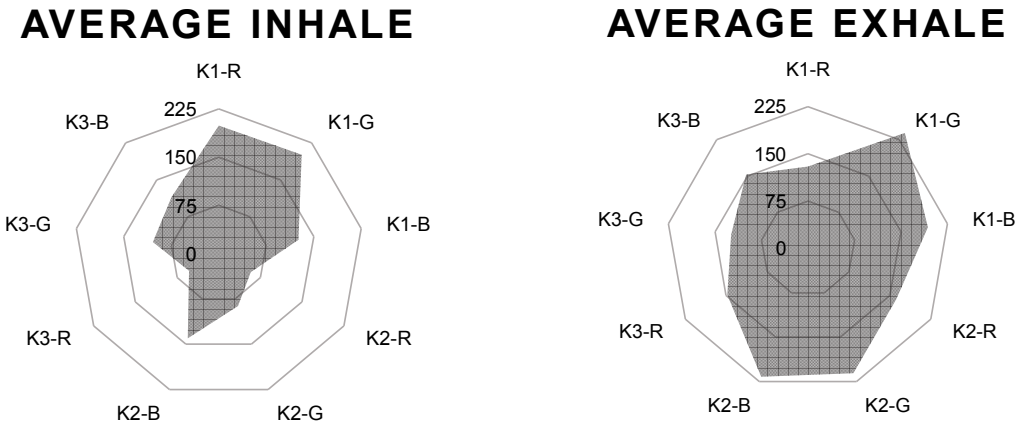

Figure 2.24. a) Colorimetric responses of KGM humidity sensors after exercising, standing and breathing through the nose. The breathing cycles for KGM I, II, and III have been aligned to compare exhale and inhale colorations. b) Radar plots of KGM I, II, and III for the exercise scenario.

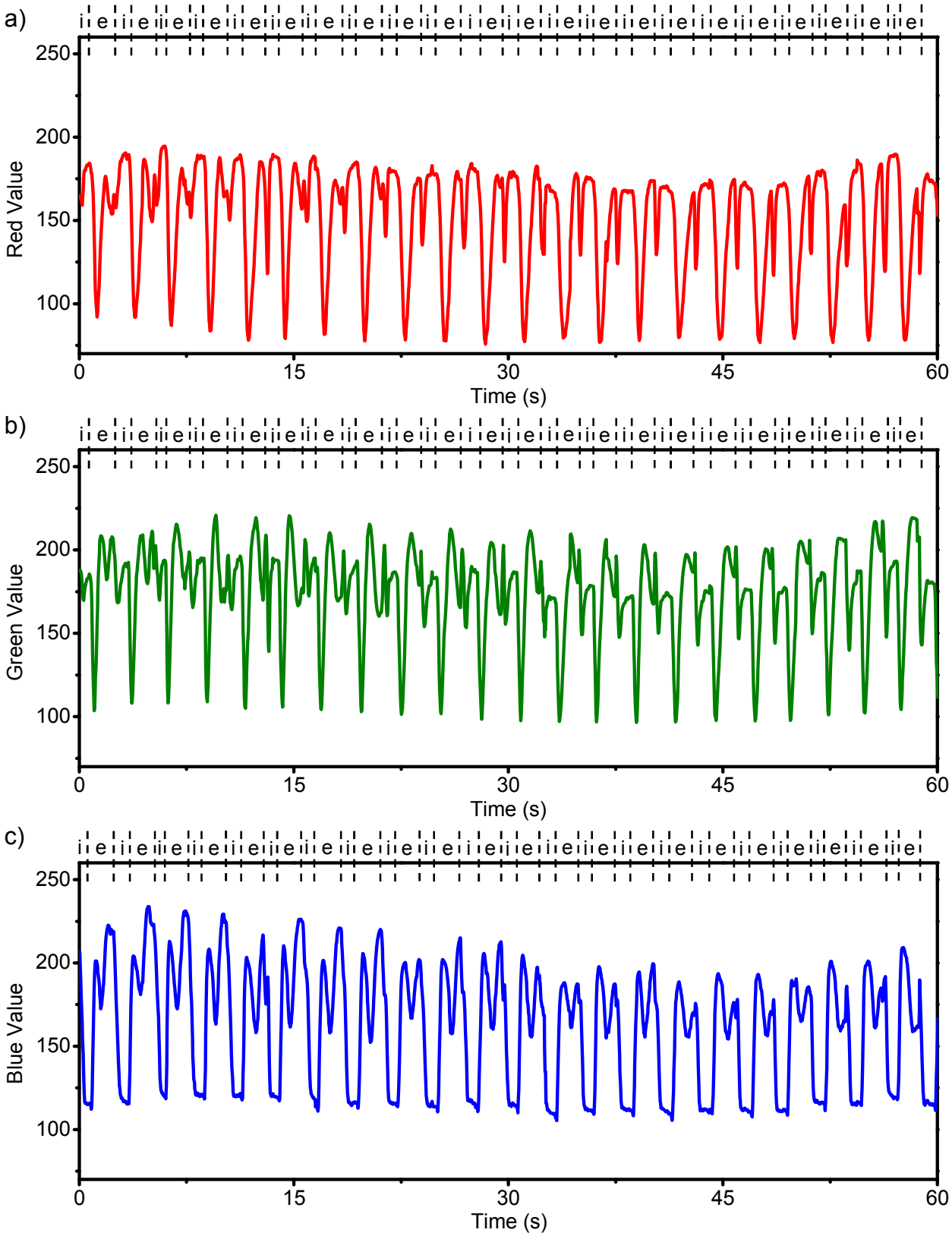

Figure 2.25. KGM I RGB plots vs. time for the exercise scenario. a) Red values, b) green values, c) blue values. Exhales are denoted as “e”, inhales as “i”.

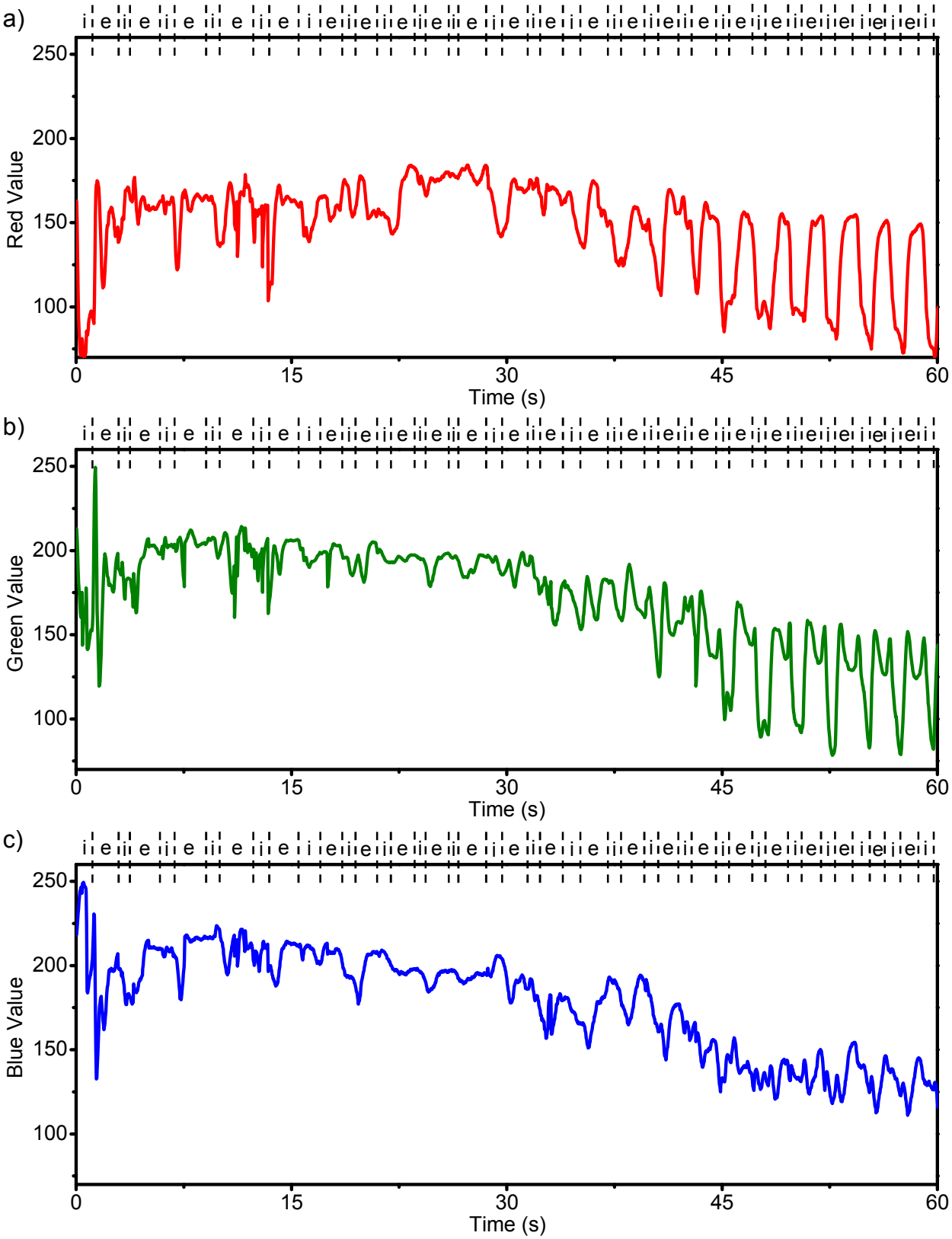

Figure 2.26. KGM II RGB plots vs. time for the exercise scenario. a) Red values, b) green values, c) blue values. Exhales are denoted as “e”, inhales as “i”.

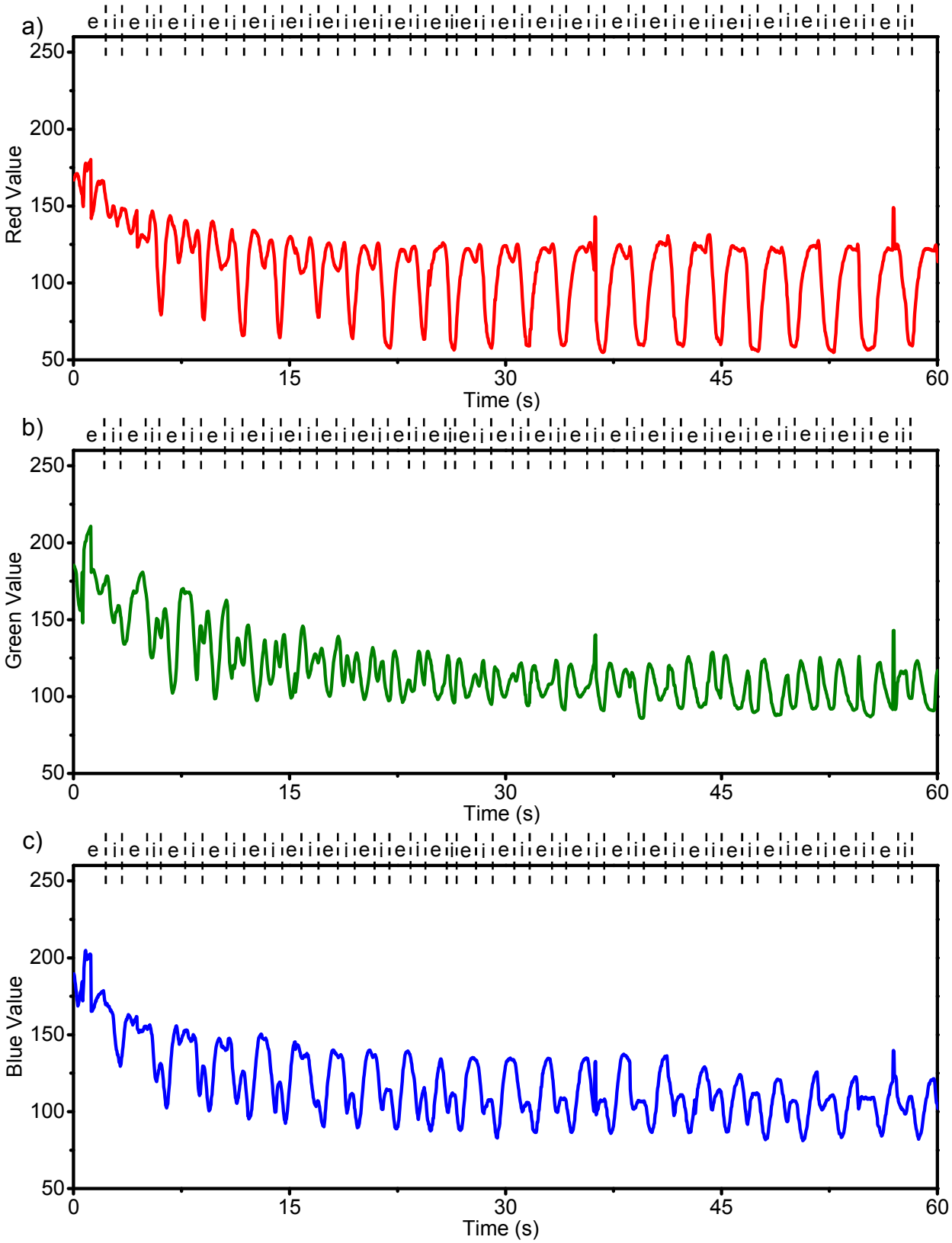

Figure 2.27. KGM III RGB plots vs. time for the exercise scenario. a) Red values, b) green values, c) blue values. Exhales are denoted as “e”, inhales as “i”.

2.3.7 Sensor Performance Analysis

The RIC sensor was successful at tracking breath cycles over time and determining the respiratory rate and breath humidity. KGM I, II, and III each exhibited a wide range of RH and bpm, as summarized in Table 2.2. On average, sensors reported lowest exhale RH in the sitting scenario, followed by the standing and after exercise scenarios. The bpm accurately tracked a faster rate of breathing immediately after exercise, much higher than the standard sitting condition.

Scenario	KGM Sensor	Peak Inhale RH %	Peak Exhale RH %	Average Breath Duration (s)	Breaths per Minute
Sitting (Back Side of Sensor)	I	33	97	5.2	11
	II	33	97	3.6	16
	III	33	97	4.0	15
Sitting	I	33	94-97	4.3	14
	II	33	94	3.9	15
	III	33	94	4.9	12
Standing	I	33	94	3.2	18
	II	33	98.5	4.3	14
	III	33	97	3.9	15
After 12 Hour Fast	I	43	97	3.4	17
	II	43	94-97	3.5	17
	III	43	94	3.8	15
After Exercise	I	43	100	2.7	22
	II	65	100	2.6	22
	III	54	100	2.6	23

Table 2.2. Performance of each KGM sensor for each scenario. Peak RH values determined by comparison with KGM sensor array at various RH[1]. Front side of sensor utilized unless noted otherwise.

The back side of the KGM sensor is not optimal for tracking breath RH. At peak exhale, the color must be inverted to find the compliment color to then compare with the KGM sensor array at various RH[1]. This analysis makes it difficult to determine breath cycles or breath RH visually, without aid of further analysis. The front side of the KGM sensor is able to clearly show breath cycles through facile visual analysis as color changes are distinct from each other. With the reference KGM array to determine RH,[1] the exhale and inhale RH can be assigned by simply viewing the sensor. Breaths per minute can also be determined visually by watching the sensor's color changes and counting the number of inhale colors seen.

When comparing KGM I, II, and III's response to humidity changes, the only differences lie within the interference colorations they reach at maximum RH. At 100% RH, KGM I exhibits fourth-order interference coloration while KGM II and III exhibit fifth-order interference coloration. KGM I does not repeat any coloration during its transition from low RH to 100% RH when it reaches fourth-order interference. This makes visual analysis and RGB plot analysis easier to interpret. When KGM II and III reach high RH, they pass through fourth-order and reach fifth-order interference, which appear as repeating colors. These repeating colors lead to difficultly in visual and RGB plot analysis. Overall, KGM I is the best candidate for breath monitoring as it is capable of clearly tracking increased respiratory rates at high relative humidities.

2.4 Conclusion

The KGM breath monitor sensor is able to not only determine the respiratory rate, but also the corresponding RH of the breath. The RH range of the KGM sensor exceeds the capability of current breath sensors as it is able to track 0-100% RH.[1] Although the breath monitor has been tested with breath cycles only as fast as 2.7 seconds, the KGM's rapid response time will allow for even faster breath cycles to be recorded at an appropriate distance from the humidity source. The breath monitor's ability to report two components of the human breath simultaneously is vital for healthcare and at-home settings.

The simplicity of visual analysis allows for easy at-home use of the breath sensor. An at-home user would be able to capture exhales by photo or video and determine the RH by matching the color to a corresponding RH color key. A 60-second video will allow for easy analysis of breaths per minute by counting the number of times their inhale color is seen. RGB analysis could also be helpful for at-home use, for example, to help those with colorblindness. Breaths can be captured by photo or video and analyzed with an application on a cell phone to determine the RGB values. These values could be matched with a corresponding RGB color key to determine the breath's RH. A few applications available for cell phone download are Color Name, Pixel Picker, and Swatches. These applications analyze a chosen point in a photo or video to determine RGB values.

In future studies, more breathing scenarios should be explored with the breath monitor. These could include a sleeping or meditative state, alcohol-induced dehydration, and a person with asthma. In addition to these scenarios, the breath

difference between a male and female would be useful to study to compare and contrast. With the positive results of this breath monitor, particularly from KGM I, further breath studies should be highly successful in monitoring both the respiratory rate and breath humidity levels.

References

(1) Momtaz, M.; Chen, J. High-Performance Colorimetric Humidity Sensors Based on Konjac Glucomannan. ACS Appl. Mater. Interfaces **2020**, 12, 48, 54104–54116.

(2) Oyefusi, A.; Chen, J. Mechanical Approaches to Dynamic, Reversible, Mechanochromism Based on Thin Film Interference. *Appl. Mater. Today* **2020**, 20, 100774.

(3) Sørensen, B. E. A Revised Michel-Lévy Interference Colour Chart Based on First-Principles Calculations. *Eur. J. Mineral.* **2013**, 25, 5-10.

(4) Datta, S.; Taghvaeian, S.; Stivers, J. Understanding Soil Water Content and Thresholds for Irrigation Management. *Oklahoma Cooperative Extension Service*, 2017, BAE-1537.

(5) Panuska, J.; Sanford, S.; Newenhouse, A. Methods to Monitor Soil Moisture. *University of Wisconsin-Extension*, 2015, A3600-02.

(6) Irrometer. https://www.irrometer.com/sensors.html (accessed Mar 1, 2020).

(7) Campbell, G.; Campbell, C.; Cobos, D.; Crawford, L.; Rivera, L.; Chambers, C. Soil Moisture Sensors – How They Work. Why Some are not Research-Grade. *METER Environment,* 2020.

(8) Campbell, C. Soil Moisture Sensors: Why TDR vs. Capacitance May be Missing the Point. *Environmental Biophysics*, 2017.

(9) Amer, A. Water Vapor Adsorption and Soil Wetting. In Wetting and Wettability; IntechOpen, 2015. 10.5772/60953.

(10) Massaroni, C.; Lopes, D.; Presti, D.; Schena, E.; Silvestri, S. Contactless Monitoring of Breathing Patterns and Respiratory Rate at the Pit of the Neck: A Single Camera Approach. *J. Sens* **2018**, 2018, 4567213.

(11) API Simply Science. https://www.api.simply.science/images/content/biology/human_physiology/respiratory_system/conceptmap/Respiratory_cycle.html (accessed Mar 6, 2020).

(12) Ferrus, L.; Guenard, H.; Vardon, G.; Varene, P. Respiratory Water Loss. *Respir. Physiol.* **1980**, 39, 367-381.

(13) Güntner, A.; Abegg, S.; Königstein, K.; Gerber, P.; Schmidt-Trucksäss, A.; Pratsinis, S. Breath Sensors for Health Monitoring. *ACS Sens.* **2019**, 4, 268-280.

(14) Mogera, U.; Sagade, A.; George, S.; Kulkarni, G. Ultrafast Response Humidity Sensor Using Supramolecular Nanofiber and its Application in Monitoring Breath Humidity and Flow. *Sci. Rep.* **2014**, 4, 4103.

(15) Duan, Z.; Jiang, Y.; Yan, M.; Wang, S.; Yuan, Z.; Zhao, Q.; Sun, P.; Xie, G.; Du, X.; Tai, H. Facile, Flexible, Cost-Saving, and Environment-Friendly Paper-Based Humidity Sensor for Multifunctional Applications. *ACS Appl. Mater.* Interfaces **2019**, 11, 21840-21849.

(16) Yan, H.; Zhang, L.; Mao, L. Sensitive and Fast Humidity Sensor Based on a Redox Conducting Supramolecular Ionic Material for Respiration Monitoring. *Anal. Chem.* **2017**, 89, 996-1001.

(17) Kano, S.; Kim, K.; Fujii, M. Fast-Response and Flexible Nanocrystal-Based Humidity Sensor for Monitoring Human Respiration and Water Evaporation on Skin. *ACS Sens.* **2017**, 2, 828-833.

(18) Zhen, Z.; Li, Z.; Zhao, X.; Zhong, Y.; Zhang, L.; Chen, Q.; Yang, T.; Zhu, H. Formation of Uniform Water Microdroplets on Wrinkled Graphene for Ultrafast Humidity Sensing. *Small* **2018**, 10.1002.

(19) Dai, J.; Zhao, H.; Lin, X.; Liu, Y.; Liu, X.; Fei, T.; Zhang, T. Ultrafast Response Polyelectrolyte Humidity Sensor for Respiration Monitoring. *ACS Appl. Mater. Interfaces* **2019**, 11, 6483-6490.

(20) Zhang, J.; Wang, X.; Zhang, B.; Ramakrishna, S.; Yu, M.; Ma, J.; Long, Y. In Situ Assembly of Well-Dispersed Ag Nanoparticles throughout Electrospun Alginate Nanofibers for Monitoring Human Breath-Smart Fabrics. *ACS Appl. Mater. Interfaces* **2018**, 10, 19863-19670.

(21) Ali, I.; Chen, L.; Huang, Y.; Song, L.; Lu, X.; Liu, B.; Zhang, L.; Zhang, J.; Hou, L.; Chen, T. Humidity-Responsive Gold Aerogel for Real-Time Monitoring of Human Breath. *Langmuir* **2018**, 34, 4908-4913.